IOWA STATE UNIVERSITY
Digital Repository

2010

Syngas fermentation to ethanol using innovative hollow fiber membrane

Po-Heng Lee
Iowa State University

Follow this and additional works at: https://lib.dr.iastate.edu/etd

Part of the Bioresource and Agricultural Engineering Commons, and the Environmental Engineering Commons

Syngas fermentation to ethanol using innovative hollow fiber membrane

by

Po-Heng Lee

A dissertation submitted to the graduate faculty

in partial fulfillment of the requirements for the degree of

DOCTOR OF PHILOSOPHY

Majors: Civil Engineering (Environmental Engineering)

Program of Study Committee:
Shihwu Sung, Major Professor
Say-kee Ong
James E. Alleman
Thomas E. Loynachan
Thomas B. Moorman

Iowa State University

Ames, Iowa

2010

TABLE OF CONTENTS

LIST OF FIGURES

Chapter 4

LIST OF TABLES

ABSTRACT

Lignocellulosic biomass like straw, wood, and agritural residues are plentiful and inexpensive, and can serve as feedstock for fuels and commercial chemicals production. These lignocellulosic biomasses of abundant supply, consisting of cellulose, hemicelluloses and lignin, however have to be pretreated to form simple sugars for further conversion into alternative fuels and chemicals. One existing technology that could convert biomass into fuels is the hybrid thermochemical/biological approach for the potential commercialization necessary to the answer of fossil fuels replacement. The process starts with the gasification of biomass to produce synthesis gas (syngas) that is a gas mixture of carbon monoxide (CO), hydrogen (H_2), carbon dioxide (CO_2) and Nitrogen (N_2). Then, syngas is served as microorganism substrates for several microbial metabolisms and produces for the synthesis of various valuable fuels including ethanol and butanol.

The low solubility of carbon monoxide and hydrogen into the aqueous fermentation broth for the microorganisms, however, limits the potential commercialization. The fermentor design for the improvement of synags-liquid mass transfer is, thus, the dominating key to determine the production of syngas fermentation. An innovative fermentor using hollow fiber membrane as a mean of gas delivery has demonstrated to be an effective method for eliminating the mass transfer limitation of syngas fermentation. The highest CO mass transfer rate of 1.49 s^{-1} which is over its counterpart (nonporous silicone HFM) and previous studies was obtained using the microporous polypropylene HFM. A model is calculated for commercialization of syngas fermentation.

Clostridium ljungdahlii, a gram-positive, motile, rod-shaped anaerobe, utilizes the CO in syngas to produce ethanol and acetate. Information is limited pertaining to the optimization of growth and production condition as well as the performance of the hollow fiber membrane fermentor. *Clostridium ljungdahlii* demonstrated its highest growth rate on PETC 1754 with 5 $g \cdot l^{-1}$ fructose and 1 $g \cdot l^{-1}$ yeast extract with pH between 6.5 and 7.5. pH at 5 in the production phase is recommended for the optimal ethanol production from *C. ljungdahlii*.

Growth and production conditions were optimized on the 40-ml hypovial test. The optimal conditions from the 40-ml hypovial test were applied to a 2-L hollow fiber membrane reactor for the optimization of ethanol production. The results demonstrated that the hollow fiber membrane reactor could produce ethanol to 6 $g \cdot L^{-1}$ by *Clostridium ljungdahlii* from the fructose-free medium and syngas with an ethanol to acetate ratio of 2.6 which was the highest ratio in compared with other previous studies.

CHAPTER 1. GENERAL INTRODUCTION

Syngas Fermentation (Chapter 15), *Anaerobic Technology for Sustainable Environment*,

Imperial College Press (expected publication in Dec, 2010)

Shihwu Sung and Po-Heng Lee

Department of Civil, Construction and Environmental Engineering,

Iowa State University, Ames, IA 50011, USA

Abstract

Using unsustainable fossil fuels for energy is a critical issue in today's society, and seeking a reliable and economical alternative energy source has raised a lot of attention recently. One of the potential solutions is to convert biomass, which is available in many forms, into fuels and commercial chemicals. The gasification of biomass followed by synthesis gas (syngas) fermentation is one of the novel methods for the potential commercialization necessary to the answer of fossil fuels replacement. An overview of fermentation from biomass-generated syngas is summarized in this chapter.

1. Introduction

Fossil fuels, which represent a significant portion of current energy supply for human activities, are of finite reserve. Moreover, burning fossil fuels result in severe environmental threats (releasing pollutants and green house gases, such as carbon dioxide and nitrogen oxides). Hence, an alternative way to produce energy and chemicals from renewable sources would reduce the stress of dependence on fossil fuels and alleviate environmental concerns (Worden *et al.,* 1991). Lignocellulosic biomass like straw, wood,

and agritural residues are plentiful and inexpensive, and can serve as feedstock for fuels and commercial chemicals production. These lignocellulosic biomasses of abundant supply, consisting of cellulose, hemicelluloses and lignin, however have to be pretreated to form simple sugars for further conversion into alternative fuels and chemicals. One pretreatment method is through acid/alkaline treatment, followed by enzymatic hydrolysis; the sugars are then fermented into fuel, such as ethanol. This process is usually extensive and leaves a large portion of un-degradable lignin.

Another pretreatment method is through gasification of lignocellulosic biomass to produce a mixture of CO, CO_2, and H_2 (known as synthesis gas, syngas or producer gas) followed by (a) a catalytic gas-conversion step or (b) anaerobic fermentation into fuels and derivative chemicals. The physicochemical limitations and disadvantages of the catalytic gas-conversion process are (Worden *et al*., 1991):

(1) Some contaminants in the syngas, primarily hydrogen sulfide and carbonyl sulfide, must be removed by an energy-intensive purification process before feeding into the catalytic reactor, making it costly.

(2) Syngas composition varies considerably from gasification processes and raw materials. However, the catalytic process requires a specific influent CO to H_2 ratio for a profitable product mix. Influent CO to H_2 ratio often needs to be adjusted by gas recompression and shift reaction mechanisms, adding significant operational costs.

(3) Catalytic processes usually operate under extreme conditions, such as high temperatures and pressures, not only creating safety concerns but also raising capital cost for reactors and other materials of construction.

(4) The catalytic processes may produce a variety of products, requiring extensive further separation.

(5) Some by-products from the catalytic process are hazardous, resulting in public health concerns.

Compared to catalytic conversion, the emerging technology of anaerobic fermentation appears to be more sustainable and attractive. It may minimize the negative impacts and produce non-toxic products. Its advantages are as follows:

(1) Microorganisms for syngas fermentation are able to tolerate hydrogen sulfide and other contaminants.

(2) Syngas fermentation is not sensitive to the syngas composition, and thus the costly gas depression procedure may be eliminated.

(3) The composition of fermentation products can be more consistent.

(4) Fermentation is operated at mild temperatures and pressures.

(5) Fermentation products are in general non-toxic.

Production of simple organic compounds from syngas is thermodynamically favorable, as shown by the negative changes of Gibbs free energy, ΔG^o, in Table 1 (Barik *et al.,* 1988). Fisher and Tropsch were the first in 1932 to demonstrate that acetate could be produced from CO by an anaerobic sewage sludge (Diekert *et al.,* 1982). Since then, microbial fermentation of syngas produced from cellulosic materials has been studied by many, and has even been demonstrated in full-scale operation. Although difficulties had been encountered in early attempts, many now believe that microbial production of fuels and

commercial products from syngas is commercially feasible through proper product formation, microbe selection, and process optimization (Barik *et al.,* 1990).

Many microbes (some have been isolated but not yet identified) capable of producing fuels and chemicals from syngas have been reported. An overview of this cutting-edge technology is summarized in the following.

2. Microbiology of anaerobic microorganisms capable of converting syngas to biofuels and chemicals

Anaerobic carboxydotrophic microorganisms known to grow on CO and H_2 as substrate are listed in Table 2. They are further discussed as follows.

2.1 Mesophiles for organic acids production

Many early researches were conducted to produce acetate and butyrate using CO as substrate. *Eubaterium limosum* isolated from various environments, e.g. human intestine, sewage, rumen, and soil, produces acetate and butyrate exclusively using CO as the sole energy source (Genthner *et al.,* 1982 and 1987). Other acetogens, including *Clostridium aceticum, Peptosteptococcus productus*, etc, were identified to be able to produce acetate from syngas gas. *Butyribacterium methylotrophicum* has demonstrated its ability to shift production from acetate to butyrate by inducing pH changes during the fermentation (Grethlein *et al.,* 1991; Lynd *et al.,* 1982; Shen *et al.,* 1999). *Acetobacterium woodii* is also one of the mesophiles capable of producing acetate from CO. However, the research trend of syngas fermentation has shifted from volatile acids production to production of fuel or other high-value derivatives (Genthner *et al.,* 1987).

2.2. Mesophiles for alcohols production with the byproducts of organic acids

Microbial production of acetate, formate, butyrate, ethanol, butanol, and hydrogen has been considered to have industrial application in recent years. Among the well-studied microbes, *Clostridium ljungdahlii*, a Gram-positive, motile, rod-shaped anaerobe, was isolated from chicken yard waste. *C. ljungdahlii* grows on syngas in pH 4-7 producing ethanol and acetate (Tanner *et al.,* 1993). It has been used in full-scale production of ethanol from syngas in a commercial process involving gasification, fermentation, and distillation. *Clostridium autoethanogenum* was also reported to be capable of producing ethanol and acetate from CO and CO_2. The conversion efficiency of *C. autoethanogenum* from syngas to alcohol and acetate, however, was much lower than that of *C. ljungdahlii* (Cotter *et al.,* 2009*)*. Another bacterium, *Clostridium carboxidivprans P7*, recently isolated from sediment of an agricultural settling lagoon*,* was reported to produce acetate, ethanol, butyrate, and butanol from CO and H_2 (Liou *et al.,* 2005). Currently, the most attractive syngas fermentation process is using *C. carboxidivprans P7* to produce butanol, which is of higher energy content, lower vapor pressure and less corrosive than ethanol.

2.3. Mesophiles for hydrogen and poly-β-hydroxyalkanoate (PHA) production

A photosynthetic purple nonsulfur bacterium, *Rhodospirillum rubrum*, can use CO as the sole carbon and energy source under anaerobic conditions, in the presence or absence of light, to produce H_2 and Poly-*β*-hydroxyalkanoate (PHA) (Kerby *et al.,* 1995; Do *et al.,* 2007). PHA is a biodegradable plastic of many potential applications, including as food additive and as the material for bone reconstruction.

2.4. Thermophiles for hydrogen and organic acid production

Thermophilic fermentation has the advantages of less cooling requirement of syngas, high conversion rates, and a separation benefit for alcohols; however, higher temperatures would reduce the syngas solubility (Henstra *et al.,* 2007). Gram-positive thermophiles that can convert CO and H_2O into H_2 and CO_2 also have been isolated recently, including *Carboxydothermus hydrogenoformans* and *Thermolithobacter carboxydivorans.* Other thermophiles, such as *Moorella thermoautotrophica* and *Moorella thermoacetic,* have been reported to use CO producing acetate. However, no thermophiles have been reported to be able to convert CO into fuels (such as ethanol or butanol).

One of the most significant factors of syngas fermentation is the CO conversion rate and superior specific products of microorganisms which could produce valuable fuels and organic compounds. Isolation of new microbes capable of converting CO into fuels and organics and research to improve efficiency will make this technology more commercially feasible.

3. **Metabolic pathways of syngas fermentation**

3.1. Acetyl-CoA pathway of bacteria for the formation of organic acids and alcohols

Products from syngas fermentation are limited to these reactions that could conserve enough energy for microbes' metabolism from syngas. The Wood-Ljungdahl pathway (Fig. 1 adopted from Henstra *et al.,* 2007) is the main mechanism for the production of acetate, ethanol, butyrate and butanol from syngas fermentation by acetogens, sulfate-

reducing bacteria, and archaea under strictly anaerobic condition. The carbonyl group (-CO) is converted from CO_2 by the bifunctional CO dehydrogenase complex. However, CO is abundant in syngas, so the bifunctional CO dehydrogenase complex is not manifestly required. The methyl group is reduced by CO_2 with some intermediates, i.e. formyl, methenyl, methylene, and methyl compounds bounded with a pterin cofactor. Acetyl-CoA-synthase/CO-dehydrogenase complex (ACS/CODH) is responsible for forming acetyl-CoA by joining a carbonyl and a methyl group (Lindahl *et al.,* 2002; Ragsdale *et al.,* 2004; Henstra *et al.,* 2007). Bacteria and Achaea have slightly different acetyl-CoA pathway. For bacteria, formate is reduced from CO_2, and then forms formyl compounds bounded to the pterin tetrahydrofolate with the utilization of ATP (Henstra *et al.,* 2007). For Achaea, a methanofuran-bound formyl reduced from CO_2 is converted to tetrahydromethanopterin. Because the formation of acetyl-CoA from H_2 and CO_2 requires energy, acetate is transferred from acetyl-CoA to recover the lost energy from the formation of acetyl-CoA. Ethanol is produced from the further reduction of acetate. Two acetyl-CoA molecules yield an acetoacetyl-CoA which further produces butanol and buyrate (Henstra *et al.,* 2007; Ragsdale and Pierce, 2008; Fischer *et al.,* 2008).

3.2. Acetyl-CoA pathway of bacteria for the formation of hydrogen

Hydrogen production from syngas is metabolized by hydrogenogenic carboxydotrophs (Fig. 2 adopted from Henstra *et al.,* 2007). The acetyl-CoA pathway with the energy-balanced conservation governs this bacterial metabolism (Henstra *et al.,* 2007). A monofunctional CO dehydrogenase releases electrons by oxidizing CO to CO_2. Energy-converting hydrogenase (ECH) receives electrons and reduces protons to yield hydrogen

(Hedderich, 2004; Singer *et al.,* 2006). ECH, which forms H_2 and translates protons or sodium ion, produces ATP from an ATP-synthase driven by a chemiosmotic ion gradient (Hedderich, 2004; Maness *et al.,* 2005).

4. Carbon monoxide gas/liquid mass transfer

Syngas predominantly consists of CO and H_2, both of which have low water solubilities. Mass transfer rates are thus crucial to syngas fermentation. The gas-liquid mass transfer rates of CO and H_2 are only 77% and 65%, respectively, of that of oxygen, (Bredwell *et al.,* 1999). The low concentrations of dissolved CO and H_2 result in insufficient supply of substrates for the microbes. This is the bottleneck for the full-scale application of syngas fermentation. This section will discuss reactor designs for improving the solubility of CO.

4.1. Determination of CO gas-liquid mass transfer

The mass transfer of a gas into liquid phase can be modeled using the following equations:

$$dC/dt = K_La(C_s-C) \qquad\qquad (1)$$

$$\ln(C_s-C)/(C_s-C_o) = (-K_La)t \qquad\qquad (2)$$

where K_La = CO gas-liquid mass transfer coefficient, (s^{-1})

C_s = saturated dissolved CO concentration $(mg \cdot l^{-1})$

C_o = dissolved CO concentration at the initial time 0 $(mg \cdot l^{-1})$

t = reaction time (s)

The gas-liquid mass transfer coefficient, K_La, depends not just on the gas species, but also the fermentor configuration and the mixing pattern.

4.2. Stirred tank rector

Stirred tank reactors (STR) are commonly used in the full-scale fermentors, in which bacterial cells are suspended in the mixed liquor. Riggs *et al.,* (2006) reported that the gas-liquid mass transfer coefficient of CO ranged from 0.003 s^{-1} to 0.043 s^{-1} (i.e. 10.8 h^{-1} to 154.8 h^{-1}) in a reactor of 7-liter working volume with stirrer speeds ranging 200-600 rpm, and CO flowrates ranging 1-6 l·min^{-1} (corresponding to a gas retention time of 1.2-7 min). A syngas consisting of 20% CO, 18% CO_2, 52% N_2, and 10% H_2 was tested to decide the CO gas-liquid mass transfer coefficient in the same reactor of 7-liter working volume. Results showed the CO gas-liquid mass transfer coefficient ranged from 0.02 s^{-1} to 0.08 s^{-1} (i.e. 72 h^{-1} to 288 h^{-1}) with stirrer speeds ranging 400-700 rpm and CO flowrates ranging 5-15 l·min^{-1} (Kapic *et al.,* 2006). Six impellers (i.e. Rushton-type, Philadelphia Mixing concave 9 hollow blade turbine, Philadelphia Mixing pitched blade turbine, Lightnin A315 fluidoil, Lightnin A310, and Philadelphia Mixing LS hydrofoil) were used to improve the CO gas-liquid mass transfer in the same reactor of 7-liter working volume. Among the six impellers tested, the Dual impeller showed the highest CO gas-liquid mass transfer with the most economical power consumption in all operational parameters (Ungerman *et al.,* 2007).

4.3. Other fermentors

Many fermentors other than STRs have different configurations and operational modes. Some have bacteria grow on surface of carriers resulting in a higher cell density, instead of dispersed in the mixed liquor. The gas-liquid mass transfer characteristics of oxygen in attached-growth reactors are listed in Table 3 (Charpentier, 1981; Bredewell *et al.,* 1999).

Results in Table 3 conclude that gas-liquid transfer rates of the different attached-growth reactor designs are better than that of the suspended growth ones . The CO-liquid mass transfer characteristic of the attached-growth fermentors was not highly dependent on the gas flow rates (Bredewell *et al.,* 1999). Carbon monoxide was dissolved at a faster rate due to a higher CO consumption rate occurred with higher cell density. Consequently, the attached growth fermentor could generally achieve a higher CO transfer rate than STR for a beneficial carbon monoxide conversion at a lower gas flow (Bredewell *et al.,* 1999).

4.4. Hollow fiber membrane fermentor

Studies have been conducted using hollow fiber membrane (HFM) to deliver oxygen and hydrogen for wastewater treatment and bio-remediation (Kim *et al.,* manuscript in progress). Application of microporous HFM as a syngas diffuser has also been developed in the authors' research lab at Iowa State University (Fig. 3). While syngas passes through the interior of the hollow fiber, CO and H_2 continuously permeate through the membrane into the aqueous phase of the reactor. Microbes grow on the exterior membrane surface with an enhanced biomass density for advancing the CO conversion. The polypropylene membrane bundles composed of 100, 250, 400 fibers (with an outside diameter of 0.042 cm, a wall thickness of 50 μm, a nominal pore size of 0.2 μm and a length of 13 cm) were used to study the CO gas-liquid mass transfer rates for a fermentor with a 2-liter working volume. For a syngas consisting of 48.5% CO, 35.5% H_2 and 16% CO_2, the CO gas-liquid mass transfer coefficients were found ranging from 0.011 to 0.177 s^{-1} for bundles consisting of 100-400 fibers and syngas flowrates of 0.025-0.140

min^{-1}. Results of the study indicate that HFM fermentor is a feasible for commercialization (Kim *et al.,* manuscript in progress).

5. Gas-liquid mass transfer rates in syngas fermentation

The standard tests on gas-liquid mass transfer, however, cannot fully simulate the actual syngas fermentation condition. In syngas fermentation, the mixed liquor is of complex composition and the dissolved CO and H$_2$ are continuously consumed by the biomass. Thus, meaningful data of syngas gas-liquid mass transfer should be obtained using the specific microbes and the fermenting mixed liquor. Table 4 summarizes the syngas gas-liquid mass transfer rates for wastewater treatment and fermentation (Bredwell *et al.,* 1999). Even though some of these studies were not used for fuels and chemicals production, the results of these studies are applicable to reactor design for syngas fermentation. CO conversion in a trickle-bed reactor by a three-culture fermentation was more than 2 fold of that in a STR (Klassson *et al.,* 1992; Bredwell *et al.,* 1999). Other studies using CO and H$_2$ as substrates for sulfate and nitrate reduction showed higher gas-liquid mass transfer rates in the fermentors with bacteria in attached growth, compared to those in STR (van Houten *et al.,* 1994; du Preez *et al.,* 1992 and 1994; Selvaraj *et al.,* 1996).

6. Performances of syngas fermentation for fuels and chemicals

6.1. Syngas fermentation for ethanol production

Ethanol is a renewable fuel and is currently used as a supplement to gasoline (10% ethanol blend). Ethanol is primarily produced from the fermentation of readily degradable

carbohydrate substrates, such as corn starch and sugarcane, causing a negative impact on global food market. Ethanol can also be produced from lignocellulosic biomass which is locally abundant. The production of fermentable sugars from lignocellulosic biomass, however, faces several challenges such as costs of pretreatment and enzymes. Another limitation is the availability of robust microbial communities capable of fermenting mixed sugars (hexose and pentose) to ethanol. Gasification of lignocellulosic biomass to produce a syngas followed by anaerobic fermentation to produce ethanol is a pioneering alternative method. Table 5 summarizes the performances of syngas fermentation to produce ethanol and acetate by *C. ljungdahlii* and *C. autoethanogenum*.

Enrichment of enough ethanol-producing biomass in a fermentor is the first task in the syngas fermentation process. Growth of *C. ljungdahlii* and *C. autoethanogenum* on solely syngas is extremely slow in comparison to growth on sugars with syngas supplement (Cotter *et al.,* 2008; Lee *et al.,* manuscript in progress). Yeast extract tended to favor the production of acetate over ethanol by *C. ljungdahlii*, removing yeast extract from a medium resulted in a 3-fold increase of ethanol production (Barik *et al.,* 1988; Berberich *et al.,* 2000). Phillips *et al.,* (1994) further developed a growth medium based on the elemental composition of *E. coli* for optimizing ethanol production in the *C. ljungdahlii* culture. With the designed medium, *C. ljungdahlii* could produce up to 23 g·l^{-1} ethanol and 27 g·l^{-1} acetate; the corresponding values were only 1.5 g·l^{-1} ethanol and 3.5 g·l^{-1} acetate in a basal medium of ATCC 1754 PETC in a STR with cell recycle (Phillips *et al.,* 1994). While *C. ljungdahlii* was able to maintain its metabolic activity with little (0.005%) to no yeast extract in the medium, the growth of *C. autoethanogenum* showed

dropped in medium completely deficient of yeast extract (Barik *et al.,* 1988; Cotter *et al.,* 2009). Investigation of the effects of nitrogen limitation in the medium has concluded that even though *C. ljungdahlii* could maintain its culture density in nitrogen limited medium with needed trace elements, vitamins and salts, it cannot produce ethanol and acetate under nitrogen limited medium (Cotter *et al.,* 2009). Similarly, *C. autoethanogenum* could not retain its culture density if the nitrogen was not provided in the medium (Cotter *et al.,* 2009). A further study on high ethanol production from metabolic activity is expected for the scale-up application of syngas fermentation.

In the syngas fermentation process, pH is also one of the critical control parameters. Previous studies suggest that higher ethanol production may be achieved by operating at a low pH environment, because the microbes would produce less acid which may prevent a further pH drop and thus result in higher ethanol production (Fordyce *et al.,* 1984; Datar *et al.,* 2004). Another study reported that ethanol may not be related to the cell growth and suggested that high ethanol yield (over acetate) could be achieved by controlling the cells in the resting phase (Gaddy and Clausen, 1992; Klasson *et al.,* 1992). However, Cotter *et al.,* (2008) showed the opposite result that low ethanol and acetate production was exhibited in the resting cell phase during batch fermentation.

Microbial fermentation for alcohol production may produce volatile fatty acids as by-products. Bioactivity inhibition by these by-products may be a crucial factor in syngas fermentation. To overcome this problem, the authors' team has developed an innovative process (Fig. 3): syngas fermentation using hollow fiber membranes with simultaneous

recovery of acetate by amine-functionalized resin or absorbent. The process utilizes the enhanced syngas-liquid mass transfer feature of the HFM, and allows the amine-functionalized resin to recover acetate as a separate saleable product and at the same time to eliminate its inhibition effect on ethanol production (Lee *et al.,* manuscript in preparation).

6.2. Syngas fermentation for butanol production

Butanol is another biofuel which has a high potential to replace gasoline, either partially or completely. Compared to ethanol, butanol has higher energy content, but lower vapor pressure, hygroscopicity and corrosivity. Butanol is traditionally produced from a sugar fermentation process called the ABE (Acetone, Butanol, and Ethanol). The process is not economical due to the high cost of sugar. The alternative is to produce butanol using lignocellulosic wastes as raw material. Lignocellulosic materials may be first converted enzymatically into sugars which are then followed by the ABE process. However, the process requires extensive pretreatments for the lignocellulose, such as acid/alkaline lignin removal and enzymatic hydrolysis in order to produce fermentable sugars. On the other hand, butanol could also be produced from syngas fermentation by a new microbial specie: *Clostridium carboxidivorans* P7 (Liou *et al.,* 2005). Most of the studies conducted on this microbe were still limited mainly on the cell growth. Ahmed *et al.,* (2006) showed that tars and nitric oxide from biomass derived syngas had an adverse influence on *C. carboxidivorans* P7. A 4.5-liter syngas bubble column fermentor produced ethanol, butanol, and acetic acid with respective yields of 0.15, 0.075, and 0.025 mole of C for each mole of CO consumed (Rajagopalan *et al.,* 2002).

7. References

Amed, A., Cateni, B.G., Huhnke, R.L., Lewis, R.S. (2006) Effects of biomass-generated producer gas constitutes on cell growth, product distribution and hydrogenase activity of *Clostridium carboxidivorans* P7, *Biomass Bioeng*. 30, 665–672.

Barik, S., Prieto, S., Harrison, S.B., Clausen, E.C., and Gaddy, J.L. (1988) Biological production of alcohols from coal through indirect liquefaction, *Appl. Biochem. Biotechnol.* 28, 363–378.

Barik, S., Prieto, S., Harrison, S.B., Clausen, E.C., and Gaddy, J.L. (1990) *Bioprocessing and Biotreatment of Coal*, I[st] Ed. Wise, D. L., Chapter 8 'Biological production of ethanol from coal synthesis gas," (Marcel Dekker In., New York) 1231–1154.

Berberich, J.A., Knutson, B.L., Strobel, H.J., Tarhan, S., Nokes, S.E., and Dawson, K.A. (2000) Product selectivity shifts in *Clostridium thermocellum* in the presence of compressed solvent, *Ind. Eng. Chem. Res.* 39, 4500–4505

Bredwell, M.D., Srivastava, P., and Worden, R.M. (1999) Reactor design issues for synthesis gas fermentations, *Biotechnol. Prog*. 15, 834–844.

Charpentier, J.C. (1981). Mass transfer in gas-liquid absorbers and reactors, *Adv. Chem. Eng.* 11, 1–103.

Cotter, J.L., Chinn, M.S., and Grunden, A.M. (2009) Influence of process parameters on growth of *Clostridium Ljungdahlii* and *Clostridium autoetahanogenum* on synthesis gas, *Enzyme Microbial Technol.* 44, 281–288.

Cotter, J.L., Chinn, M.S., and Grunden, A.M. (2008) Ethanol and acetate production by *Clostridium ljungdahlii* and *Clostridium autoethanogenum* using resting cells, *Bioprocess Biosyst. Eng.* 32, 369–380.

Datar R.P., Shenkman, R.M., Cateni, B.G., Huhnke, R.L, and Lewis, R.S. (2004) Fermentation of biomass-generated producer gas to ethanol, *Biotechnol. Bioeng*. 86, 587–594

Diekert, G.B., and Thayer, R.K. (1982) Carbon monoxide oxidation by *Clostridium thermoaceticum* and *Clostridium formicoaceticum*, *J. Bacteriol.* 136, 597–606.

Do, Y.S., Smeenk, J., Broer, K.M., Kisting, C., Brown, R., Heindel, T.J., Bobik, T.A., and Dispirito, A.A. (2007) Growth of *Rhodospirillum rubrum* on synthesis gas: conversion of CO to H_2 and poly-beta-hydroxyalkanoate, *Biotechnol. Bioeng*. 97, 279–86.

Drake, H.L. (1994) *Acetogenesis,* 1st ed. (Chapman and Hall, New York).

du Preez, L.A., Opendaal, J.P., Maree, J.P., Ponsonby, M. (1992) Biological removal of sulfate from industrial effluents using producer gas as energy source, *Environ. Technol*. 13, 875–882.

du Preez, L.A., and Maree, J.P. (1994) Pilot-scale biological sulfate and nitrate removal utilizing producer gas and energy source, *Wat.. Sci. Technol*. 30, 275–285.

Fischer, C.R., Klein-Marcuschamer, D., and Stephanopoulos, G. (2008) Selection and optimization of microbial hosts for biofuels production, *Metabolic Eng*. 10, 295–304.

Fordyce, A.M., Crow, V.L., and Thomas, T.D. (1984) Regulation of product formation during glucose or lactose limitation in nongrowing cells of streptococcus, *Appl. Environ. Microbiol.* 48, 332–337.

Gaddy, J.L. and Clausen, E.C. (1992) US Patent 612:221

Genthner, B.R.S. and Bryant, M.P. (1987) Additional characteristics of one-carbon-compound utilization by *Eubacterium limosum* and *Acetobacterium woodii*, *Appl. Environ. Microbiol.* 53, 471–476.

Genthner, B.R.S. and Bryant, M.P. (1982) Growth of *Eubacterium limosum* with carbon monoxide as the energy source. *Appl. Environ. Microbiol.* 43, 70–74.

Grethlein, A.J., Worden, R.M., Jain, M.K., and Datta, R. (1991) Evidence for production of n-butanol from carbon monoxide by *Butyribacterium methylotrophicum*, *J. Ferment. Bioeng*. 72, 58–60.

Hedderich, R. (2004) Energy-converting [NiFe] hydrogenases from archaea and extremophiles: ancestors of complex I. *J. Bioenerg. Biomembr.* 36, 65–75.

Henstra, A.M., Sipma, J., Rinzema, A., and Stams, A.J.M. (2007) Microbiology of synthesis gas fermentation for biofuel production, *Current Option in Biotechnol.,* 18, 200–206.

Kapic, A., Jones, S.T., and Heindel, T.J. (2006) Carbon monoxide mass transfer in a syngas mixture, *Ind. Eng. Chem. Res*. 45, 9150–9155.

Kerby, R.L., Ludden, P.W., and Roberts, G.P. (1995) Carbon monoxide dependent growth of *Rhodospirillum rubrum*, *J. Bacteriol.* 177, 2241–2244.

Kim, S.H., Lee, P.H., Chang, H.I., and Sung, S. Carbon monoxide mass transfer characteristics of hollow-fiber membranes for syngas fermentation, manuscript in progress.

Klasson, K.T., Ackerson, M.D., Clausen, E.C. and Gaddy, J.L. (1992) Bioconversion of synthesis gas into liquid or gaseous fuels. *Enzyme Microbial Technol. 14*, 602–608.

Lee, P.H., Ni, S.Q., Choi, D.W., and Sung, S. pH effect on the growth of *Clostridium ljungdahlii* for ethanol production from syngas fermentation, manuscript in progress.

Lindahl P.A. (2002). The Ni-containing carbon monoxide dehydrogenase family: light at the end of the tunnel?. *Biochem*. 41, 2097–2105.

Liou, J.S.C., Balkwill, D.L, Drake, G.R., and Tanner, R.S. (2005) *Clostridium carboxidivorans* sp. nov., a solvent-producing clostridium isolated from an agricultural settling lagoon, and reclassification of the acetogen *Clostridium scatologenes* strain SL1 as *Clostridium drakei* sp. nov. *Int. J. Syst. Evol. Microbiol*. 55, 2085–2091.

Lynd, L., Kerby, R., Zeikus, J.G. (1982) Carbon monoxide metabolism of the methylotrophic acidogen *Butyribacterium methylotrophicum*, *J. Bacteriol*., 149, 255–263.

Maness, P. C., Huang, J., Smolinski, S., Tek, V., Vanzin, G. (2005) Energy generation from the CO oxidation-hydrogen production pathway in *Rubrivivax gelatinosus*, *Appl. Environ. Microbiol*. 71, 2870–2874.

Najafpour, G. and Younesi, H. (2006) Ethanol and acetate synthesis from waste gas using batch culture of *Clostridium ljungdahli*, *Enzyme Microbial Technol*. *38*, 223–228.

Phillips, J.R., Clausen, E.C., Gaddy, J.L. (1994) Synthesis gas as substrate for biological production of fuels and chemicals., *Appl. Biochem. Biotechnol*. 45, 145–157.

Ragsdale, S.W. (2004) Life with carbon monoxide, *Crit. Rev. Biochem. Mol. Biol*, 39, 165–195

Ragsdale, S.W. and Pierce, E. (2008) Acetogenesis and Wood-Ljungdahl pathway of CO_2 fixation, *Biochimica et Biophysica Acta* 1784, 1873–1898.

Riggs, S.S. and Heindel, T.J. (2006) Measuring carbon monoxide gas-liquid mass transfer in a stirred tank reactor for syngas fermentation, *Biotechnol. Prog*. 22, 903–906.

Rajagopalan, S., Datar, R.P., and Lewis, R.S. (2002) Formation of ethanol from carbon monoxide via a new microbial catalyst, *Biomass Bioenergy* 23, 487–493.

Selvaraj, P.T., Little, M.H., Bredwell, M.D., and Kaufman, E.N. (1996) Bioreactors for flue gas biodesulfurization using coal synthesis gas as feedstock. *Proc. American Insti. of Chem. Eng. Fall Annual Meeting.*, 10-15, 1996, (in Chicago, IL).

Shen, G.J., Shieh, J.S., Grethlein, A.J., Jain, M.K., and Zeikus, J.G. (1999) Biochemical basis for carbon monoxide tolerance and butanol production by *Butyribacterium methylotrophicum*, *Appl. Microbiol. Biotechnol.* 51, 827–832.

Singer S.W., Hirst, M.B., Ludden, P.W. (2006) CO-dependent H_2 evolution by *Rhodospirillum rubrum*: role of CODH:CooF complex, *Biochim. Biophys. Acta. – Bioenerg.* 1757, 1582–1591

Tanner, R.S., Miller, L.M., and Yang, D. (1993) *Clostridium ljungdahlii* sp. nov., an acetogenic species in clostridial ribosomal-RNA homology group-I. *Int. J. Syst. Bacteriol*. 43, 232–236.

Ungerman, A.J. and Heindel, T.J. (2007) Carbon monoxide mass transfer for syngas transfer for syngas fermentation in a stirred tank reactor with dual impeller configurations, *Biotechnol. Prog.* 23, 613–620.

van Houten, R.T., Hulshoff Pol, L.W., Lettinga, G. (1994) Biological sulfate reduction using gas-lift bioreactors fed with hydrogen and carbon dioxide as energy and carbon source, *Biotechnol Bioeng.* 44, 586–594.

Worden, R.M., Grethlein, A.J., Jain, M.K., and Datta, R. (1991) Production of butanol and ethanol from synthesis gas via fermentation, *Fuel* 70, 615–619.

Younesi, H., Najafpour G., Mohamed, A.R. (2005) Ethanol and acetate production from synthesis gas via fermentation processes using anaerobic bacterium, *Clostridium ljungdahlii*, *Biochem. Eng. J.* 27, 110–119.

Younesi, H., Najafpour G., Mohamed, A.R. (2006) Liquid fuel production from synthesis gas via fermentation process in a continuous tank bioreactor (CSTR) using Clostridium ljungdahlii, *Iranian J. Botechnol.* 4, 45–53.

Fig. 1. Schematics of the reductive acetyl-CoA/ Wood-Ljungdahl pathway (adopted from Henstra *et al.,* 2007). [a]Formate (HCOOH), [b]methylene-tetrahydrofolate (CH-THF), [c]methenyl-tetrahydrofolate (CH_2-THF), and [d]methyl-tetrahydrofolate (CH_3-THF) (adopted from Henstra *et al.,* 2007).
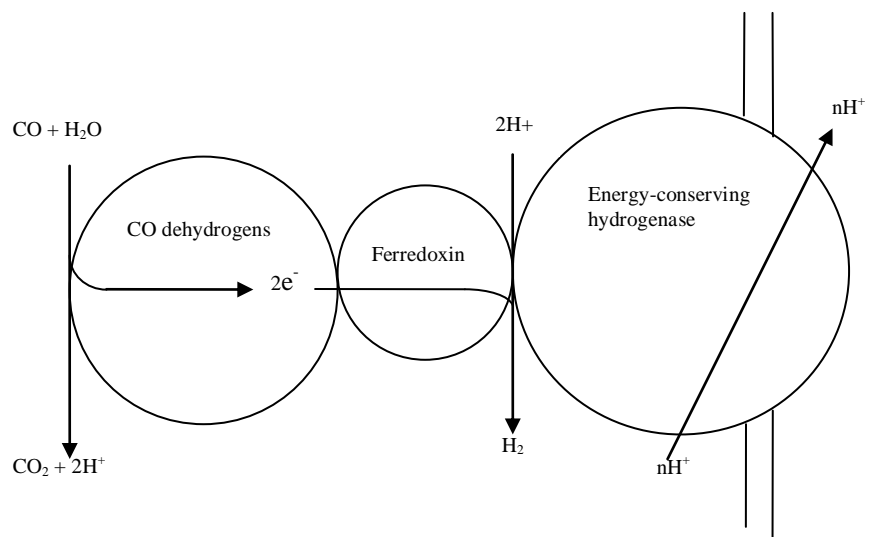
Fig.2. Schematics of membrane-bound CO-oxidizing, hydrogen-evolving enzyme complex of carboxydotrophic hydrogen (adopted from Henstra *et al.,* 2007).
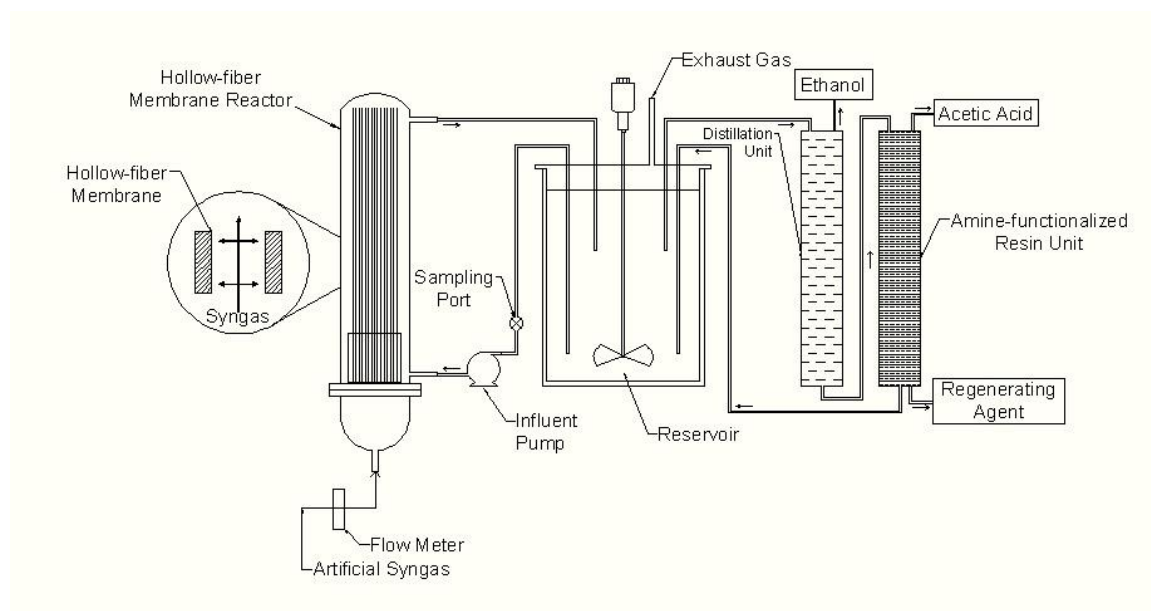
Fig. 3. Schematics of microporous hollow fiber membrane fermentor set-up.

Table 1. Theoretically Feasible Reactions Using CO, CO_2, and H_2 (adopted from Barik *et al.,* 1990).

Products	Equation	ΔG^o (kcal·mol^{-1})
Formic acid	$CO + H_2O \rightarrow HCOOH$	+5.57
	$CO_2 + H_2 \rightarrow HCOOH$	+10.35
Methanol	$CO + 2H_2 \rightarrow CH_3OH$	-9.14
	$CO_2 + 3H_2 \rightarrow CH_3OH + H_2O$	-4.35
Ethanol	$2CO + 4H_2 \rightarrow C_2H_5OH + H_2O$	-34.56
	$2CO_2 + 6H_2 \rightarrow C_2H_5OH + 3H_2O$	-24.99
Butanol	$4CO + 8H_2 \rightarrow CH_3(CH_2)_2CH_2OH + 3H_2O$	-80.0
	$4CO + 12H_2 \rightarrow CH_3(CH_2)_2CH_2OH + 7H_2O$	-60.86
	$12CO + 5H_2O \rightarrow CH_3(CH_2)_2CH_2OH + 8C_2O$	-116.16
Acetic acid	$CO + 2H_2 \rightarrow CH_3COOH$	-22.73
	$2CO_2 + 4H_2 \rightarrow CH_3COOH + 2H_2O$	-13.15
Propionic acid	$3CO + 4H_2 \rightarrow CH_3CH_2COOH + H_2O$	-44.65
	$3CO_2 + 7H_2 \rightarrow CH_3CH_2COOH + 4H_2O$	-30.29
Acetone	$3CO + 5H_2 \rightarrow CH_3COCH_3 + 2H_2O$	-53.55
	$3CO_2 + 8H_2 \rightarrow CH_3COCH_3 + 5H_2O$	-39.20

Table 2. Anaerobic carboxydotrophic microorganisms (adopted from Henstra *et al.,* 2007).

Species	T_{opt} (°C)	pH_{opt}	t_d (h)	Products
Mesophilic bacteria				
Clostridium antoethanogenum	37	5.8-6.0	n.a.	Acetate, ethanol
Clostridium ljungdahlii	37	6	3.8	Acetate, ethanol
Clostridium carboxidivprans P7	38	6.2	6.25	Acetate, ethanol, butyrate, butanol
Oxobacter pfennigii	36-38	7.3	13.9	Acetate, n-butyrate
Peptostreptococcus productus	37	7	1.5	Acetate
Acetobacterium Woodii	30	6.8	13	Acetate
Eubacterium Limosum	38-39	7.0-7.2	7	Acetate
Butyribacterium methylotrophicum	37	6	12-20	Acetate, ethanol, butyrate, butanol
Rubrivivax Gelatinosus	34	6.7-6.9	6.7	H_2
Rhodopseudomonas palustris P4	30	nr	23	H_2
Rhodospirillum rubrum	30	6.8	8.4	H_2
Citrobacter sp Y19	30-40	5.5-7.5	8.3	H_2
Mesophilic archaea				
Methanosarcina barkerkeri	37	7.4	65	CH_4
Methanosarcina acetivorans strain C2A	37	7	24	Acetate, formate, CH_4
Thermophilic bacteria				
Moorella thermoacetica	55	6.5-6.8	10	Acetate
Moorella thermoautotrophica	58	6.1	7	Acetate
Moorella strain AMP	60-65	6.9	n.a.	H_2
Carboxydothermus hydrogenoformans	70-72	6.8-7.0	2	H_2
Carboxydibrachium pacificus	70	6.8-7.1	7.1	H_2
Carboxydocella sporoproducens	60	6.8	1	H_2
Carboxydocella thermoautotrophica	58	7	1.1	H_2
Thermincola carboxydiphila	55	8	1.3	H_2
Thermincola ferriacetica	57-60	7.0-7.2	n.a.	-
Thermolithobacter carboxydivorans (Known as *Carboxydothermus restrictus R1*)	70	7	8.3	H_2
Thermosinus carboxydivorans	60	6.8-7.0	1.2	H_2
Desulfotomaculum Kuznetsovil	60	7	n.a.	Acetate, H_2S
Desulfotomaculum thermobenzoicum subsp. thermosyntrophicum	55	7	n.a.	Acetate, H_2S
Desulfotomaculum carboxydivorans	55	7	1.7	H_2, H_2S
Thermophilic archaea				
Methanothermobacter	65	7.4	140	CH_4
Thermococcus strain AM4	82	6.8	n.a.	H_2
Archaeoglobus fulgidus	83	6.4	n.a.	Acetate, formate, H_2S

n.a.: not available

Table 3. Oxygen gas-liquid mass transfer coefficients for different attached-growth reactors (Charpentier 1981; Bredwell *et al.,* 1999).

Reactor type	Gas void fraction (Gas volume/liquid volume)	K_La (h^{-1})
Packed columns		
Countercurrent	0.02-0.25	0.001-0.2
Cocurrent	0.60-0.98	0.001-2.8
Plate columns		
Bubble cap	0.10-0.95	0.027-0.56
Sieve plates	0.10-0.95	0.027-1.1
Bubble columns	0.60-0.98	0.014-0.67
Packed bubble columns	0.60-0.98	0.014-0.33
Tube reactors		
Horizontal and coiled	0.05-0.95	0.014-1.94
Vertical	0.05-0.95	0.056-2.8
Spray columns	0.20-0.95	0.002-0.042
Submerged and plunging jet	0.94-0.99	0.0008-0.017

Table 4. Syngas gas-liquid mass transfer coefficients for wastewater treatment and fermentation (adopted from Bredwell *et al.,* 1999**).**

Reactor type	Biological system	Feedstock	K_La (h^{-1})
Stirred tank -200 rpm	*B. methylotrophicum*	CO	14.2
Stirred tank -300 rpm	SRB mixed culture	Syngas mix	31 for CO
			75 for H$_2$
Stirred tank -300 rpm	*C. ljungdahlii*	Syngas mix	35 for CO
Stirred tank -300 rpm	*R. rubrum, M. formicum, M. barkeri*	Syngas mix	28.1 for CO
Stirred tank -450 rpm	*R. rubrum, M. formicum, M. barkeri*	Syngas mix	101 for CO
Stirred tank -200 rpm	*B. methylotrophicum*	CO	90.6 for CO
Stirred tank -300 rpm Microbubble sparging	SRB mixed culture	Syngas mix	104 for CO 190 for H$_2$
Packed-bubble column	*R. rubrum, M. formicum, M. barkeri*	Syngas mix	2.1
Trickle bed	*R. rubrum, M. formicum, M. barkeri*	Syngas mix	55.5
Trickle bed	SRB mixed culture	Syngas mix	121 for CO 335 for H$_2$
Trickle bed	*C. ljungdahlii*	Syngas mix	137 for CO

Table 5. Performances of syngas fermentation for ethanol and acetate production

Species	Reactor type	Feed stock	pH	Temp (^oC)	Medium	Maximum production	References
C. ljungdahlii	STR with cell recycle (13.5 l)	55% CO, 20% H_2, 10% CO_2, and 15% Ar (agitation rate: 300-500 ppm)	4.5	37	ATCC 1754 PETC medium	1.5 g·l⁻¹ ethanol 3.5 g·l⁻¹ acetate	Phillips *et al.*, 1994
C. ljungdahlii	CSTR with cell recycle (13.5 l)	55% CO, 20% H2, 10% CO2, and 15% Ar (flow rare: 14 ml·min-1, agitation rate: 300-500 rpm)	4.5	37	Designed medium based on *E. Coli*	23 g·l⁻¹ ethanol 27 g·l⁻¹ acetate	Phillips *et al.*, 1994
C. ljungdahlii	CSTR (20 l)	70% CO, 15% H_2, and 15% Ar (flow rare: 14 ml·min⁻¹, agitation rate: 550 rpm)	4.5	37	ATCC 1754 PETC medium (flow rate : 0.55 ml·min⁻¹)	11 g·l⁻¹ ethanol and acetate	Younesi *et al.*, 2006
C. ljungdahlii	Batch (125 ml)	55% CO, 20% H_2, 10% CO_2, and 15% Ar (Initial syngas pressure: 1.6 and 1.8 atm)	-	37	ATCC 1754 PETC medium	0.60 g·l⁻¹ ethanol 1.11 g·l⁻¹ acetate	Younesi *et al.*, 2005
C. ljungdahlii	Batch (163 ml)	55% CO, 20% H_2, 10% CO_2, and 15% Ar (Initial syngas pressure: 1.8 atm)	-	37	ATCC 1754 PETC medium	0.012 g·l⁻¹ ethanol 0.024 g·l⁻¹ acetate	Najafpour and Younesi, 2006
C.ljungdahlii (growth phase)	Batch (250 ml)	20% CO, 10% H_2, 20% CO_2, and 50% N_2 (flow rare: 7.5 ml·min⁻¹)	6.8	37	Modified reinforced Clostridial medium	0.23 g·l⁻¹ ethanol 2.10 g·l⁻¹ acetate	Cotter *et al.*, 2008
C.ljungdahlii (growth phase)	Batch (80 ml)	n.a.	6.8	37	Modified ATCC 1754 PETC medium	0.60 g·l⁻¹ ethanol 5.34 g·l⁻¹ acetate	Cotter *et al.*, 2009
C.ljungdahlii (resting phase)	Batch (80 ml)	n.a.	4.5	37	Modified nitrogen limitation medium	0.02 g·l⁻¹ ethanol > 0.06 g·l⁻¹ acetate	Cotter *et al.*, 2009
C. autoethanogenum (growth phase)	Batch (250 ml)	20% CO, 10% H_2, 20% CO_2, and 50% N_2 (flow rare: 10 ml·min⁻¹)	6.0	37	DSMZ 640	0.66 g·l⁻¹ ethanol 1.40 g·l⁻¹ acetate	Cotter *et al.*, 2008
C. autoethanogenum (growth phase)	Batch (80 ml)	n.a.	6.0	37	DSMZ 640 supplemented with 5 g·l⁻¹ xylose	0.24 g·l⁻¹ ethanol 2.40 g·l⁻¹ acetate	Cotter *et al.*, 2009
C. autoethanogenum (resting phase)	Batch (80 ml)	n.a.	6.0	37	Modified DSMZ 640	0.44 g·l⁻¹ ethanol 2.51 g·l⁻¹ acetate	Cotter *et al.*, 2009

CHAPTER 2. CARBON MONOXIDE MASS TRANSFER USING HOLLOW FIBER MEMBERANCE FOR SYNGAS FERMENTATION

Sang-Hyoun Kim, Po-Heng Lee, and Shihwu Sung

Department of Civil, Construction and Environmental Engineering,

Iowa State University, Ames, IA 50011, USA

Abstract

The mass transfer of carbon monoxide (CO) to liquid through hollow fiber membrane was examined for syngas fermentation in which gas transfer is regarded as limiting step. Hollow fiber membrane would be beneficial, as the membrane enabled higher CO mass transfer than previous studies. The maximum observed volumetric CO mass transfer coefficient of 0.107 s^{-1} was observed at 400 fibers, cross flow velocity of 2.20 cm·sec^{-1}, and specific gas flow rate of 1.02 min^{-1}. The mass transfer would be improved along with increasing cross flow velocity, specific gas flow rate, and fiber numbers.

1. Introduction

Fuel and chemical production from non-food biomass, such as lignocellusic biomass has received considerable interests. The typical conversion route of physicochemical and/or enzymatic hydrolysis followed by fermentation of the formed sugars, however, faces several challenges. These include high enzyme cost and unwanted by-products in

physicochemical hydrolysis (Henstra *et al.,* 2007). Furthermore, lignin composing 10-40% lignocellulose cannot be converted to sugars in any known hydrolysis method (Bredwell *et al.,* 1999). An alternative approach is gasification of biomass to syngas with subsequent conversion to fuels and chemicals. Carbon monoxide (CO) and hydrogen (H_2) in syngas are substrates for several microbial metabolisms, which can be exploited for the synthesis of various interesting products including ethanol and butanol (Henstra *et al.,* 2007). Syngas fermentation could offer several potential advantages over metal catalytic conversion, which include higher specificity of the biocatalyst and lower energy costs (Klasson *et al.,* 1992). However, the poor solubility of syngas in the aqueous phase (e.g. the solubility of CO is 77% that of oxygen) would limit the overall rate of syngas fermentation in a bioreactor using bubble sparging (Chang *et al.,* 2001; Kapic *et al.,* 2006; Henstra *et al.,* 2007).

Microporous hollow fiber membrane with a hydrophobic surface would enhance the gas-to-liquid mass transfer. The syngas fed to the inside of the hollow fiber membrane diffuses through the wall of the membrane and dissolves into the aqueous phase on the outside of membrane. The gaseous diffusion by membrane is known to be more efficient than bubble sparging in oxygen and H_2 transfer (Cote *et al.,* 1988; Ahmed *et al.,* 2004; Nerenberg and Rittmann, 2004). Mass transfer of CO, the most abundant and useful component in syngas, however, has not been reported yet using hollow fiber membrane. The objective of this study was to evaluate the performance of the hollow fiber membrane for CO transfer under different fiber numbers, water velocities, and specific gas flow rates.

2. Materials and Methods

Polypropylene hollow fiber membranes manufactured by C2L ENVIRONMENTAL MEMBRANE, LLC (Hangzhou, China) were used in this study. The outer diameter, wall thickness, porosity, and nominal pore size were 426 μm, 50 μm, 40%, and 0.2 μm, respectively. 100 to 400 fibers were potted into a Plexiglas insert (inner diameter of 1.90 cm) using Alumilite Regular (Alumilite Corp., Kalamazoo, MI). The length of fibers above the insert was controlled to be 25.0 cm. The other free ends of the fibers were heat-sealed. The insert with fibers was then combined to an external glass shell (inner diameter of 2.54 cm) as shown in Figure 1(a). The working volume of the hollow fiber membrane reactor was 0.13 L.

A schematic of CO transfer experimental setup is shown in Figure 1(b). The membrane reactor was connected to an artificial syngas supply and a reservoir. The artificial syngas was composed of 50.0% CO, 30% H_2, and 20% CO_2 (Ciferno and Marano, 2002). The 2.4-L reservoir was employed for liquid recirculation and CO mass transfer assay (Ahmed *et al.,* 2004). In the experiment, the membrane reactor and the reservoir were filled with distilled water. The water was re-circulated using a peristaltic pump (Masterflex I/P 7521-50, Cole-Parmer Inc., Vernon Hills, IL, USA) at a flow rate of 0.31 to 1.07 L/min providing cross flow velocity of 1.02 to 3.52 cm/sec in the membrane reactor. The reservoir was mixed at 90 rpm. Artificial syngas was transferred across the membrane at 35 to 140 ml/min (specific gas flow rate of 0.256 to 1.02 min^{-1}). The liquid samples were withdrawn through the septa in sampling port using 10-μL syringe

(Hamilton Gastight 1701). The experiment was performed at 35°C which would be adequate for typical syngas utilizing bacteria (Bredwell *et al.*, 1999).

Dissolved CO concentration was measured by CO-myoglobin assay with a spectrophotometer from Ocean Optics (model CHEMUSB2-VIS-NIR) and SpectraSolve software (Ames Photonics) (Kapic *et al.*, 2006). The CO transfer characteristics were then evaluated using the following equation (1) (Ahmed *et al.*, 2004).

$$\ln(\frac{C^*}{C^* - C}) = \frac{Q}{V}[1 - \exp(k_L a \frac{L}{v_L})]t$$

(1)

where C^* = aqueous phase CO concentration in equilibrium with the gas phase (mg/L), 456 in this study, C = measured dissolved CO concentration, Q = Liquid flow rate (L/min), V = reservoir volume (L), 2.4 in this study, k_L = CO mass transfer coefficient (cm/sec) in the hollow fiber membrane reactor, a = gas-liquid interfacial area in the hollow fiber membrane reactor (cm^{-1}), (fiber number) x 0.026 in this study, L = fiber length (cm), 25 in this study, v_L = cross flow velocity in the hollow fiber membrane reactor (cm/sec), t = time (sec).

3. Results

The dissolved CO concentrations in the reservoir plotted against the time collected during each test generated a linear relationship (R^2>0.90) according to equation (1) as shown in Figure 2, and the mass transfer coefficient was derived from the slope. Table 1 summarizes the CO volumetric mass transfer coefficient ($k_L a$) data observed in this study.

Assuming CO was transferred through all the pores in the hollow fiber membrane (Ahmed *et al*., 2004), mass transfer coefficient, k_L, could be separated from the k_La. The relationship between the cross flow velocity, the specific gas flow rate, and the CO mass transfer coefficient was derived as a two-full quadratic equation (2).

$$(k_L) = 0.0462 + 0.00665v_L - 0.0272q_{gas}$$
$$- 0.00160(v_L)^2 - 0.000536(q_{gas})^2 + 0.0189(v_L)(q_{gas})$$
$$(R^2 = 0.7009, F = 3.7489) \tag{2}$$

where q_{gas}= specific gas flow rate (min^{-1}). The calculated values of F was higher than $F_{0.05,5,14}$ = 2.96 (table value), which meant a statistically significant regression was obtained. Figure 3 illustrates that the CO mass transfer coefficient increases with rising cross flow velocity and gas flow rate.

4. Discussion

The maximum observed volumetric mass transfer coefficient (k_La), 0.107 s^{-1} at 400 fibers, a cross flow velocity of 2.20 cm·sec^{-1}, and specific gas flow rate of 1.02 min^{-1}, was higher than reported values for CO mass transfer as shown in Table 2. The gaseous diffusion, direct CO transfer from membrane pore to water would result in the efficient mass transfer (Cote *et al.,* 1988). As gas-to-liquid mass transfer is typically the rate-limiting factor in syngas fermentation, the enhanced mass transfer using hollow fiber would provide improved productivity and yield (Henstra *et al.,* 2007).

CO mass transfer would be increased as increasing cross flow velocity, specific gas flow rate, and fiber numbers. The curves of mass transfer coefficient (k_L) in Figure 3, which is dependent on fiber numbers, had the shape of a ridge system for both cross flow velocity

and specific gas flow rate in the tested ranges. Shear flow of liquid would improve gas-to-liquid mass transfer by mitigating resistance of the stagnant water layer on the membrane surface (Cote *et al.,* 1998). Gas flow is regarded to reduce the liquid film thickness, which determines gas-to-liquid mass transfer (Lemoine *et al.,* 2004). Higher cross flow velocity and/or specific gas flow rate could yield better volumetric mass transfer coefficient than observed in this study. It should be considered, however, that excessive cross flow velocity and gas flow rate would result in over-consumption of operating power and the loss of feedstock gas respectively. The cross flow velocity range in this study (1.02 to 3.52 cm/sec) was 3 to 8-fold lower than the value (9.5 cm/sec) in a hollow fiber membrane reactor for H_2 delivery (Nerenberg and Rittmann, 2004), while the specific gas flow rate range (0.256 to 1.02 min^{-1}) was similar to that (0.71 to 2.14 min^{-1}) of a CSTR for syngas transfer (Kapic *et al.,* 2006). Since it was regarded that all the pores in the hollow fibers were substantially used for the gaseous diffusion, increase of fiber numbers would also increase CO mass transfer. The data obtained at a same cross flow velocity and specific gas flow rate shown in Table 1 also prove it. However, too many fibers might cause clogging and channeling, because biofilm would be formed in syngas fermentation using the hollow fiber membrane. Packing factor (volume of membranes/volume of reactor) of this study was 2.8 to 12.7%, which is comparable to 7.0% of the reported value (Nerenberg and Rittmann, 2004).

5. References

Ahmed T, Semmens MJ, Voss MA (2004) Oxygen transfer characteristics of hollow-fiber, composite membranes. Adv Environ Res 8: 637-646.

Bredwell MD, Srivastava P, Worden RM (1999) Reactor design issues for synthesis-gas fermentations. Biotechnol Prog 15: 834-844.

Chang IS., Kim BH, Lovitt RW, Bang JS (2001) Effect of CO partial pressure on cell-recycled continuous CO fermentation by *Eubacterium limosum* KIST612. Process Biochem 37: 411-421.

Cote PL, Bersillon J-L, Huyard A (1988) Bubble-free aeration using membranes: Mass transfer analysis. J Membrane Sci 47: 91-106.

Ciferno JP, Marano JJ (2002) Benchmarking biomass gasification technologies for fuels, chemicals and hydrogen production. Prepared for US Department of Energy, National Energy Technology Laboratory.

Henstra AM, Sipma J, Rinzema A, Stams AJM (2007) Microbiology of synthesis gas fermentation for biofuel production. Curr Opin Biotechnol 18: 200-206.

Nerenberg R, Rittmann BE (2004) Hydroge-based, hollow-fiber membrane biofilm reactor for reduction of perchlorate and other oxidized contaminants. Water Sci Technol 49(11-12): 223-230.

Lemoine R, Behkish A, Morsi B (2004) Hydrodynamic and mass-transfer characteristics in organic liquid mixtures in a large-scale bubble column reactor for the toluene oxidation process. Ind Eng Chem Res 43: 6195-6212.

Kapic A, Jones ST, Heindel TJ (2006) Carbon monoxide mass transfer in a syngas mixture. Ind Eng Chem Res 45: 9150-9155.

Klasson KT, Ackerson MD, Clausen EC, Gaddy JL (1993) Biological conversion of coal and coal-derived synthesis gas. Fuel 72: 1673-1678.

Figure 1. Schematic diagram of experimental setup. (a) Hollow fiber membrane reactor, (b) CO transfer experiment
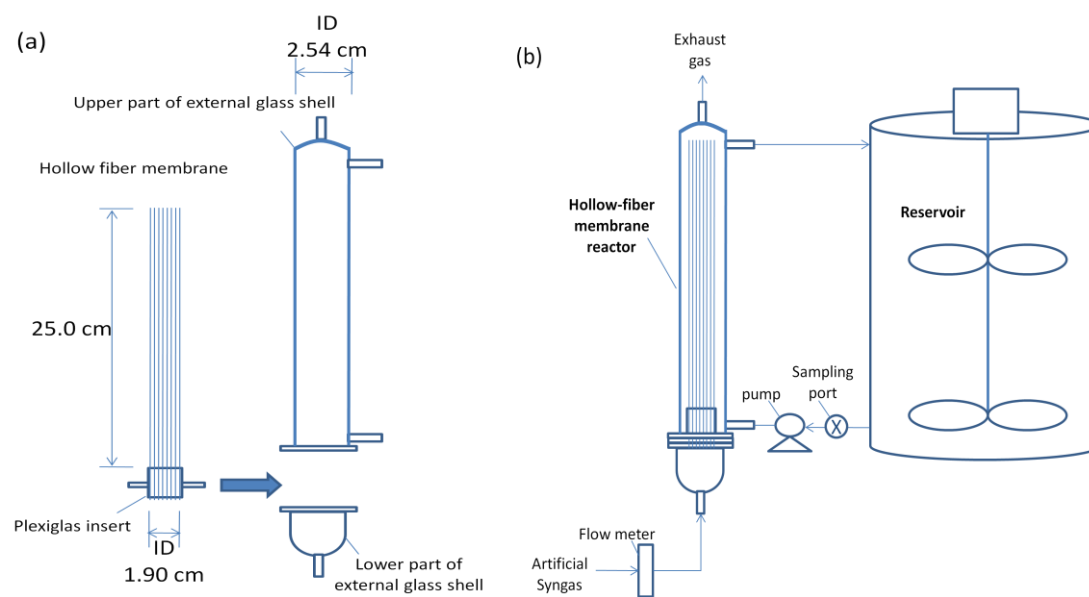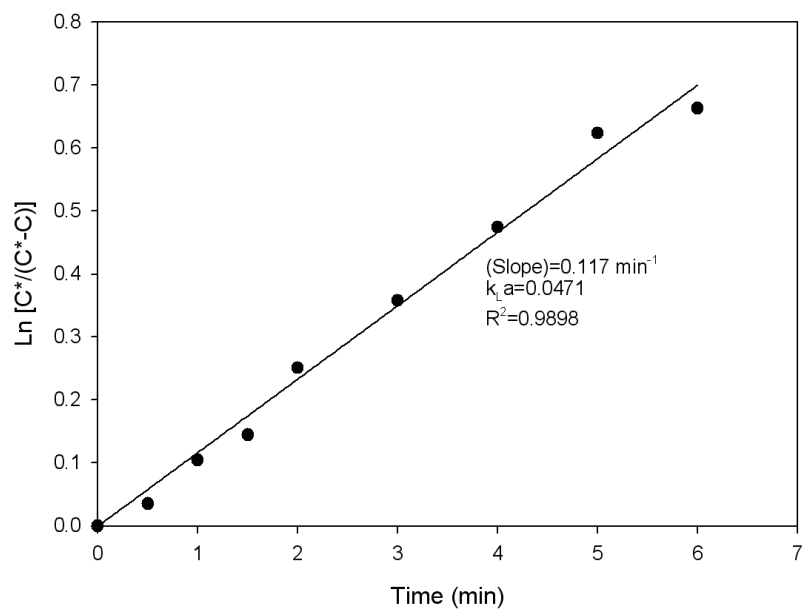
Figure 2. Dissolved CO concentration according to time at the fiber number, cross flow velocity, and specific gas flow rate of 350, 2.20 cm·sec^{-1}, and 0.511 min^{-1}, respectively.
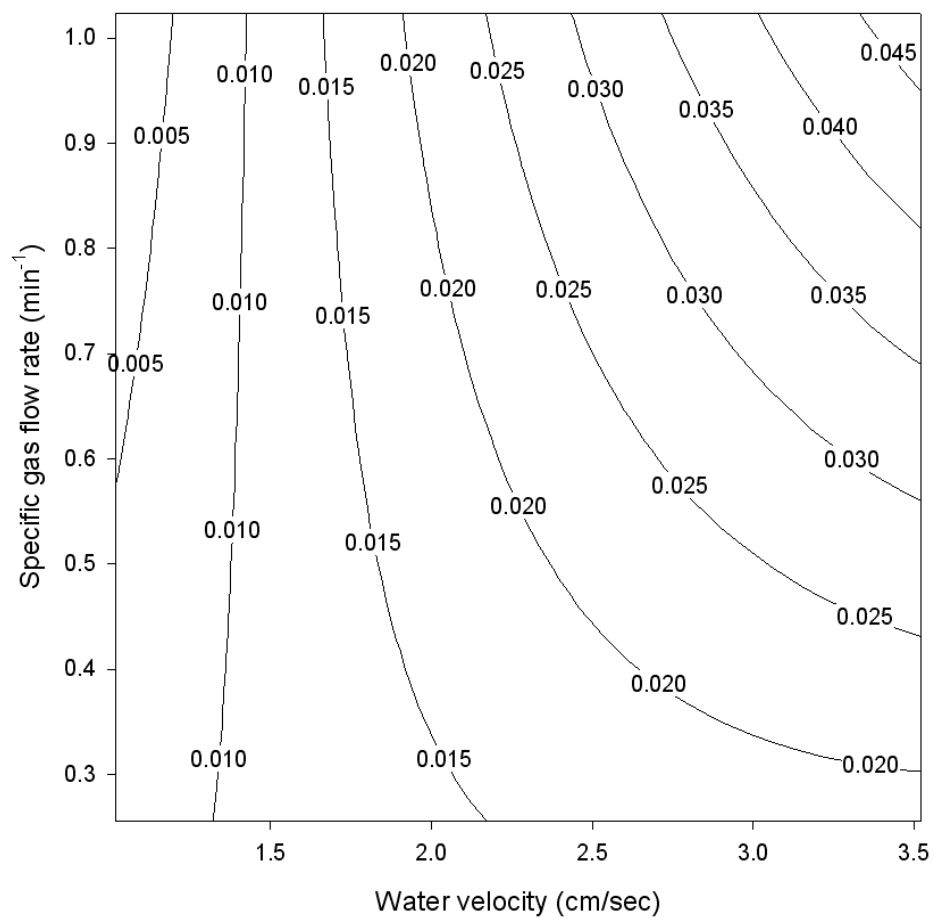
Figure 3. Contour lines of constant mass transfer coefficient (k_L, cm·sec^{-1}) versus cross flow velocity (v_L, cm·sec^{-1}) and specific gas flow rate (q_{gas}, min^{-1}).

Table 1. CO volumetric mass transfer coefficient (k_La) in the hollow fiber membrane reactor

Fiber no.	Cross flow velocity (cm·sec^{-1})	Specific gas flow rate (min^{-1})	k_La (s^{-1})
100	1.02	0.256	0.00586
100	1.38	0.256	0.00932
100	1.55	0.256	0.0162
100	2.20	0.256	0.0170
100	3.52	0.256	0.0182
100	2.20	0.512	0.0178
100	2.20	1.02	0.0249
200	2.20	1.02	0.0314
250	2.20	0.256	0.0290
250	2.20	0.767	0.0679
250	2.20	1.023	0.0787
350	2.20	0.511	0.0471
400	2.20	1.02	0.1070
450	1.38	1.02	0.0400

Table 2. Comparison of the maximum k_La values for CO mass transfer

Reactor type	Specific gas flow rate (min^{-1})	k_La (s^{-1})	Reference
Hollow fiber membrane reactor	1.02	0.107	This study
CSTR	2.14	0.082	Kapic *et al.,* 2006
Trickle bed[a]	-	0.095	Bredwell *et al.,* 1999
Bubble column	0.4	0.05	Chang *et al.,* 2001

[a]Shown at a table in the review paper without a specific reference

CHAPTER 3. ENHANCEMENT OF CARBON MONOXIDE MASS TRANSFER BY HOLLOW FIBER MEMBRANE

A paper to be submitted to Journal of Membrane Science

Po-Heng Lee, Sang-Hyoun Kim, Shouqing Ni, and Shihwu Sung

Department of Civil, Construction and Environmental Engineering,

Iowa State University, Ames, IA 50011, USA

Abstract

Synthesis gas (syngas) fermentation, in which gas transfer is regarded as a limiting step, is one of the alternative renewable energy processes. The mass transfer rates of carbon monoxide (CO) to liquid through a microporous polypropylene hollow fiber membrane and nonporous silicone hollow fiber membrane (HFM) were examined in this study for improving CO-liquid mass transfer in the syngas fermentation process. The study was conducted using a statistical experimental design: Box-Behnken design to determinate the significant operational parameters (water recirculation velocity, specific gas flow rate, and mixing power input per volume) and to fit a model for full-scale applications. The highest CO mass transfer rate of 1.49 s^{-1} was obtained using the microporous polypropylene HFM; this value is over its counterpart (nonporous silicone HFM) and previous studies. A model was calculated for commercialization of syngas fermentation.

1. Introduction

Seeking an alternative energy source for replacing fossil fuels is a critical subject in today's society. Biomass, which is an abundant resource, has the potential to serve as feedstock for replacing petroleum-based products and for generating transportation fuels and commercial chemicals. Synthesis (syngas) fermentation, one of the biomass conversion technologies for the products described above, offers cost and efficiency advantages [1, 2]. Syngas derived from the gasification of biomass is a gaseous mixture of carbon monoxide (CO), hydrogen (H_2), carbon dioxide (CO_2) and a variety of trace gases. The low solubility of carbon monoxide and hydrogen into the aqueous fermentation medium for the microorganisms, however, limits the potential commercialization. The fermentor design for the improvement of synags-liquid mass transfer is, thus, the dominating key to determine the production of syngas fermentation.

Stirred–tank reactors (STRs), which are commonly used in the fermentation industry, have been extensively applied in the syngas fermentation process [3]. A 7-liter CSTR fermentor equipped with a six-bladed rushton impeller by stirrer speeds and CO gas (99.99% pure) at the flow rates ranging 200-600 rpm and 1-6 L/min was carried out in the lab, and the result of its CO mass transfer rates were from 0.003 to 0.043 s^{-1} [4]. A syngas composition of 20% CO, 18% CO_2, 52% N_2, and 10% H_2 was tested to determine the CO gas-liquid mass transfer rates in the same 7-liter working volume reactor by the same impeller. CO gas-liquid mass transfer rates ranged from 0.02 to 0.08 s^{-1} were reported with stirrer speeds of 400-700 rpm and syngas flow rates of 5-15 L/min [5]. To increase the CO mass transfer rates in the CSTRs, the impeller configurations play an

essential role. Six impellers were examined to determine the CO gas-liquid mass transfer in the same reactor of 7-liter working volume. Dual impeller schemes showed the highest CO gas-liquid mass transfer performance with the most economical power consumption among all of these tested impellers [6]. Nevertheless, increasing the agitation speed of the full-scale fermentor's impellers results in higher energy consumption and causes negative impact on shear-sensitive microorganisms [6, 7]. Also, un-dissolved CO gas, which could not be used for CO-utilizing microorganisms, in a syngas fermentator is wasted to the exhausted line. It therefore reduces the substrate utilization rate, reducing its application attraction economically.

CO mass transfer rates in the fermentor within the CO utilizing microorganisms would be higher than that without CO utilizing ones, because soluble CO in the bulk solution would be consumed by the microorganisms resulting in more gaseous CO dissolving into bulk solution. Improved syngas-liquid mass transfer efficiency in the syngas fermentation process resulting from higher biomass retention is expected. In reality, the CO mass transfer reactor design which considers the microorganisms within the syngas fermentation processes would be more valuable in the industrial application. A tricked bed reactor and a STR at different cell recycle rates were conducted for the comparison of their individual CO mass transfer rates with the presence of a CO utilizing bacterium, *Rhodospirillum rubrum* [8]. Another similar study with the same microorganism in a STR was carried out. CO mass transfer rates of 13 to 35 h^{-1} were obtained with the agitation speeds of 300 to 700 rpm [9]. A review article was targeted to overview various reactor configurations, which could be divided into the attached packed and suspended

growth categories. In general, higher CO mass transfer rates of the attached growth processes over suspended ones were concluded [10]. Besides reactor designs, the operating parameters, including temperature, CO partial pressure, and specific gas velocity, affecting CO mass transfer rates and biomass density were also evaluated in a slurry bubble column and in a bubble column [11, 12].

Using a gas permeable hollow fiber membrane (HFM) as an oxygen and hydrogen delivery diffuser has been evaluated in water and wastewater treatment processes [13, 14, 15]. Two types of membranes, microporous polypropylene membrane and nonporous silicone membrane, were commonly used for oxygen transfer studies in water and wastewater treatment applications [13]. HFM membranes have the characteristic of high surface area, resulting in an optimal small footprint reactor for fermentation [13, 16]. HFM, therefore, could be utilized in syngas delivery systems to improve low solubility of carbon monoxide to resolve the bottleneck of syngas fermentation [16, 17]. Kim *et al.,* identified the fiber number of hollow fiber membrane as the most significant parameter affecting CO mass transfer rate over two other parameters, i.e. cross flow velocity and specific gas flow [17]. However, besides the parameter of the hollow fiber membrane surface area, other energy-consuming operational parameters, such as water recirculation velocity, specific gas flow rate, and mixing speed (power input for mixing per volume), have not yet been studied systemically in the HFM reactor for syngas fermentation.

The aim of this study was to examine CO mass transfer from two typical kinds of membranes (microporous polypropylene hollow fiber membrane and nonporous silicone

hollow fiber membrane) to determine which one could have better performance. The Box-Behnken method, a statistical experimental design method, was used to define a simplified model to investigate the operational parameters of water recirculation velocity, specific gas flow rate, and power input per working volume for mixing and their effects on CO mass transfer performance. The model should be used to design the full-scale HFM reactors for syngas fermentation.

2. Materials and methods

2.1. Membrane module

Microporous polypropylene hollow fiber membrane by C2L Environmental Membrane, LLC (Hangzhou, China) and nonporous silicone hollow fiber (silicone-rubber type) by Fuji System Corporation (Tokyo, Japan) were investigated for CO mass transfer study. The outer diameter, wall thickness, porosity, and nominal pore size of microporous polypropylene HFM were 426 μm, 50 μm, 40%, and 0.2 μm, respectively. The outer diameter and wall thickness of the other membrane (nonporous silicone HFM) were 400 μm and 50 μm, respectively. The length of each working membrane fiber was 25.0 cm. One end of the fibers was opened, and the other free end of the fibers was heat-sealed. 400 fibers of both membranes were potted into a Plexiglas insert (inner diameter of 1.90 cm) using Alumilite Regular (Alumilite Corp., Kalamazoo, MI), set into the membrane modules (Figure 1 (a)). The membrane fiber modules were then combined with an external glass shell (inner diameter of 2.54 cm) as shown in Figure 1(b). The working volume of the hollow fiber membrane reactor was 0.13 L. These two membrane fiber modules were dimensionally identical and were both fit into the same external glass shell.

A schematic of CO transfer experimental setup is shown in Figure 1 (c). The membrane reactor was connected to an artificial syngas supply and a reservoir with a working volume of 2.4 L. The artificial syngas was composed of 50.0% CO, 30% H_2, and 20% CO_2 (Ciferno and Marano, 2002). The reservoir was employed for water recirculation and CO mass transfer assay [13]. In the experiment, the membrane reactor and the reservoir were filled with distilled water. The water was re-circulated using a peristaltic pump (Masterflex I/P 7521-50, Cole-Parmer Inc., Vernon Hills, IL, USA) at a flow rate of 0.27 to 1.07 L/min corresponding to the water recirculation velocity of 0.89 to 3.52 cm/sec in the membrane reactor. The reservoir was mixed between 70 rpm to 250 rpm, which was converted to the ungassed power input per unit volume (Pg/V) of from 5.2×10^{-11} to 1.67 $W \cdot m^{-3}$. The ungassed power input (P_u) was not measured. It could be expressed as follow [18]:

$$\frac{Pu}{V} = \frac{(Po\rho n^3 D^5)}{\pi T^2 (\frac{H}{4})} \quad (1)$$

Where P_o is the power number for a six-bladed Rushton impeller (W), 4.75 in this study, ρ is the water density (kg/m^3), D is the impeller diameter (m), T is the reactor diameter (m), n is the mixing speed (rps), and H is the height of the water level in the reservoir (m).

Artificial syngas was transferred across the membrane at 25 to 170 ml/min^{-1} (specific gas flow rate of 0.19 to 1.35 min^{-1}) into water in the membrane reactor. Then, the exhaust was vented from the top of the membrane reactor. To monitor the CO concentration gradient with time, the water samples were withdrawn through the septa in sampling port

using 10-µL syringe (Hamilton Gastight 1701). The experiment was operated at 35°C which was adequate for thermophilic syngas utilizing bacteria [4].

2.2. Measuring Dissolved CO Concentrations

Dissolved CO concentration was measured by CO-myoglobin assay with a spectrophotometer from Ocean Optics (model CHEMUSB2-VIS-NIR) and SpectraSolve software (Ames Photonics) [5]. Myoglobin was purchased through Sigma-Aldrich with 90% purity and is derived from horse heart as lyophilized powder. Samples were prepared in a 1.5 mL nominal volume semi-micro special optical glass cuvettes. These cuvettes have a 10 mm path length and are usable for wavelengths in the range 320-2500 nm. The dissolved CO concentrations in the liquid samples were obtained spectrophotometrically using a Cary-50 Bio spectrophotometer from Varian (Mulgrave, Victoria, Australia). The peak for myoglobin is obtained at a wavelength of 423 nm. The spectrophotometer is therefore setup to measure light absorption in the wavelength of ranging from 400 to 700 nm. The CO concentrations were determined by the measured peak areas [7].

The CO transfer rate characteristics were then evaluated using the following equation (2) [13].

$$ln\left(\frac{c^*}{c^*-c}\right) = \frac{Q}{V}\left[1 - exp\,(k_L a \frac{L}{V_L})\right]t \qquad (2)$$

where C^* = aqueous phase CO concentration in equilibrium with the gas phase (mg/L), 456 in this study, C = measured dissolved CO concentration (mg/L), Q = water recirculation flow rate (L/min), V = reservoir volume (L), 2.4 in this study, k_L = CO mass transfer coefficient (cm/sec) in the hollow fiber membrane reactor, a = gas-water interfacial area in the hollow fiber membrane reactor (cm^{-1}), L = fiber length (cm), 25 in this study, v_L = water recirculation velocity in the hollow fiber membrane reactor (cm/sec), t = time (sec).

2.3. Experimental design

Three variables, water recirculation velocity (V_L, cm·s^{-1}), specific gas flow rate (V_g, min^{-1}), and mixing power input per volume (P_u/V, W·m^{-3}), will be surveyed at three levels using Box-Behnken design. The variable levels have been chosen under the conditions of the practical ranges (Table 1 shows the variables and their respective levels for this membrane study). The list of the experimental runs based on Table 1 is shown in Table 2. The experimental combination of variables was selected at random by the JMP statistical software. Experimental runs 2, 3, and 12 (Table 2) are the central variable points; these runs have been repeated three times for calculating errors (mean and standard deviation) based on the Box-Behnken design. The Box-Behnken design among the response surface designs allows the estimation of an empirical second-order model shown below:

$$y = b_0 + b_1 x_1 + b_2 x_2 + b_3 x_3 + b_{11} x_1^2 + b_{22} x_2^2 + b_{33} x_3^2 + b_{12} x_1 x_2 + b_{13} x_1 x_3 + b_{23} x_2 x_3$$

(3)

Where x_i are the variables, y is the response, b_o is the constant term (intercept parameter), b_1, b_2, and b_3 are single factor effects, b_{11}, b_{22}, and b_{33} are quadratic terms, and b_{12}, b_{13}, and b_{23} are interaction effect terms.

The Box-Behnken design experimentations, statistical data analysis, and graphics in this study were conducted using the statistical software package JMP[TM] version 8.0.1 (©SAS Institute Inc., Cary NC).

3. Results and Discussion

3.1. Summary of the experimental results

Table 3 shows the experimental results of the CO-liquid mass transfer coefficients on the performances of two membranes using an experimental method: Box-Behnken design. The experimental errors are evaluated on the basis of the experimentation runs 2, 3, and 12, the three repetitions of the center point of the design. They are expressed by the K_La standard deviations of 0.0105 for the microporous polypropylene HFM and 0.0053 for the nonporous silicone HFM, respectively. The highest CO-liquid mass transfer coefficient for the polypropylene HFM was 1.49 s^{-1} at run 10 with the operating conditions of 0.89 cm/s (V_L), 0.77 min^{-1} (V_g), and 75.70 W·m^{-3} (P_u/V), while the highest mass transfer coefficient for the silicone HFM was 1.05 s^{-1} at run 7 with the operating conditions of 0.89 cm/s (V_L), 1.35 min^{-1} (V_g), and 38.69 W·m^{-3} (P_u/V). It reveals that the microporous polypropylene HFM has a better performance on CO-liquid mass transfer over the nonporous silicone HFM. Since the nonporous silicone membrane transfers CO gas only by gaseous diffusion. The microporous polypropylene HFM, however, could

break down CO gas into micron size bubbles through the pores of the microporous polypropylene HFM, and its CO-liquid mass transfer is not only limited by the gaseous diffusion. On the other hand, the higher syngas supply by the microporous polypropylene HFM may not result in the higher mass transfer rate, because the micron size CO bubbles which are diffused from the microporous polypropylene HFM could be further dissolved into the bulk solution by convection from the recirculation pump and mixing from the mixer. Furthermore, the micron size CO bubbles from the microporous polypropylene HFM increase the contact surface area, indirectly improving the CO-liquid mass transfer performance. Thus, the performance of the microporous polypropylene HFM CO-liquid mass transfer is better than the CO-liquid mass transfer of the silicone HFM. The same outcome of the better performance of the microporous HFM over the nonporous silicone HFM as a gas delivery system also was found in the oxygen transfer study [19].

For syngas fermentation, the un-dissolved CO bubbles in the traditional stirred-tank reactors are usually wasted into the exhausted vent, because the low solubility of CO results in increasing the syngas supply. Using HFM as a gas delivery system could eliminate the CO-liquid mass transfer limitation so that it decreases the amount of the un-dissolved CO bubbles into the exhausted vent. It thus improves the syngas fermentation productivity.

3.2 Fitted models

The experimental results were evaluated by an empirical second-order model shown in eq. (3). A summary of the regression coefficients is listed in Table 4 and 5 for the microporous polypropylene HFM and nonporous silicone HFM, respectively. For the experimental results of the microporous polypropylene HFM, the coefficients of b_2, b_3, and b_{12}, which are V_g, P_u/V, and $V_L \cdot V_L$ in coded variables, are the three largest in the model. These coefficients (V_g, P_u/V, and $V_L \cdot V_L$) are significant to the 90% confidence level. However, the coefficient of b_1 corresponding to V_L in the coded variables has a negative impact to the 95% confidence level in the model. For nonporous silicone HFM, the results of the fitted model show the same trend of its counterpart, the polypropylene HFM. However, the coefficients of the nonporous silicone HFM fitted model are smaller. The F test has been used to evaluate the two membrane models. p-values calculated from the ratio of lack-of-fit and the pure error are given as 0.0014 for the microporous polypropylene HFM and 0.0003 for the nonporous silicone HFM, respectively. Because the p-values are small and F values are big, these two models are statistically satisfied.

The response surfaces are plotted as Fig. 2 for K_La. These graphs represent the effect of two variables (specific gas flow rate and liquid velocity) at their studied range with one maintained variable, P_u/V, at its zero level. The CO-liquid mass transfer rate was found to increase with decreased water recirculation velocity and specific gas flow rate on both of the two HFMs. From Fig. 2 (a) and (b), the higher CO-liquid mass transfer rates for both of the HFMs were obtained when V_L was at the minimum point and V_g was at the maximum point within the range studied. This result was consistent at the three levels of P_u/V within the range tested.

3.3. Interaction plots

The interaction profile on the CO-liquid mass transfer tests for these two membranes is presented in Figs. 3 (a) and (b). Both of the results for the two membranes represent a similar trend. In both of the interaction plots, evidence of interaction between V_g vs P_u/V shows as parallel lines. However, the interactions between V_L vs P_u/V and V_L vs V_g show nonparallel relationship. In the V_L vs P_u/V and V_L vs V_g plots, the CO-mass transfer efficiency decreases with increasing of V_L regardless of the P_u/V and V_g values. It shows that V_L is the predominant parameter over the others. In the V_g vs P_u/V and V_g vs V_L plots the effect of V_g is positive toward the CO-liquid mass transfer rate at the low values of V_L. Similarly, in the P_u/V vs V_g and P_u/V_g vs V_L plots the P_u/V plays a positive effect on the CO-liquid mass transfer rate at the low values of V_L. The interaction of V_L with P_u/V and V_g tends to mask the effect of V_L as a main effect

3.4. Contour plots

The contour plots of V_L vs V_g at three levels of P_u/V obtained from the experimental results are shown in Figs. 4 and 5. The results of these two membranes showed that V_L has negative effect toward the CO-liquid mass transfer efficiency, while P_u/V is over the level of zero (power input pre working volume of 38.69 $W \cdot m^{-3}$). In general, the optimal parameters in terms of CO mass transfer efficiency for syngas fermentation are at the V_L of 1.0 $cm \cdot s^{-1}$ and the V_g of 1.25 min^{-1}, regardless of P_u/V. The highest CO-mass transfer coefficients (K_L) are predicted as 1.75 for the polypropylene HFM and 1.50 for the silicone HFM, respectively.

4. Conclusion

Evaluation of the CO-liquid mass transfer rates in a microporous polypropylene HFM and a nonporous silicone HFM reactors were conducted using a myoglobin protein method. The maximum observed volumetric mass transfer coefficients (k_La) were 1.4912 s^{-1} for the polypropylene HFM at Run 10 (recirculation velocity of 0.89 cm/sec, specific gas flow rate of 0.77 min^{-1}, and power input pre working volume of 75.70) and 1.0549 for the silicone HFM at Run 7 (recirculation velocity of 0.89 cm/sec, specific gas flow rate of 1.35 min^{-1}, and power input pre working volume of 38.69 $W{\cdot}m^{-3}$). These values were higher than the reported values of CO mass transfer as shown in Table 6. For a microporous polypropylene HFM, the CO gaseous mass transfer from membrane pore to water would require higher agitation speed to mix microporous CO gases for researching the highest mass transfer rate. For the nonporous silicone HFM, the CO mass transfer is only dependent on diffusion, so the highest CO mass transfer rate results from the highest specific gas transfer rate. Since the optimal condition of the CO mass transfer rate in the microporous polypropylene is not only relient on the gas supply parameter (the gas specific velocity), the microporous HFM syngas fermentor could improve the transfer rate by agitation. Because the energy consumption in the microporous HFM is much less than the energy consumption in the nonporous HFM, the enhanced mass transfer using the microporous HFM would provide better productivity and less energy consumption over other syngas fermentors.

Acknowledgement

5. Nomenclature

a: gas-liquid interfacial area in the hollow fiber membrane reactor, cm^{-1}

b_o: the constant term (intercept parameter)

b_1, b_2, and b_3: the single factor effects

b_{11}, b_{22}, and b_{33}: the quadratic terms

b_{12}, b_{13}, and b_{23}: the interaction effect term

C^*: aqueous phase CO concentration in equilibrium with the gas phase, $mg \cdot L^{-1}$

C: measured dissolved CO concentration, $mg \cdot L^{-1}$

D is the impeller diameter (m)

H: the height of the water level in the reservoir, m

k_L: CO mass transfer coefficient, $cm \cdot sec^{-1}$

L: fiber length, cm

n: the mixing speed, rps

P_o: the power number for a six-bladed Rushton impeller, W

P_u: the ungassed power input for a six-bladed Rushton impeller, W

Q: Liquid flow rate, $L \cdot min^{-1}$

T: the reactor diameter, m

t: time, sec

V: reservoir volume, L

v_L: cross flow velocity in the hollow fiber membrane reactor, $cm \cdot sec^{-1}$

x_i: the variables

y: the response

ρ: the water density, $kg \cdot m^{-3}$

6. References

[1] R.M. Worden, M.D. Bredwell, A.J. Grethlein, Engineering Issues in Synthesis-Gas Fermentations, in: M.L. Sinnott, J. Woodward, (EDs), Fuels and Chemicals from Biomass, American Chemical Society, Washington, DC, 1997, 320-335.

[2] L.R. Lynd, Overview and Evaluation of Fuel Ethanol from Cellulosic Biomass: Technology, Economics, the Environment, and Policy. Annu. Rv. Energy Environ. 21(1996) 403-465.

[3] M.H. Siegel, C.W. Robinson, Application of airlift gas-liquid solid reactors in biotechnology, Chem. Eng. Sci. 47(1992) 3215-3229.

[4] S.S. Riggs, T.J. Heindel, Measuring carbon monoxide gas-liquid mass transfer in a stirred tank reactor for syngas fermentation, Biotechnol. Prog. 22 (2006), 903–906.

[5] A. Kapic, S.T. Jones, T.J. Heindel, Carbon monoxide mass transfer in a syngas mixture, Ind. Eng. Chem. Res. 45 (2006) 9150–9155.

[6] A.J. Ungerman, T.J. Heindel, Carbon monoxide mass transfer for syngas transfer for syngas fermentation in a stirred tank reactor with dual impeller configurations, Biotechnol. Prog. 23 (2007) 613–620.

[7] M.D. Bredwell, R.M. Worden, Mass-transfer properties of microbubbles. 1. Experimental studies. Biotechnol. Prog. 14(1998) 31-38.

[8] J.P. Cowger, K.T. Klasson, M.D. Ackerson, E.C. Clausen, J.L. Gaddy, Mass-transfer and kinetic aspects in continuous bioreactors using *Rhodospirillum rubrum*, Appl. Biochem. Biotechnol. 34/35 (1992) 613-624.

[9] K.T. Klasson, A. Gupta, E.C. Clausen, J.L. Gaddy, Evaluation of mass-transfer and kinetic parameters for *Rhodospirillum rubrum* in a continuous stirred tank reactor. Appl. Biochem. Biotechnol. (37/40) 1993 549-557.

[10] M.D. Bredwell, P. Srivastava, R.M. Worden, Reactor design issues for synthesis-gas fermentations, Biotechnol. Prog. 15(1999) 834-844.

[11] W. Yang, J. Wang, Y. Jin, Mass transfer characteristics of syngas components in slurry system at industrial conditions. Chem. Eng. Technol. 24(2001) 651-657.

[12] I.S. Chang, I. S. B.H. Kim, R.V. Lovitt, J.S. Bang, Effect of CO partial pressure on cell-recycled continuous CO fermentation by *Eubacterium limosum* KIST612, Process Biochem. 37 (2001) 411-421.

[13] T. Ahmed, J.M. Semmens, Use of sealed end hollow fibers for bubbleless membrane aeration: experimental studies, J. of Membr. Sci. (69) 1991 1-10.

[14] K.C. Lee, B.E. Rittmann, Applying a novel autohydrogenotrophic hollow-fiber membrane biofilm reactor for denitrification of drinking water, Water Res. 36 (2001) 2040–2052.

[15] R. Nerenberg, B.E. Rittmann, Hydrogen-based, hollow-fiber membrane biofilm reactor for reduction of perchlorate and other oxidized contamitants, Water Sci. Technol. 49(2004) 223–230.

[16] P.C. Munasinghe, S.K. Khanal, Biomass-derived syngas fermentation into biofuels: opportunities and challenges, Biores. Technol. 2010 doi: 10, 1016/j. biortech.2009.12.098.

[17] S.H. Kim, P. H. Lee, H.I. Chang, S. Sung, Carobon monoxide mass transfer using hollow fiber membrane for syngas fermentation, Biotechnol. Let.

[18] X.Ni, S. Gao, R.H. Cumming, D.W. Pritchard, A comparative study of mass transfer in yeast for a batch pulsed bioreactor and a stirred tank fermentor. Chem. Eng. Sci. 50 (1995) 2127-2136.

[19] M.C. Yang and E.L. Cussler, Designing hoolow-fiber contactors, AIChE J., 32(11) (1986) 1910-1916.
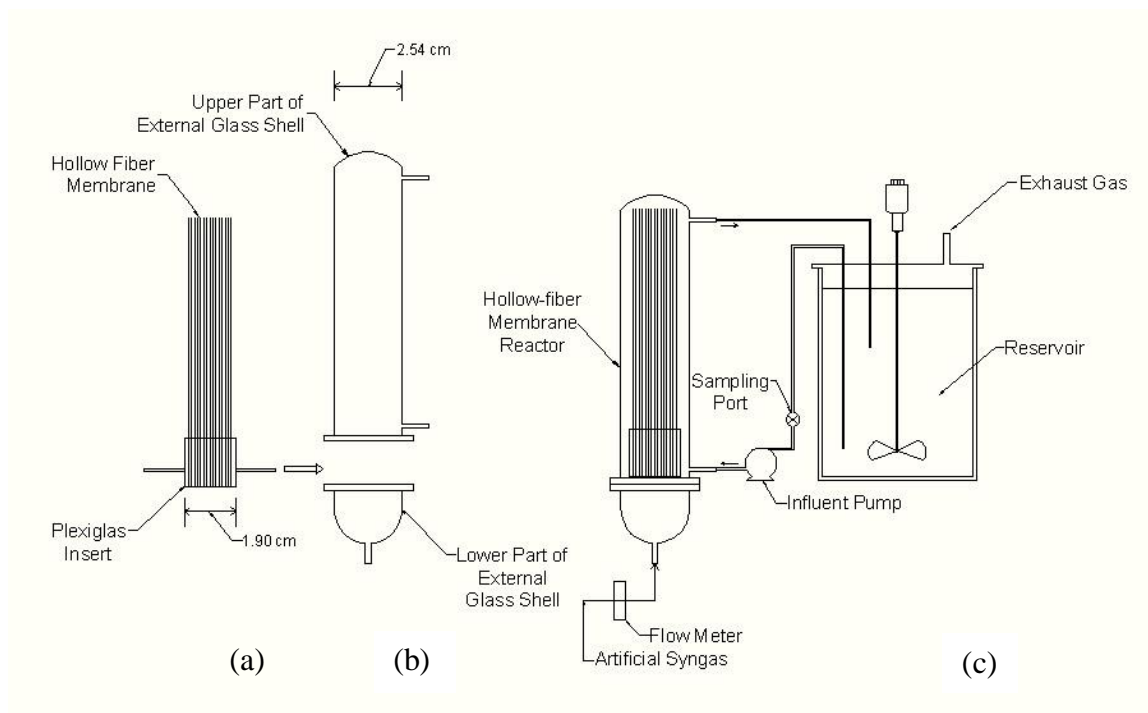
Figure 1. Schematic diagram of experimental setup. (a) Hollow fiber membrane module, (b) Hollow fiber membrane reactor, (c) CO transfer experiment.
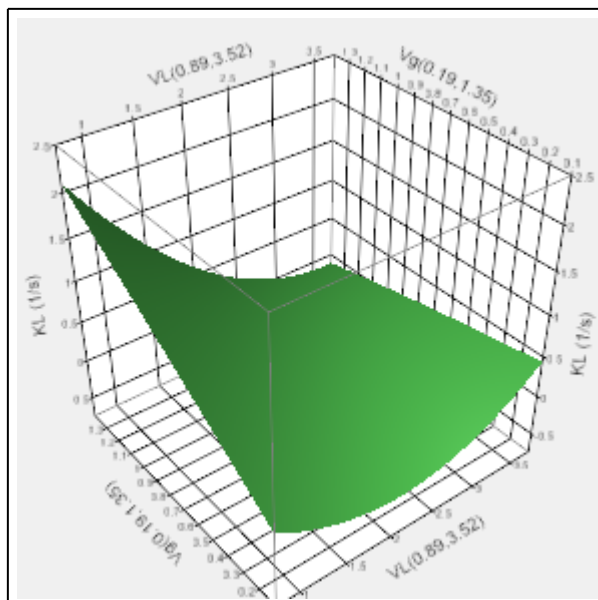
(a) Microporous polypropylene hollow fiber membrane
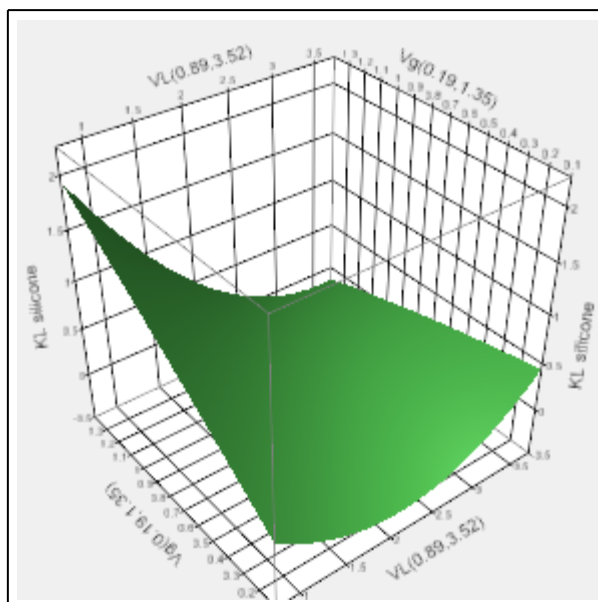
(b) Nonporous silicone membrane

Fig. 2 Response surface for K_La dependence on specific gas flow rate and liquid velocity at 0 level of P_u/V
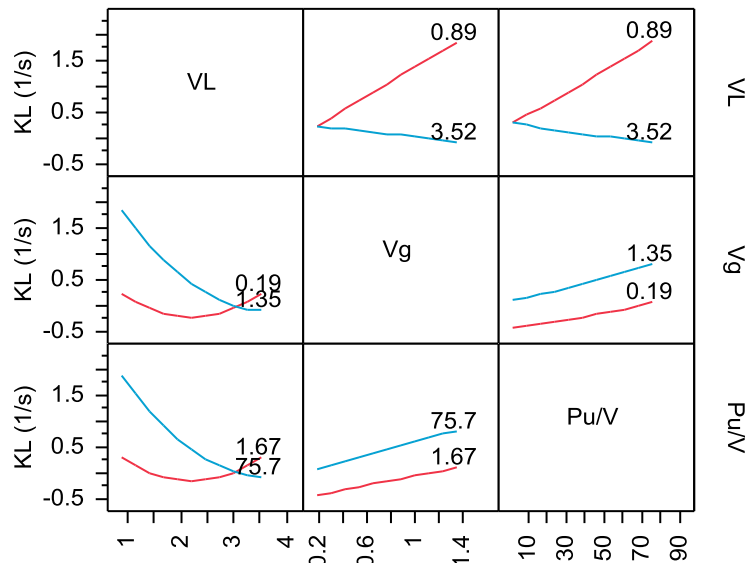
(a) Microporous polypropylene hollow fiber membrane
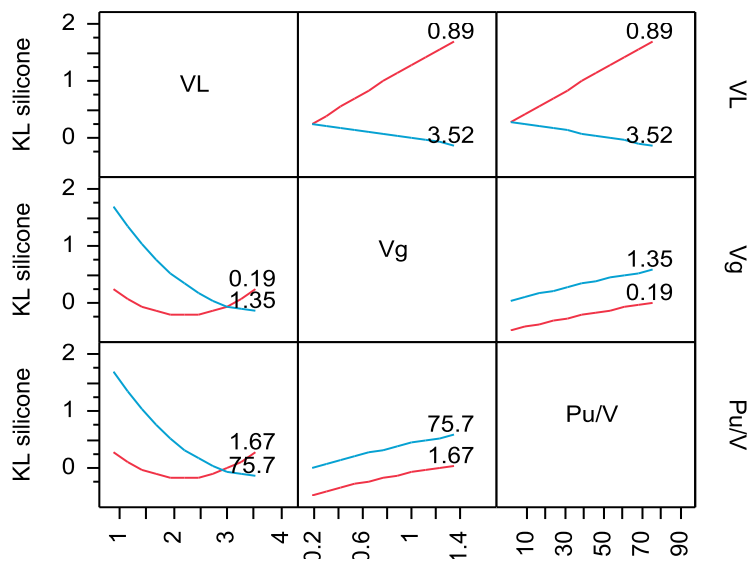
(b) Nonporous silicone hollow fiber membrane

Fig. 3 Interaction Profiles (Units: K_L: s$^-$1, V_L: cm·s^{-1}, V_g: min^{-1}, and Pu/V: W·m^{-3})
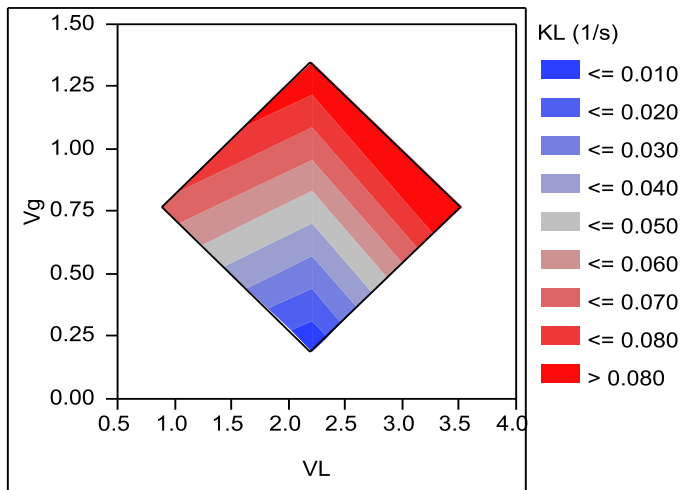
(a) Contour Plot for K_L (s^{-1}) at the P_u/V of 1.67
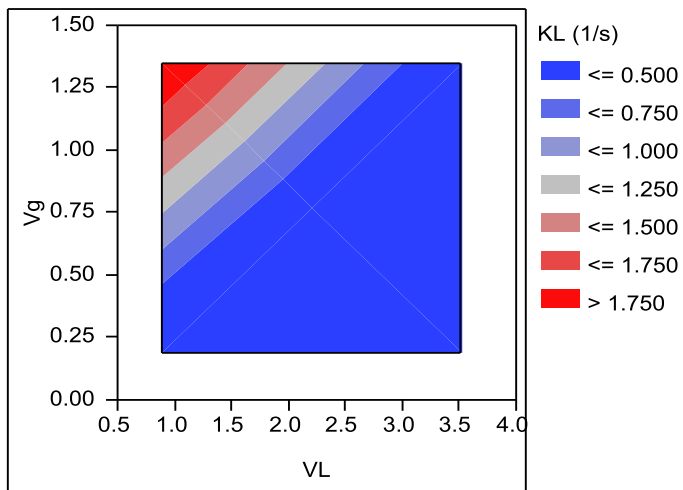
(b) Contour Plot for K_L (s^{-1}) at the P_u/V of 38.68
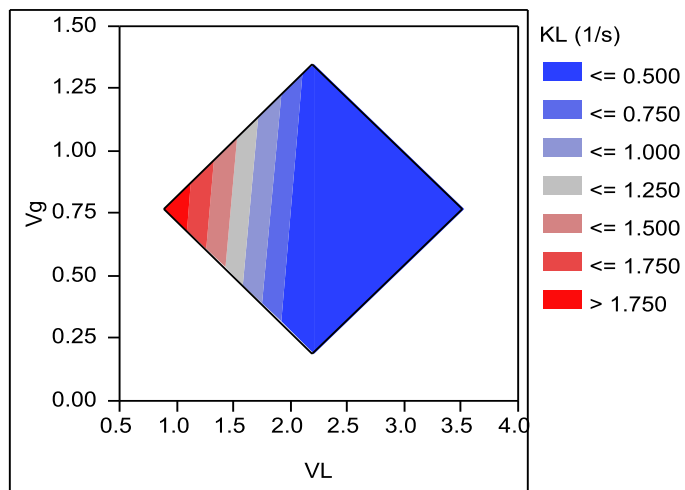
(c) Contour Plot for K_L (s^{-1}) at the *Pu/V* of 75.7
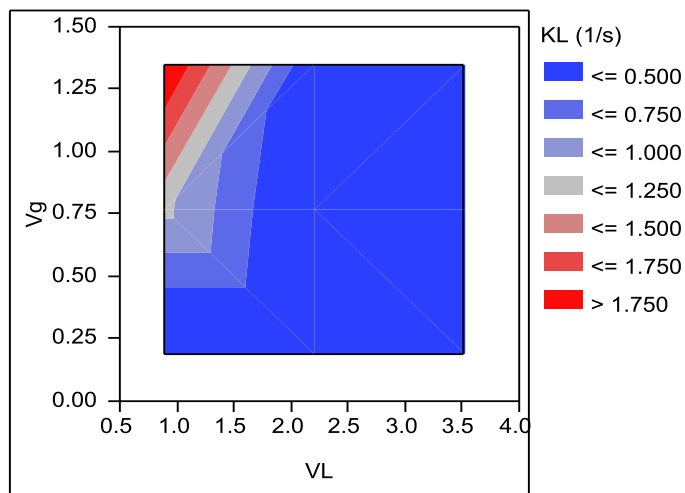
(d) Contour Plot for K_L (s^{-1}) regardless of P_u/V

Fig. 4 Contour Plot for K_L (s^{-1}) on polypropylene hollow fiber membrane test
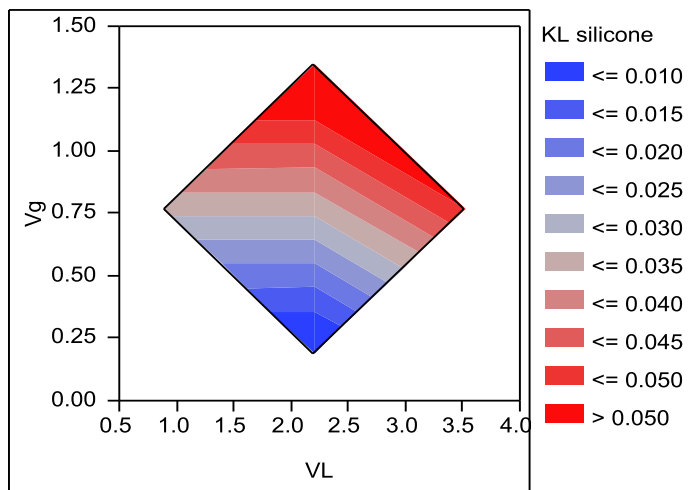
(a) Contour Plot for K_L (s^{-1}) at the P_u/V of 1.67
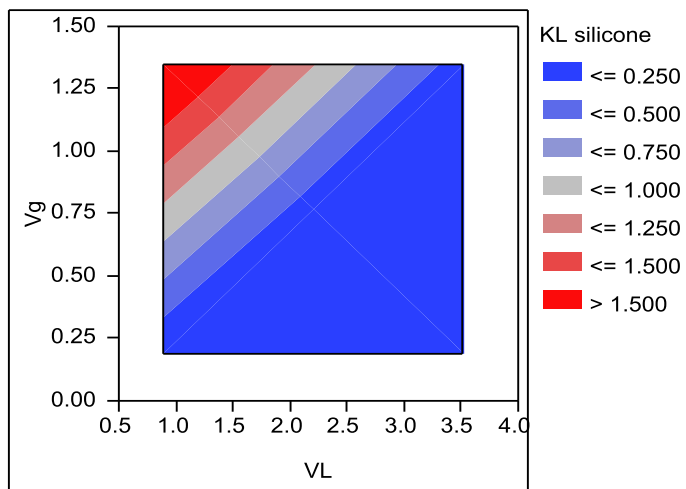
(b) Contour Plot for K_L (s^{-1}) at the P_u/V of 38.68
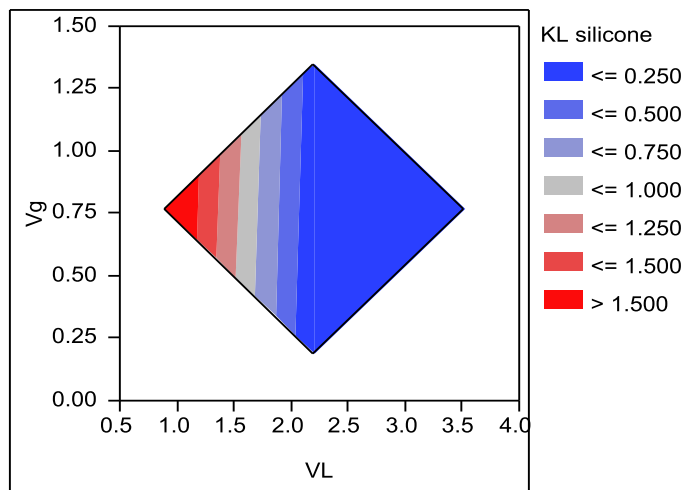
(c) Contour Plot for K_L (s^{-1}) at the *Pu/V* of 75.7
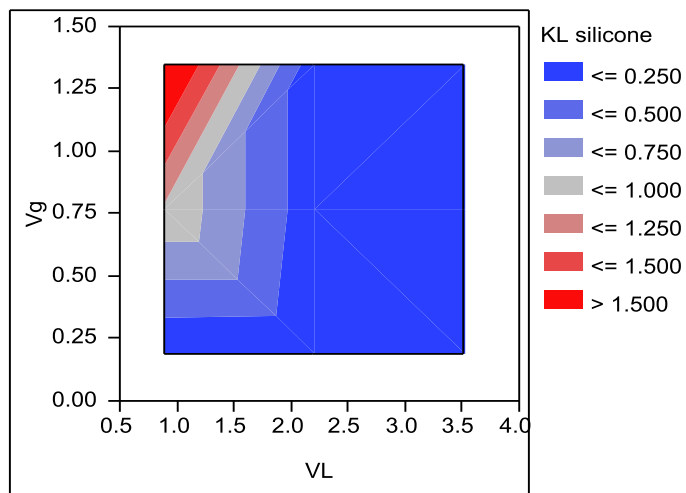
(d) Contour Plot for K_L (s^{-1}) regardless of P_u/V

Fig. 5 Contour plot on nonporous silicone membrane test

Table 1. Variables and their respective levels on both of the membranes

Variables	Levels		
	-1	0	+1
Cross flow velocity (V_L, cm·s^{-1})	0.89	2.21	3.52
Specific gas flow rate (V_g, min^{-1})	0.19	0.77	1.35
Power input for mixing per volume (Pu/V, W·m^{-3})	1.67	38.69	75.70

Table 2. The list of experimentations on both of the membranes

Systematic run	Pattern	V_L (cm·s^{-1})	V_g (min^{-1})	P_u/V (W·m^{-3})
1	+-0	3.52	0.19	38.69
2	000	2.21	0.77	38.69
3	000	2.21	0.77	38.69
4	+0+	3.52	0.77	75.70
5	+0-	3.52	0.77	1.67
6	0--	2.21	0.19	1.67
7	-+0	0.89	1.35	38.69
8	++0	3.52	1.35	38.69
9	0-+	2.21	0.19	75.70
10	-0+	0.89	0.77	75.70
11	0+-	2.21	1.35	1.67
12	000	2.21	0.77	38.69
13	--0	0.89	0.19	38.69
14	-0-	0.89	0.77	1.67
15	0++	2.21	1.35	75.70

Table 3 Results of CO-liquid mass transfer coefficients for the polypropylene and silicone HFMs

Statistical errors	Run	Polypropylene HFM $(K_L a, s^{-1})^b$	Silicone HFM $(K_L a, s^{-1})^c$	Polypropylene HFM $(K_L, cm \cdot s^{-1})$	Silicone HFM $(K_L, cm \cdot s^{-1})$
	1	0.0004	0.0020	0.0007	0.0036
	2	0.0785	0.0558	0.1408	0.1015
	3	0.0604	0.0511	0.1083	0.0909
	4	0.0926	0.0583	0.1661	0.1060
	5	0.0547	0.0275	0.0981	0.0500
	6	0.0002	0.0007	0.0003	0.0012
	7	1.1489	1.0549	2.0603	1.9200
	8	0.0616	0.0550	0.1105	0.1000
	9	0.0324	0.0032	0.0581	0.0059
	10	1.4912	1.0489	2.0605	1.9078
	11	0.0503	0.0342	0.0902	0.0618
	12	0.0602	0.0452	0.1080	0.0822
	13	0.0136	0.0050	0.0244	0.0092
	14	0.0378	0.0174	0.0678	0.0317
	15	0.2138	0.0672	0.3834	0.1223
Mean[a]		0.0664	0.0503	0.1190	0.0916
STD[a]		0.0105	0.0053	0.0188	0.0097

[a]Mean and Standard Deviation calculated for data runs 2, 3, and 12.

[b]a is the gas-water interfacial area (polypropylene HFM surface area) in the reactor (0.557 cm^{-1})

[c]a is the gas-water interfacial area (silicone HFM surface area) in the reactor (0.549 cm^{-1})

Table 4 Estimates of the coefficients and t-test of significance using microporous polypropylene hollow fiber membrane

	Key	Estimate	Std. Error	t value	Prob > $|t|$
b_0	Intercept	-0.119	0.222	0.54	0.6154
b_1	V_L	-0.480	0.136	-3.52	0.0169
b_2	V_g	0.320	0.136	2.35	0.0655
b_3	P_u/V	0.301	0.136	2.21	0.0778
b_{12}	$V_L \cdot V_g$	-0.482	0.193	-2.50	0.0545
b_{23}	$V_L \cdot P_u/V$	-0.482	0.193	-2.50	0.0546
b_{13}	$V_g \cdot P_u/V$	0.059	0.193	0.31	0.7722
b_1^2	$V_L \cdot V_L$	0.447	0.200	2.23	0.0759
b_2^2	$V_g \cdot V_g$	-0.018	0.200	-0.09	0.9336
b_3^2	$P_u/V \cdot P_u/V$	0.032	0.200	0.16	0.8812

$F = 4.50$, $F_{0.01,9,5} = 3.32$, $R^2 = 88.7\%$

Table 5 Estimates of the coefficients and t-test of significance using nonporous silicone hollow fiber membrane

	Key	Estimate	Std. Error	t value	Prob > |t|
b_0	Intercept	0.091	0.238	0.38	0.7171
b_1	V_L	-0.451	0.146	-3.09	0.0273
b_2	V_g	0.273	0.146	1.87	0.1208
b_3	P_u/V	0.250	0.146	1.71	0.1484
b_{12}	$V_L \cdot V_g$	-0.454	0.207	-2.19	0.0797
b_{23}	$V_L \cdot P_u/V$	-0.455	0.207	-2.20	0.0790
b_{13}	$V_g \cdot P_u/V$	0.014	0.207	0.07	0.9488
b_1^2	$V_L \cdot V_L$	0.446	0.215	2.07	0.0927
b_2^2	$V_g \cdot V_g$	-0.030	0.215	-0.14	0.8956
b_3^2	$P_u/V \cdot P_u/V$	-0.014	0.215	-0.07	0.9505

$F=3.33$, $F_{0.01,9,5} = 3.32$, $R^2 = 85.5\%$

Table 6 Comparison of the maximum k_La values for CO mass transfer studies

Reactor type (N/rpm)	Biological system	Feedstock	K_La (h^{-1})	References
Stirred tank -200	*B. methylotrophicum*	CO	14.2	[10]
Stirred tank -300	SBR mixed culture	Syngas mix	31 for CO 75 for H_2	[10]
Stirred tank -300	*C. ljungdahlii*	Syngas mix	35 for CO	[10]
Stirred tank -300	*R. rubrum, M. formicum, M. barkeri*	Syngas mix	28.1 for CO	[10]
Stirred tank -450	*R. rubrum, M. formicum, M. barkeri*	Syngas mix	101 for CO	[10]
Stirred tank -200	*B. methylotrophicum*	CO	90.6 for CO	[10]
Stirred tank -300	SRB mixed culture	Syngas mix	104 for CO	[10]
Microbubble sparging	n/a		190 for H_2	
Packed-bubble column	*R. rubrum, M. formicum, M. barkeri*	Syngas mix	2.1	[10]
Trickle bed	*R. rubrum, M. formicum, M. barkeri*	Syngas mix	55.5	[10]
Trickle bed	SRB mixed culture	Syngas mix	121 for CO 335 for H_2	[10]
Trickle bed	*C. ljungdahlii*	Syngas mix	137 for CO	[10]
Bubble column	n/a	CO	72.0	[12]
Stirred tank-400	n/a	CO	75.6	[4]
Stirred tank-500	*R. rubrum*	Syngas mix	71.8	[4]
Microporous Polypropylene hollow fiber member reactor	none	Syngas mix	385	[17]
Microporous Polypropylene Hollow fiber member reactor	none	Syngas mix	4136	This study
Nonporous silicone hollow fiber member reactor	none	Syngas mix	3798	This study

N: Mixing speed

CHAPTER 4. EFFECTS OF SYNTHESIS GAS FERMENTATION ON CELL GROWTH PHASE AND ETHANOL PRODUCTION PHASE

Po-Heng Lee, Dong-Won Choi, Sang-Hyoun Kim, and Shihwu Sung

Department of Civil, Construction and Environmental Engineering,

Iowa State University, Ames, IA 50011, USA

Abstract

The process of gasification followed by fermentation using biomass as feedstocks could potentially replace fossil fuels. Gasification generates a gas mixture of CO, CO_2, H_2, N_2 (Synthesis gas), with smaller amounts of trace gaseous compounds, ash, char, and tars. *Clostridium ljungdahlii* is an anaerobic bacterium that can convert synthesis gas (syngas) into ethanol. This study was designed to investigate different operating conditions for improving the culture density in the growth phase and increasing ethanol-to-acetate ratios in the production phase using batch hypovials with a working volume of 125 mL. The results showed that the highest cell density among the experiment in this study could be reached by controlling pH in a natural rage without adding additional buffer and with fructose in the medium. Supplementing hydrogen in the head space of the hypovials can improve the productivity of ethanol and the cell density of *Clostridium ljungdahlii* when the hydrogen concentration is kept as low as 15 % in this study. The condition of pH 5

maximizes the ethanol production using the medium without fructose in the production phase.

1. Introduction

Seeking an alternative renewable energy is a critical issue in today's society, since a significant portion of fossil fuels consumed for current energy supply causes a lot of problems. For example, burning fossil fuels result in negative environmental impacts: releasing pollutants and green house gases, such as carbon dioxide and nitrogen oxides. On the other hand, the fossil fuels are of finite reserve. Thus, these resources will be depleted sometime. Hence, alternative methods to produce energy and chemicals from renewable sources are a good solution to the concerns described above. Renewable resources including straw, wood, and corn stover (which are categorized as lignocellulosic biomass) are the most inexpensive, abundant carbohydrates in the world. Therefore, it makes perfect sense for these renewable products to serve as lignocellulosic biomass feedstock for fuels and commercial chemical production. Converting the lignocellulosic biomass into fuels and commercial chemicals could be achieved by one of the existing technologies: gasification of lignocellulosic biomass to produce a mixture of CO, CO_2, and H_2 (known as synthesis gas, syngas or producer gas) followed by anaerobic fermentation (Worden *et al*., 1991). Syngas fermentation, therefore, has raised a lot of interest recently.

Syngas fermentation to commercial chemicals, especially volatile acids, is reported to be thermodynamically favorable by the reactions of their negative changes of Gibbs free

energy (Barik *et al.,* 1988). As early as 1932, Fisher and Tropsch were the first to demonstrate that acetate could be produced from CO in an anaerobic sewage sludge (Diekert *et al.,* 1982). Since then, many anaerobic microbes (some have been isolated but not yet identified) capable of producing fuels and chemicals from syngas have been reported. For example, *Eubaterium limosum*, which can produce acetate and butyrate exclusively using CO as the sole energy source, was isolated from various environments, e.g. human intestine, sewage, rumen, and soil (Genthner *et al.,* 1982 and 1987). Other acetogens, including *Clostridium aceticum, Peptosteptococcus productus*, etc, were identified to be capable of producing acetate from syngas gas. Acetate and butyrate production from syngas by *Butyribacterium methylotrophicum* has been demonstrated as well. This microbe's ability to shift production from acetate to butyrate by inducing pH changes during the fermentation was found in the following studies (Grethlein *et al.,* 1991; Lynd *et al.,* 1982; Shen *et al.,* 1999). *Acetobacterium woodii* is also one of the mesophiles able to yield acetate from CO (Genthner *et al.,* 1987).

Since the finding of syngas fermentation to fuels, which was calculated to be thermodynamically favorable, was discovered, the research trend of syngas fermentation has shifted from volatile acids production to production of fuels or other high-value derivatives (Genthner *et al.,* 1987). For example, *Clostridium autoethanogenum* and *Clostridium carboxidivprans P7* were reported to be capable of generating ethanol and butanol (Liou *et al.* 2005; Cotter *et al.,* 2008 and 2009). A gram-positive, motile, rod-shaped syngas utilizing bacterium, *Clostridium ljungdahlii*, for ethanol creation was isolated from chicken yard waste. A full-scale plant involving gasification, fermentation,

and distillation using this microorganism has been operating for ethanol production with syngas serving as a gas substrate (Tanner *et al.,* 1993).

Syngas fermentation process parameters for *Clostridium ljungdahlii* have been manipulated for achieving higher ethanol yield. A study showed that ethanol was a non-growth associated metabolite by *Clostridium ljungdahlii* while acetate was a growth related product (Klasson *et al.,* 1992). It demonstrates that *Clostridium ljungdahlii* produces acetate in the growth phase by maintaining a natural pH range and yields ethanol in a non-growth phase by a pH drop condition (Fordyce *et al.,* 1984). Another autotrophic bacterium, *Clostridium carboxidivprans P7*, has also showed the correlation of acetate production in a growth phase and ethanol production in a non-growth phase which is the same as *Clostridium ljungdahlii* (Datar *et al.,* 2004). Collectively, a new operating strategy, breaking the syngas fermentation process into (1) increasing microorganism density stage (growth phase) and (2) rest cell stage (ethanol production phase), is proposed for use in syngas fermentation. In short, the operating point is to divide the process into two phases. The first stage (growth phase) is designed to increase the microorganism density in a short period of time. The second stage (ethanol production phase) is intended to maintain the microorganism population, and then switch its metabolism to the rest cell phase for ethanol production. Even though the strategy of manipulating the growth and production phases has been studied by some researchers (Fordyce *et al.,* 1984; Klasson *et al.,* 1992; Datar *et al.,* 2004; Cotter *et al.,* 2008 and 2009), some operating parameters, e.g. end product inhibition, buffer solutions and syngas fermentation, of switching between growth phase and ethanol production phase separately has not been studied yet.

The goal of this study was to examine the effects of different parameters 1) for rapidly reaching the maximum cell density in the growth phase and 2) for triggering a controlled metabolic shift from the growth phase into the production phase. Consequently, the study focuses on determining the effects of ethanol and acetate production capabilities on both phases. *Clostridium ljungdahlii*, a well-studied, anaerobic autotroph is used to identify the effects of the operating parameters, i.e. buffer solutions, syngas composition, carbon source influence, and pH for improvement of ethanol production by syngas fermentation.

2. Material and methods

2.1. Organisms and anaerobic medium preparation

In this study, a pure culture of *Clostridium ljungdahlii* purchased from American Type Culture Collection (ATCC), 55383, University Boulevard, Manassa, Virginia, 20110-2209 USA, was used. The bacterium was grown on ATCC 1754 PETC medium at $35^{o}C$ in sealed stopper hypovials (total volume, 120 ml). This basal medium composition is summarized in Table 1. All media for the studies were prepared anaerobically. Heat stable ingredients were combined and the medium was boiled and cooled under an argon purge to drive off dissolved oxygen. 40 ml of the deoxygenated medium was transferred to each hypovial in a Coy anaerobic chamber with an atmosphere containing 3% H_2 97% Ar (Coy Laboratory Products, Inc.). Hypovials were capped with stoppers, removed from the chamber, and sterilized at $121^{o}C$ for 15 min. After autoclaving, the hypovials were purged with a 100 % CO gas. Heat sensitive ingredients were brought into the

chamber and reconstituted with anaerobic de-ionized water in the anaerobic chamber. These ingredients were filter sterilized and injected into the medium in the autoclaved hypovials. The medium was inoculated with 4 ml inoculums.

2.2. Test on the growth phase

Different operating parameters, i.e. different buffer solutions, carbon source in the medium, pH conditions, and syngas supply composition, were used to evaluate the effects on *C. ljungdahlii* for its optimal growth condition in the growth phase. Citrate, Phosphate, and Citrate-Phosphate, $NaHCO_3$, $NaHCO_3$-Phosphate, and MES (2 (*N*-morpholino) ethanesulfonic acid) were varied to examine the effect of the buffer solutions on pH and then the impacts on growth phase and ethanol production. Three different syngas supply compositions, (1)100% CO, (2) 15% H_2, 10% CO, 20% CO_2, and 55% N_2, (3) 50% H_2 and 50% CO, were also used to observe their effects on the microbe in the growth phase.

2.3 Test on the production phase

A varied-pH range of the medium without fructose for optimizing *C. ljungdahlii* production phase was prepared and conducted. The inoculums contained 5 ml from an active culture to investigate the optimal pH for ethanol production in the production phase (cell rest stage).

2.4. Analytical procedures

Cell density: A 200 µl aliquot from the well-mixed hypovail sample was diluted to 1,000 µl by adding dI water in a 1.5 ml disposable polystyrene cuvette (Fisher Scientific). A Cary 50 Conc UV-Visible spectrophotometer (Varian) equipped with the Varian software, Simple Reads, was used to determinate cell density. The measured values were obtained by setting the spectrophotometer at an absorbance of 600 nm, a sampling rate of 80 Hz, and a reading period of 3 second. A blank of deionized (dI) water was used as a zero reference. The blank cuvette was re-read at the end of each session in order to check for baseline drift during analysis.

Lactic acid, acetic acid, and ethanol concentration determination: The concentrations of lactic acid, acetic acid, and ethanol were analyzed for lactic acid, acetic acid, and ethanol concentrations by using a Waters high pressure liquid chromatograph (HPLC). The HPLC system (Millipore Corporation, Milford, MA, USA) included a Waters model 401 refractive index detector, column heater, auto-sampler and computer controller. The Bio-Rad Aminex HPX-87H column (7.8 × 300 mm; Bio-Rad Chemical Division, Richmond, CA, USA) was used to separate the samples with 0.012 N sulfuric acid as a mobile phase at 0.8 ml/min, an injection volume of 20 µl, and a column temperature of 65 $^\circ$C. After harvesting the samples, the samples were centrifuged at 9000 rpm for 10 min and filtered by using Whatman PP 0.45 µm syringe filters. All analyses were carried out in triplicate with the same samples and the mean values reported.

3. Results and discussion

3.1. Buffer solution effects

pH is an important growth factor on *Clostridium ljungdahlii.* The optimal growth rate for *Clostridium ljungdahlii* has been reported in a range of 7.5 to 6.0 (Tanner *et al.,* 1993). *Clostridium ljungdahlii* produces the product of acetate, which inhibits the metabolic activity of itself, in the fermentation process, even though the ATCC medium includes 2 g/l of $NaHCO_3$. In the hypo-vials tests, a variety of the additional buffer solutions, i.e. citrate, $NaHCO_3$, $NaHCO_3$-Phosphate, MES (2 (*N*-morpholino) ethanesulfonic acid), phosphate, and citate-phosphate, was investigated to control the pH in the natural condition of the fermenting broth with a 10 psig pressurized CO gas, while the ATCC medium includes bicarbonate as the buffer solution. Figure 1 shows the additional buffer (citrate) influence on *Clostridium ljungdahili* growth in a range of 0 to 25 mM. The results demonstrated that the citrate concentrations of 5 mM and 10 mM in the medium do not increase the biomass in comparison with the medium without the citrate as the buffer solution. In the medium with the citrate concentration of 25 mM, the biomas was increased from the OD (600 nm) of 0.74, compared to the ones of OD of 0.72 for 5 mM and 10 mM. There was no significant increase of the biomass by using citrate as the buffer solution in the medium. pH values of the hypovial samples without citrate and with citrate as high as 10 mM were not much different. pH values were about 4.2 when these hypovails reached the stationary phase (Figure 1 (b)). However, the pH value of the hypovial with 25 mM citrate was 4.8. It indicates that 25 mM of citrate in the medium has a positive effect on *Clostridium ljungdahlii*, compared to other different hypovials with the lower concentrations of citrate in them.

Figure 2 (a) shows the phosphate influence on *Clostridium ljungdahlii* growth in a range of 0 to 25 mM. The results confirmed that the phosphate concentrations of 5, 10, and 25 mM, which served as the additional buffer in the medium, do not increase the biomass in comparison with the medium without the phosphate as the buffer solution. pH values of these hypovials, which were added at varied concentrations of phosphate in the buffer solutions, were all around 4.2 (Figure 2 (b)). The values of optical density (OD) in the different concentrations of phosphate were 0.70 to 0.79, which proved there was no significant enhancement on the growth of *Clostridium ljungdahlii*.

From the results above, the hypotheses of the buffer solution inhibition and the bicarbonate used as the carbon source were proposed. The buffer solution inhibition of the hypovial tests were conducted by the combined phosphate and citrate solution and the bicarbonate solution in the medium, respectively. Fig. 3 (a) shows the influence of the various concentrations in the medium on *Clostridium ljungdahlii* growth. It implied that the medium with citrate-phosphate as the buffer solution does not improve cell density on *Clostridium ljungdahlii*, even though pH values of these hypovails were about 4.5 in comparison with the tests on either citrate or phosphate as the buffer solutions. The results confirmed that the combined phosphate and citrate concentrations of 25 mM which served as the buffer in the medium do not improve the biomass growth, compared to the medium without the buffer solution. Figure 4 depicts the influence of phosphate and bicarbonate in the medium affects the microbe. It demonstrates that using phosphate as the buffer solution has shown the increase of biomass up to 0.85, while the pH decrease gradually occurred. The stationary phase of *Clostridium ljungdahlii* was shown

to be delayed in the medium with the phosphate as the buffer solution. The ODs at 600

nm in the different concentrations of the combined phosphate and citrate as the buffer

solution were similar, which proved there was no significant enhancement on the growth

of *Clostridium ljungdahlii*. The buffer solution inhibiting concern from acetate

production on *Clostridium ljungdahli* is eliminated. Therefore, the metabolic product of

acetic acid from *Clostridium ljungdahlii* should be eliminated in the fermenting broth to

prevent syngas fermentation failure.

Another test using (2-(*N*-morpholino) ethanesulfonic acid) as the buffer solution in the

medium was conducted. The result demonstrates that MES does not have a positive

effect on the microbe growth in the syngas fermentation (Figure 5). Adding 5mM of HCl

for controlling a pH range of 7.5 to 6.5 manually in every four hours was conducted

(Figure 6). The results confirmed that maintaining pH between 6.5 and 7.5 positively

affects the OD value (0.92) of *Clostridium ljungdahlii*, compared to the OD value of 0.81

without pH control. Table 2 summarizes the results of the buffer solutions in this study.

Apparently, controlling pH in a natural condition has proved to be the most efficient

method to reach the optimal cell density among all of tests in this study. Manual pH

control every 4 hours was not physically achieved, so the auto pH controller is required to

maintain the optimal condition in the fermentation study.

3.2. Carbon source effects

Fructose is one of the components in the *Clostridium ljungdahlii* medium provided by

ATCC. It is critical to test whether *Clostridium ljungdahlii* could grow without fructose

so that it could reduce the operating cost and make the process more attractive. Figure 7 shows the influence of the medium with and without fructose on the microbe. Obviously, the microbe did not grow well in the medium without fructose. However, the microbe did grow within a long lag phase. Table 3 summarizes the carbon source effect on *Clostridium ljungdahlii*. It implied that the microbe could grow either by other carbon sources in the medium or dissolved CO from the headspace. The full-scale application should include fructose in the medium for *Clostridium ljungdahlii* to reach a high cell density for ethanol production.

3.3. Syngas composition effects

The composition of syngas depends on the types of gasifier, the operating conditions of the gasifier, and the sources of biomass. Definitely, syngas composition is one of the parameters that influence the syngas fermentation process. Three different syngas compositions, (1) 15% H_2, 10% CO, 20% CO_2, and 55% N_2, (2) 50% H_2 and 50% CO, and (3) 100% were used to observe their effects on *Clostridium ljungdahlii* in the growth phase. Figure 8 (A) presents the cell density using the syngas composition of 15% H_2, 10% CO, 20% CO_2, and 55% N_2 in various fructose concentration media. The values of optical density increased with 2.5 and 5.0 g/L fructose in the media after 2 day. It concludes that the microbe could utilize hydrogen as an energy source to increase its cell density. Also, the threshold of the fructose concentration in the medium for triggering the growth is 2.5 g/L. Without enough fructose as the initial energy and carbon source, *Clostridium ljungdahlii* could not grow well and rapidly.

Figure 9 (a) presents the cell density using the syngas composition of 50% H_2 and 50% CO in various fructose concentration of the medium. It shows that the medium with 1.25 g/L fructose could have the highest cell density in the syngas composition of 50% H_2 and 50% CO. Because hydrogen could enhance the metabolic reaction resulting in producing a large amount of acetic acid, the end product inhibition occurred from acetic acid production in the medium that had fructose concentrations over 2.5 g/L. Table 4 summarizes the syngas fermentation effect on *Clostridium ljungdahlii*. Hydrogen does increase the biological reaction of *Clostridium ljungdahlii* and also increases its cell density.

3.4. Ethanol, acetic acid, and lactic acid production

The main purpose of syngas fermentation is to produce ethanol from syngas for replacing fossil fuels. Ethanol production results in this study are presented in this section. Ethanol, acetic acid, and lactic acid production using 100% CO gas supply were shown in Figs. 10 (a), (b), and (c) , respectively. As the fructose concentration was increased, the ethanol production was increased. MES was added as the buffer solution in two samples, and the end products presented 120 mM of acetic acid and 45 mM of lactic acid. *Clostridium ljungdahlii* is considered a CO utilizing bacterium that uses CODH (carbon monoxide dehydrogenase) for converting syngas into ethanol and acetic acid. While lactic acid is a fermenting end product from sugar fermentation by *Clostridium ljungdahlii*. It was observed that the high acid yield was from MES which might have the concern of the acid inhibition on *Clostridium ljungdahlii*.

Ethanol, acetic acid, and lactic acid yields using 100% CO gas supply with pH controlled between 6.5 to 7.5 are shown in Figs. 11 (a), (b), and (c) , respectively. *Clostridium ljungdahlii* apparently has higher ethanol yield (10 mM) and less acid yield corresponding to their high cell density by consuming lactic acid. Ethanol, acetic acid, and lactic acid yields using the syngas composition of 15% H_2, 10% CO, 20% CO_2, and 55% N_2 are shown in Figs. 12 (a), (b), and (c), respectively. The ethanol yield was as high as 12.3 mM with hydrogen in the head space. The trend of higher acetic acid production (18.3 mM in the 5 g/L fructose medium) was also triggered by hydrogen. However, the lactic acid production was consistently around 47.4 mM. It explains that hydrogen increases the activity of CODH resulting in ethanol and acetcic acid production. Ethanol, acetic acid, and lactic acid yields using the syngas composition of 50% H_2 and 50% CO are shown in Figs. 13 (a), (b), and (c), respectively. The ethanol yield was as high as 10.5 mM with hydrogen in the head space within 12 hrs. The trend of higher acetic acid production (18.3 mM in the 5 g/L fructose medium) was also triggered by hydrogen. Even though hydrogen demonstrated its ability to improve the syngas fermentation process for yielding ethanol and acetic acid rapidly, the end product inhibition occurred on *Clostridium ljungdahlii* growth within 12 hrs. Less lactic acid production and lower cell density were also observed.

Table 5 summarizes the results of the yield ratios of the end products (ethanol, acetic acid, and lactic acid) by *Clostridium ljungdahlii*. For 100% CO as the gas supply, it showed that the highest ethanol yield occurred in 5 g/L fructose with pH control. Additionally, lactic acid could be used as a carbon source for *Clostridium ljungdahlii*

growth. However, acetic acid and ethanol are the end products of the syngas fermentation by CODH. Also, acetic acid has negative impact on its growth. With hydrogen in the gas supply, *Clostridium ljungdahlii* could improve its cell density as well as the productivity of ethanol, acetic acid, and lactic acid.

3.5. pH effect in ethanol production phase

Clostridium ljungdahlii non-growth cultures were prepared, and the inoculums were obtained before the stationary phase. The test was conducted for 58 hrs. The medium for the ethanol production were without fructose so that *Clostridium ljungdahlii* non-growth cultures could be maintained in the ethanol production phase with 100% CO supply. The five different pH condition media cosnsisted of pH values of 4.0, 4.6, 4.9, 5.3, and 6.0. Table 6 summarizes ethanol and acetic acid production at the fermentation time of 56 hr. Only the medium at a pH of 4.9 produced the ethanol concentration of 0.6 mM. The result was reported from previous studies that pH of 5 maximizes ethanol production by *Clostridium ljungdahlii* even though the compostions of the media varied among previous studies.

4. Conclusions

In this study, the effect of different operating parameters on syngas conversion and product formation of *Clostridium ljungdahlii* was studied. The buffer solution is one of the parameters investigated in this study. Among all of the tested buffer solutions, phosphate and MES-bicarbonate had a positive influence on *Clostridium ljungdahlii* cell growth. Phosphate as the buffer solution had a long lag phase for *Clostridium*

ljungdahlii. The highest cell density among the experiments in this study was reached by controlling pH in a natural rage without adding additional buffer.

Fructose is a component in the medium recommended by ATCC. Because the hypovial study could not consistently supply CO, fructose is a vital energy and carbon resource for *Clostridium ljungdahlii*. For the full-scale application, adding fructose in the medium fits the requirement of rapid cell density increase.

Ethanol, acetic acid, and lactic acid were major products of syngas fermentations by *Clostridium ljungdahlii*. Supplementing hydrogen can advance the productivity of ethanol, when the hydrogen concentration is kept as low as 15 % in this study. Also, the suitable hydrogen concentration (15% in this study) could improve the cell density of *Clostridium ljungdahlii* without producing too much acetic acid resulting in the end product inhibition. The final results of this study show that the syngas composition has a significant effect on the growth rate and the product spectrum. The condition of pH 5 maximizes the ethanol production using the medium without fructose in the production phase.

5. Referenecs

Barik, S., Prieto, S., Harrison, S.B., Clausen, E.C., and Gaddy, J.L. (1988) Biological production of alcohols from coal through indirect liquefaction, *Appl. Biochem. Biotechnol.* 28, 363–378.

Cotter, J.L., Chinn, M.S., and Grunden, A.M. (2008) Ethanol and acetate production by *Clostridium ljungdahlii* and *Clostridium autoethanogenum* using resting cells, *Bioprocess Biosyst. Eng.* 32, 369–380.

Cotter, J.L., Chinn, M.S., and Grunden, A.M. (2009) Influence of process parameters on growth of *Clostridium Ljungdahlii* and *Clostridium autoetahanogenum* on synthesis gas, *Enzyme Microbial Technol.* 44, 281–288

Datar R.P., Shenkman, R.M., Cateni, B.G., Huhnke, R.L, and Lewis, R.S. (2004) Fermentation of biomass-generated producer gas to ethanol, *Biotechnol. Bioeng.* 86, 587–594

Diekert, G.B., and Thayer, R.K. (1982) Carbon monoxide oxidation by *Clostridium thermoaceticum* and *Clostridium formicoaceticum*, *J. Bacteriol.* 136, 597–606.

Fordyce, A.M., Crow, V.L., and Thomas, T.D. (1984) Regulation of product formation during glucose or lactose limitation in nongrowing cells of streptococcus, *Appl. Environ. Microbiol.* 48, 332–337.

Genthner, B.R.S., and Bryant, M.P. (1987) Additional characteristics of one-carbon-compound utilization by *Eubacterium limosum* and *Acetobacterium woodii*, *Appl. Environ. Microbiol.* 53, 471–476.

Genthner, B.R.S., and Bryant, M.P. (1982) Growth of *Eubacterium limosum* with carbon monoxide as the energy source. *Appl. Environ. Microbiol. 43*, 70–74.

Grethlein, A.J., Worden, R.M., Jain, M.K., and Datta, R. (1991) Evidence for production of n-butanol from carbon monoxide by *Butyribacterium methylotrophicum*, *J. Ferment. Bioeng*. 72, 58–60.

Liou, J.S.C., Balkwill, D.L., Drake, G.R., and Tanner, R.S. (2005) *Clostridium carboxidivorans* sp. nov., a solvent-producing clostridium isolated from an agricultural settling lagoon, and reclassification of the acetogen *Clostridium scatologenes* strain SL1 as *Clostridium drakei* sp. nov. *Int. J. Syst. Evol. Microbiol. 55*, 2085–2091

Lynd, L., Kerby, R., and Zeikus, J.G. (1982) Carbon monoxide metabolism of the methylotrophic acidogen *Butyribacterium methylotrophicum*, *J. Bacteriol*., 149, 255–263.

Klasson, K.T., Ackerson, M.D., Clausen, E.C. and Gaddy, J.L. (1992) Bioconversion of synthesis gas into liquid or gaseous fuels. *Enzyme Microbial Technol. 14*, 602–608.

Shen, G.J., Shieh, J.S., Grethlein, A.J., Jain, M.K., and Zeikus, J.G. (1999) Biochemical basis for carbon monoxide tolerance and butanol production by *Butyribacterium methylotrophicum*, *Appl. Microbiol. Biotechnol. 51*, 827–832.

Tanner, R.S., Miller, L.M., and Yang, D. (1993) *Clostridium ljungdahlii* sp. nov., an acetogenic species in clostridial ribosomal-RNA homology group-I. *Int. J. Syst. Bacteriol. 43*, 232–236.

Worden, R.M., Grethlein, A.J., Jain, M.K., and Datta, R. (1991) Production of butanol and ethanol from synthesis gas via fermentation, *Fuel 70*, 615–619.
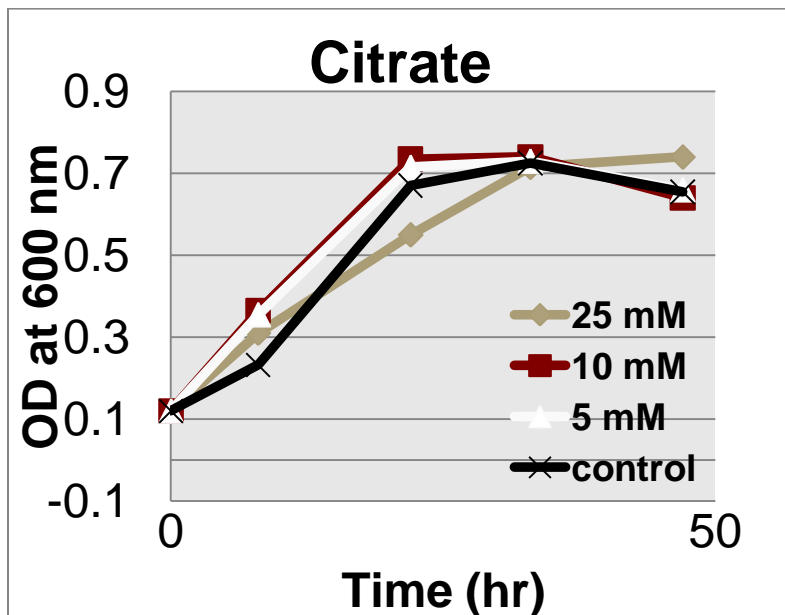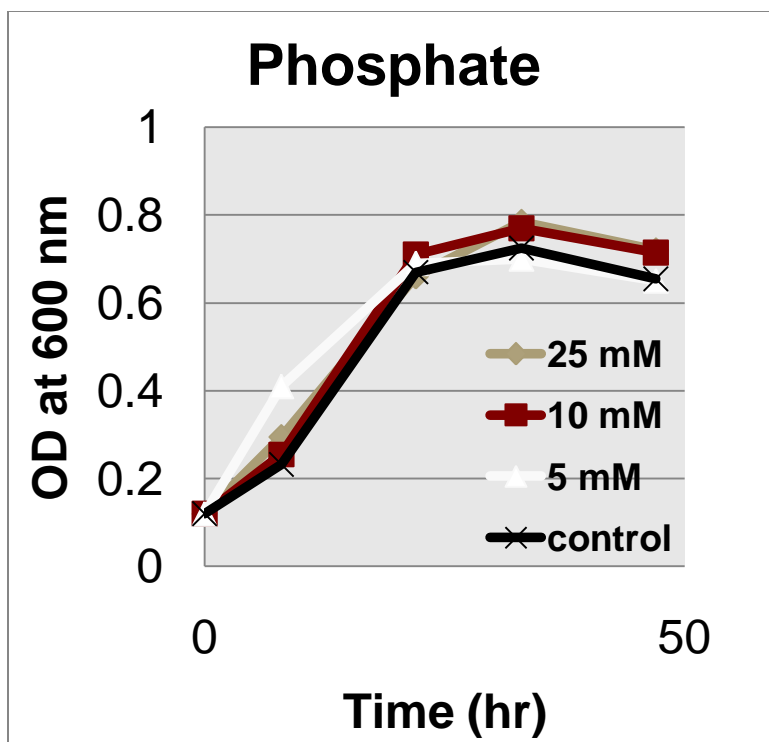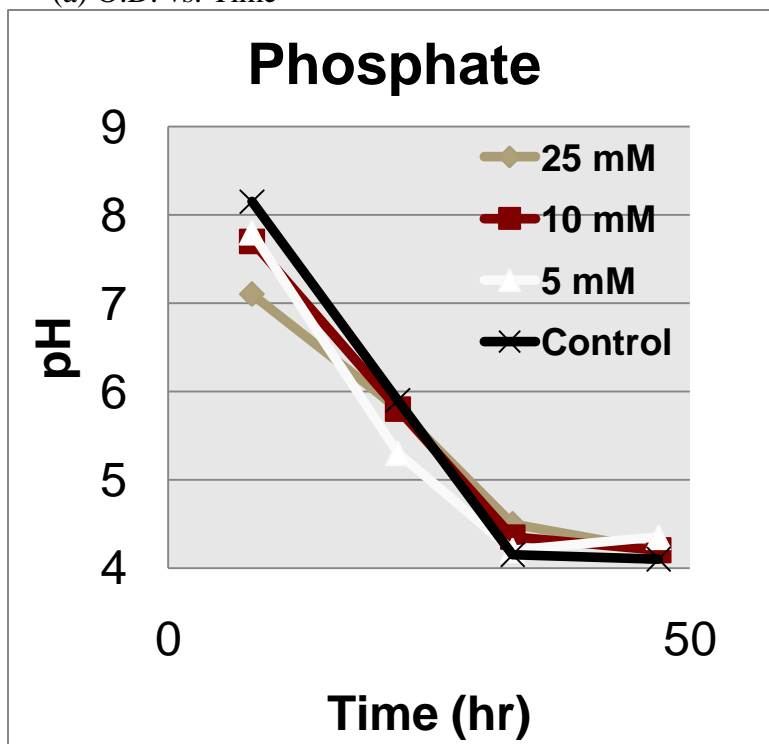
(a) O.D. vs. Time
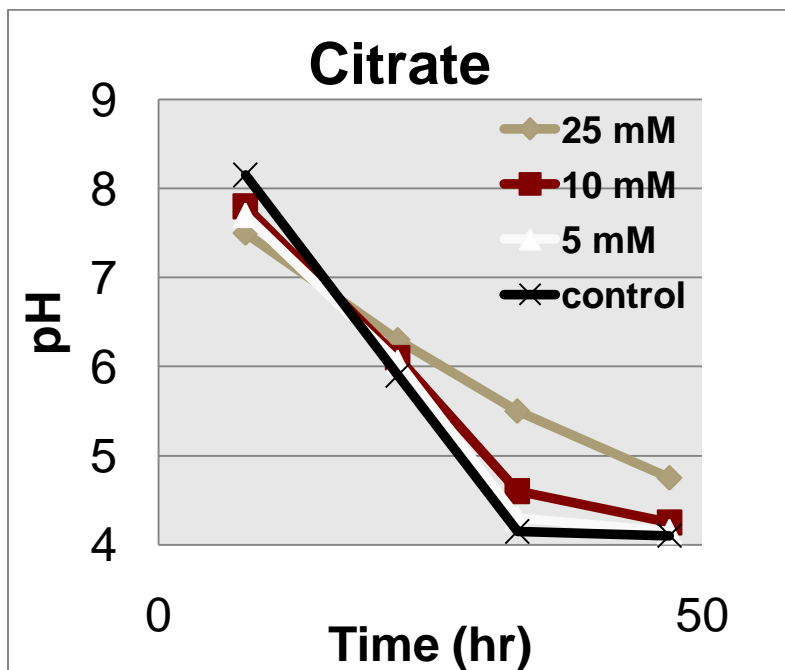
(b) pH vs. Time

Fig. 1. The effect of citrate as the buffer solution on *Clostridium ljungdahlii*
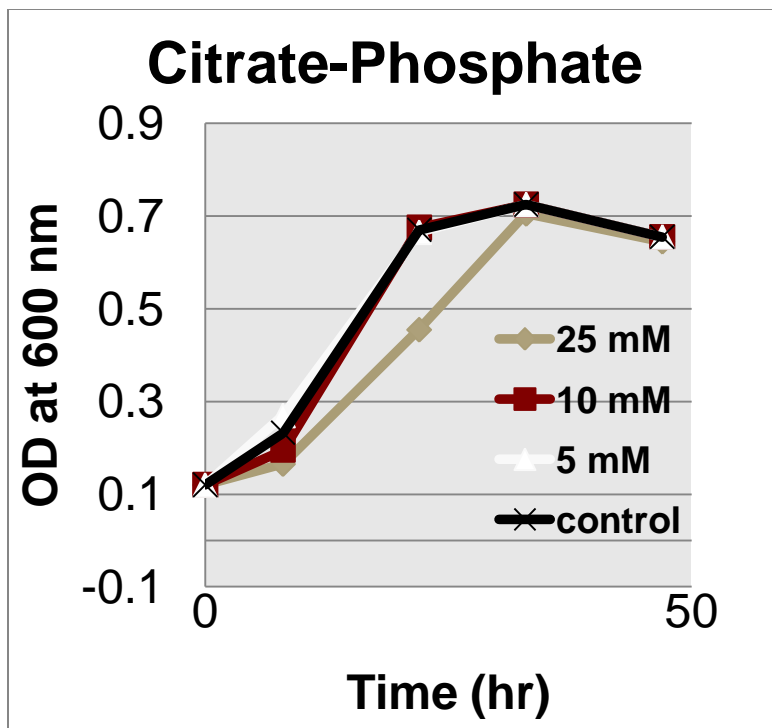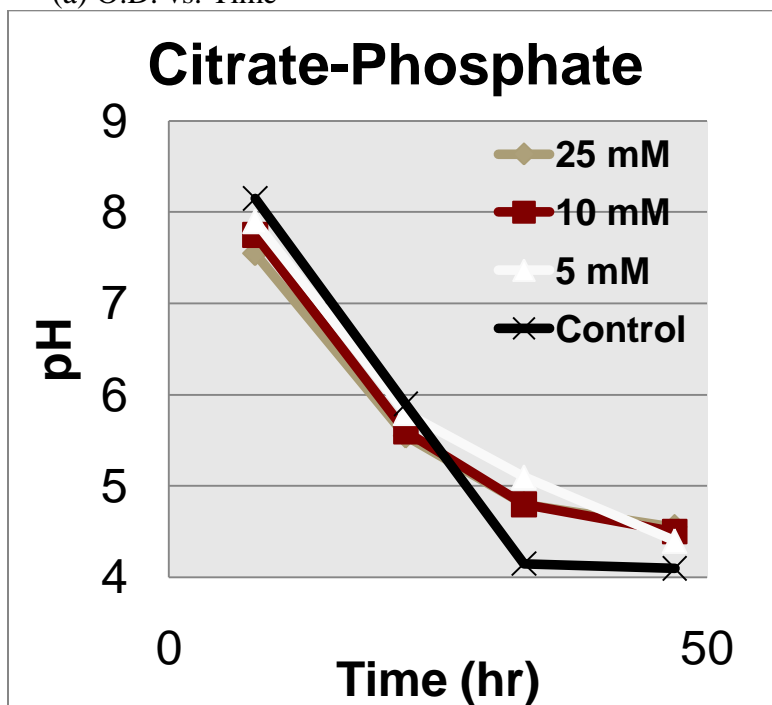
(a) O.D. vs. Time

(b) pH vs. Time

Fig. 2. The effect of phosphate as the buffer solution on *Clostridium ljungdahlii*
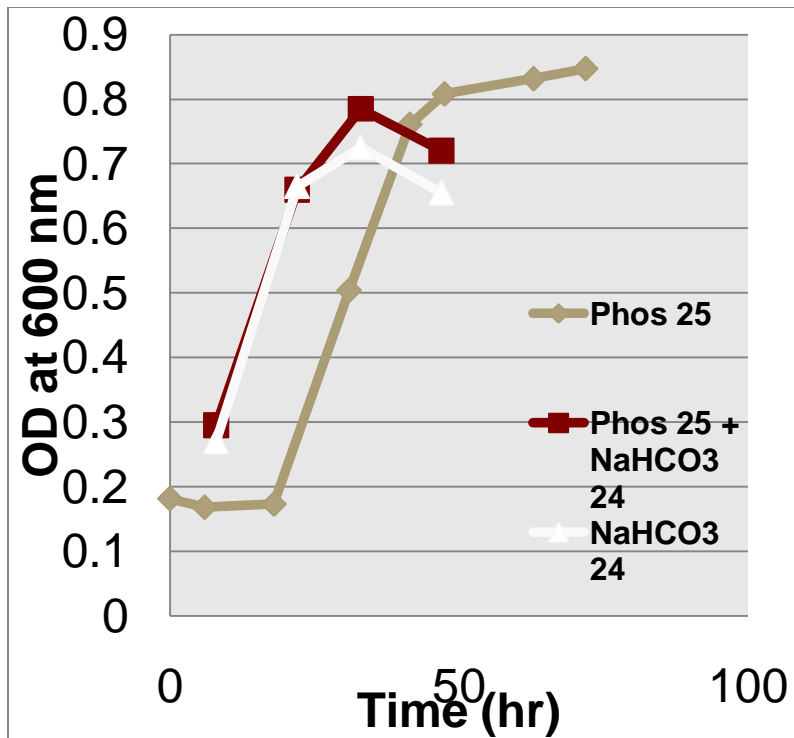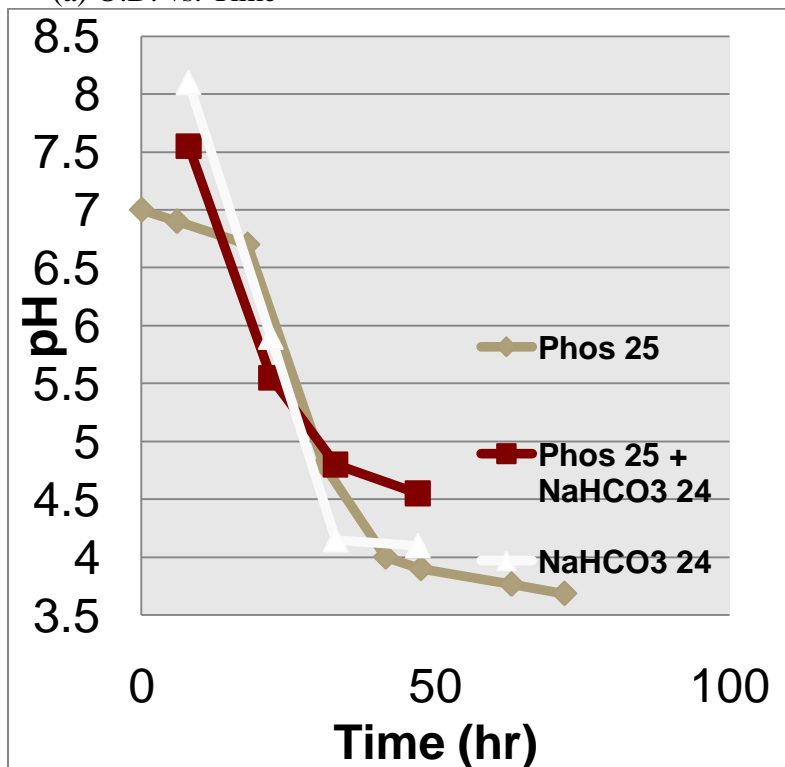
(a) O.D. vs. Time

(b) pH vs. Time

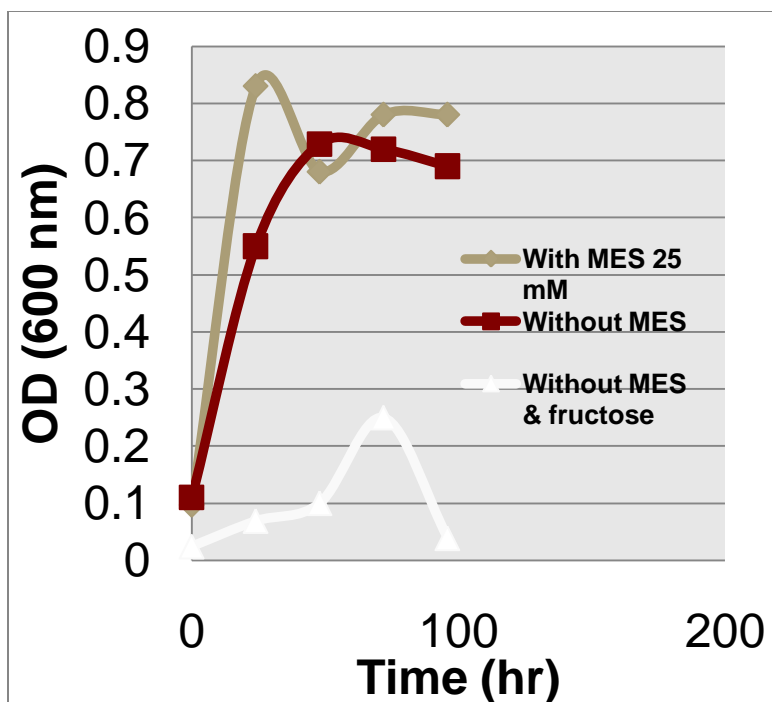Fig. 3. The effect of citrate-phosphate as the buffer solution on *Clostridium ljungdahlii*
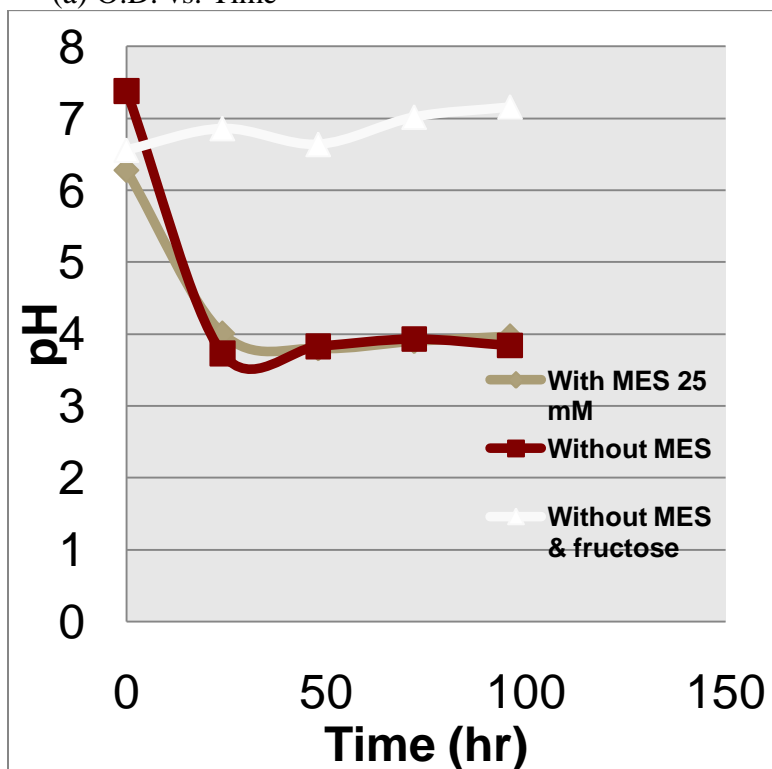
(a) O.D. vs. Time

(b) pH vs. Time

Fig. 4. The effect of phosphate-NaHCO$_3$ as the buffer solution on *Clostridium ljungdahlii*
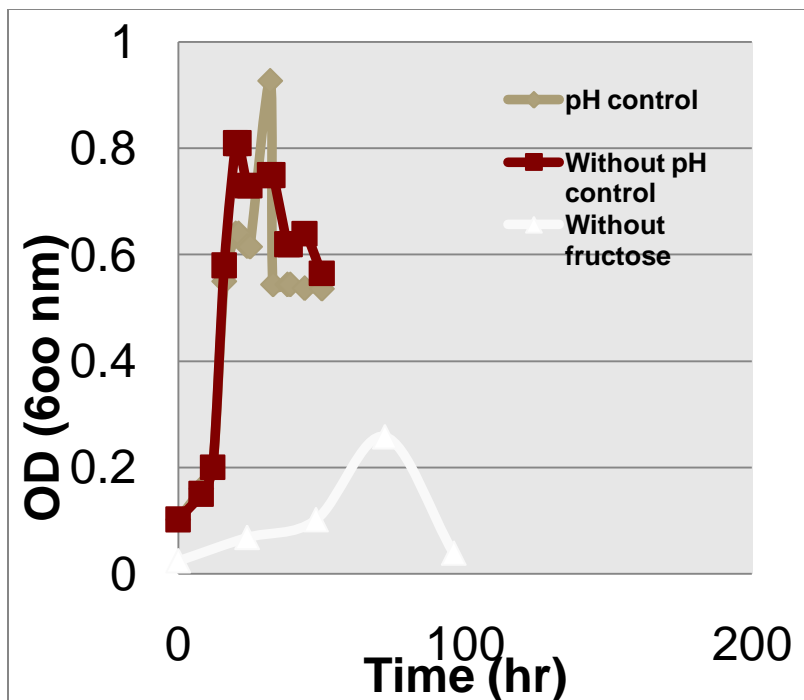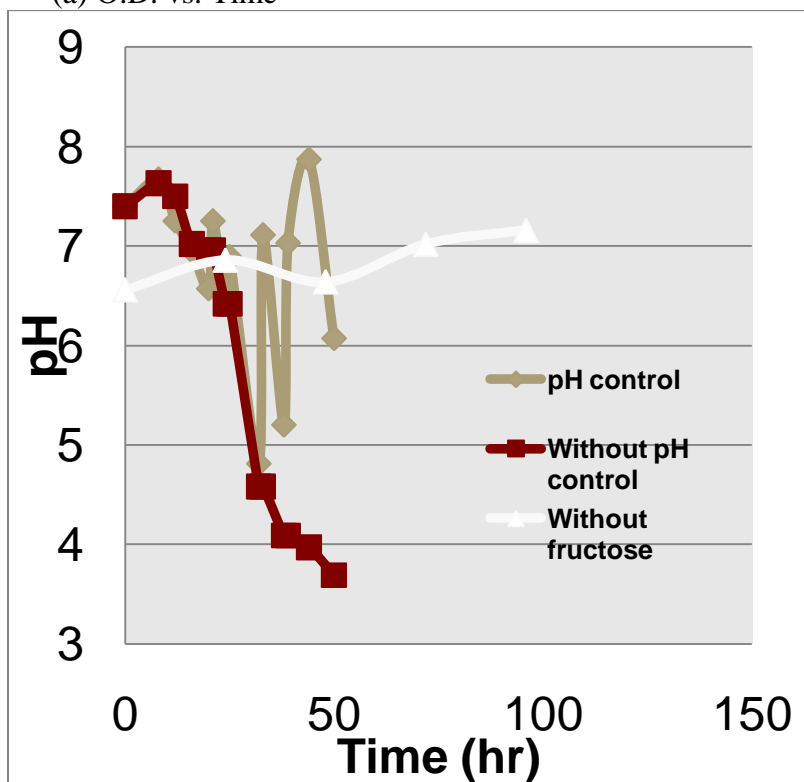
(a) O.D. vs. Time

(b) pH vs. Time

Fig. 5. The effect of MES (2-(*N*-morpholino) ethanesulfonic acid) as the buffer solution on *Clostridium ljungdahlii*

(a) O.D. vs. Time

(b) pH vs. Time

Fig. 6. The effect of controlling pH between 7.5 and 6.5 on *Clostridium ljungdahlii*
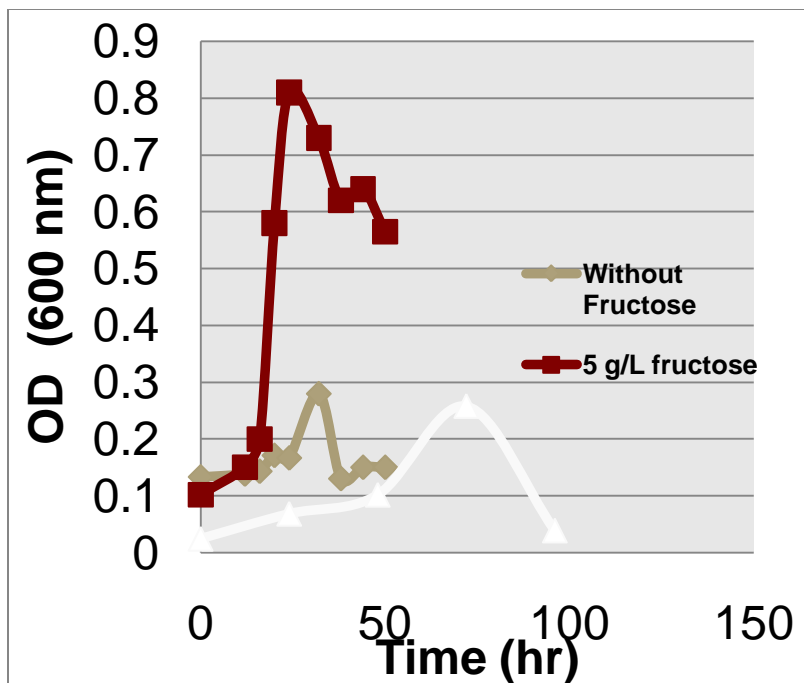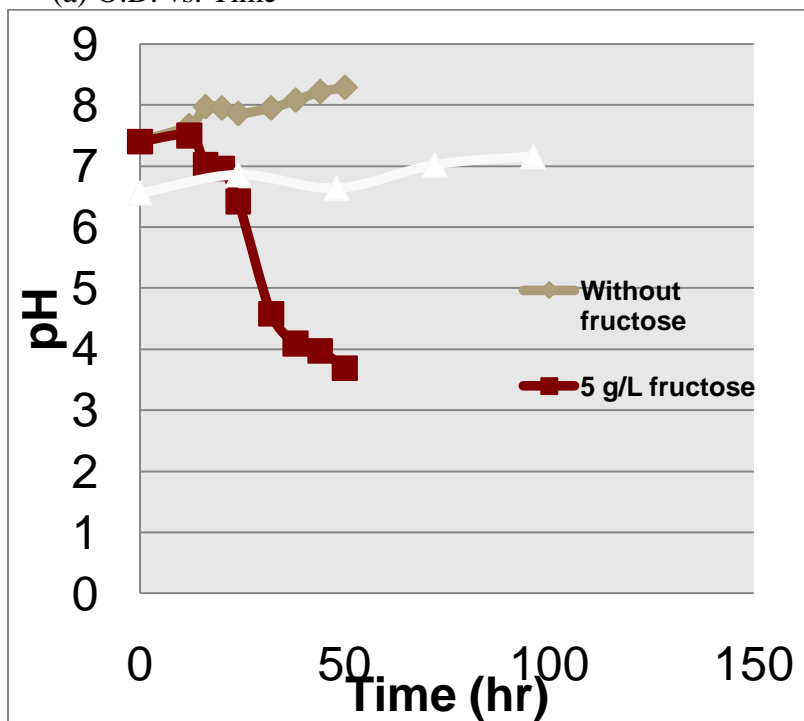
(a) O.D. vs. Time

(b) pH vs. Time

Fig. 7. The effect of the carbon source with and without fructose on *Clostridium ljungdahlii*
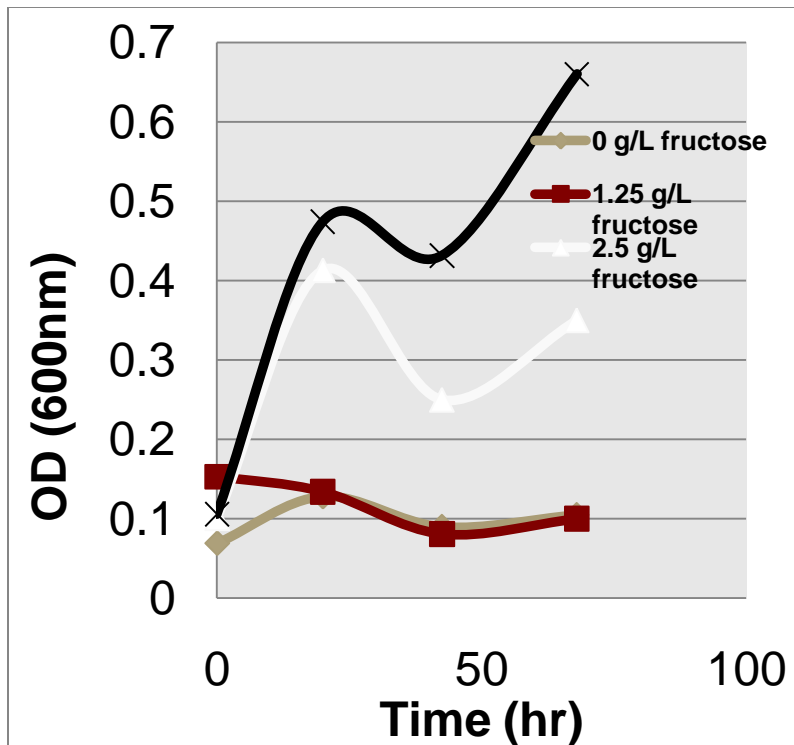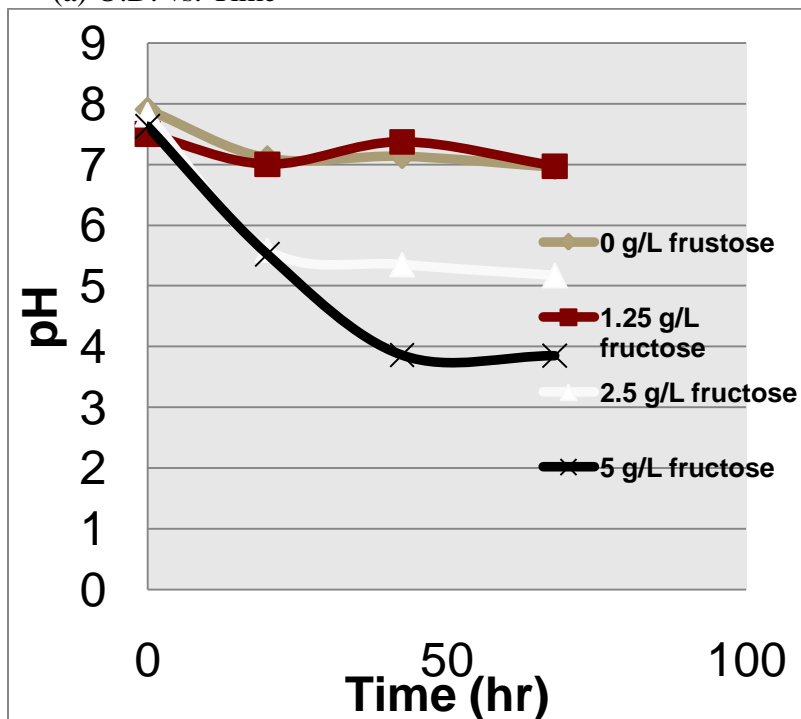
(a) O.D. vs. Time

(b) pH vs. Time

Fig. 8. The effect of the syngas supply composition of 15% H_2, 10% CO, 20% CO_2, and 55% N_2 with and without fructose on *Clostridium ljungdahlii*
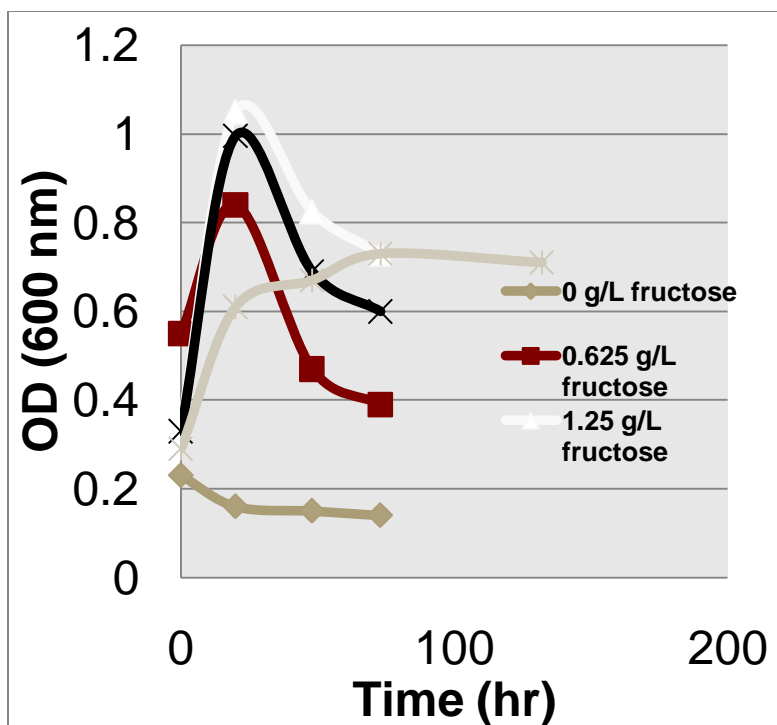
(a) O.D. vs. Time
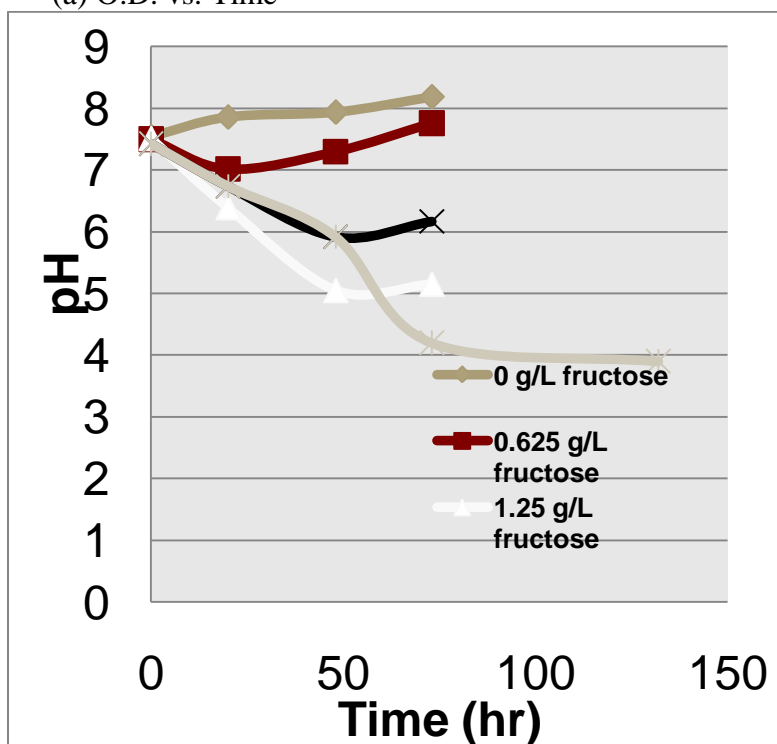
(b) pH vs. Time

Fig. 9. The effect of the syngas supply composition of 50% H_2 and 50% CO with and without fructose on *Clostridium ljungdahlii*
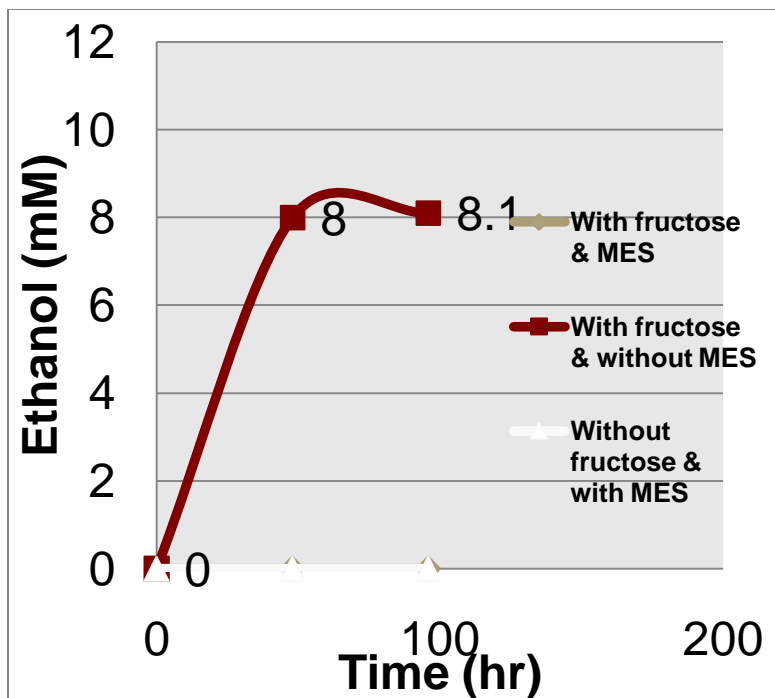
(a) Ethanol production vs. Time
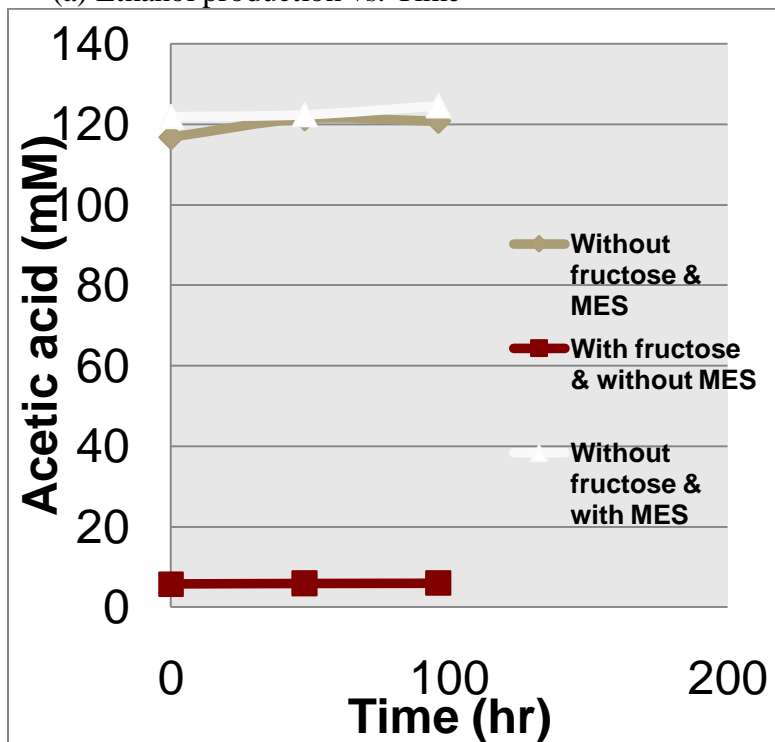
(b) Acetic acid production vs. Time
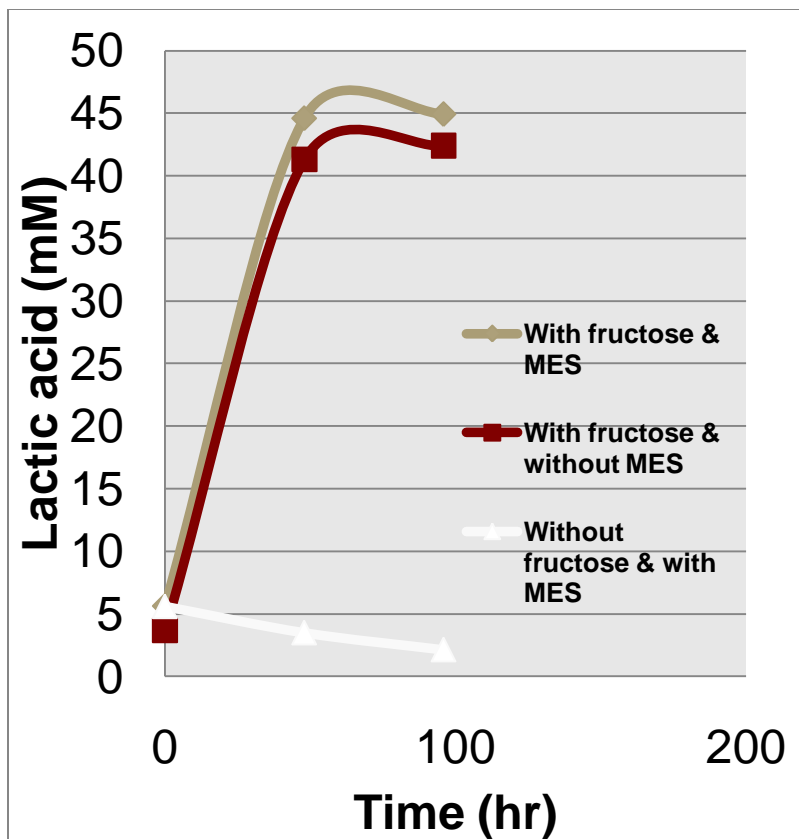
(c) Lactic acid production vs. Time

Fig. 10. Ethanol, acetic acid, and lactic acid production using 100% CO supply with and without fructose and MES on *Clostridium ljungdahlii*
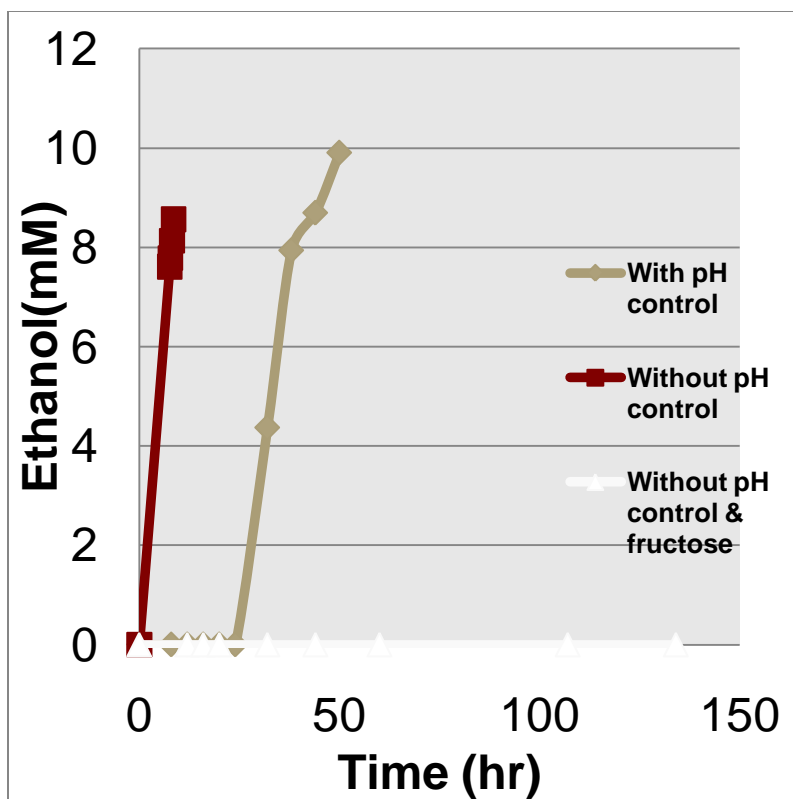
(a) Ethanol production vs. Time
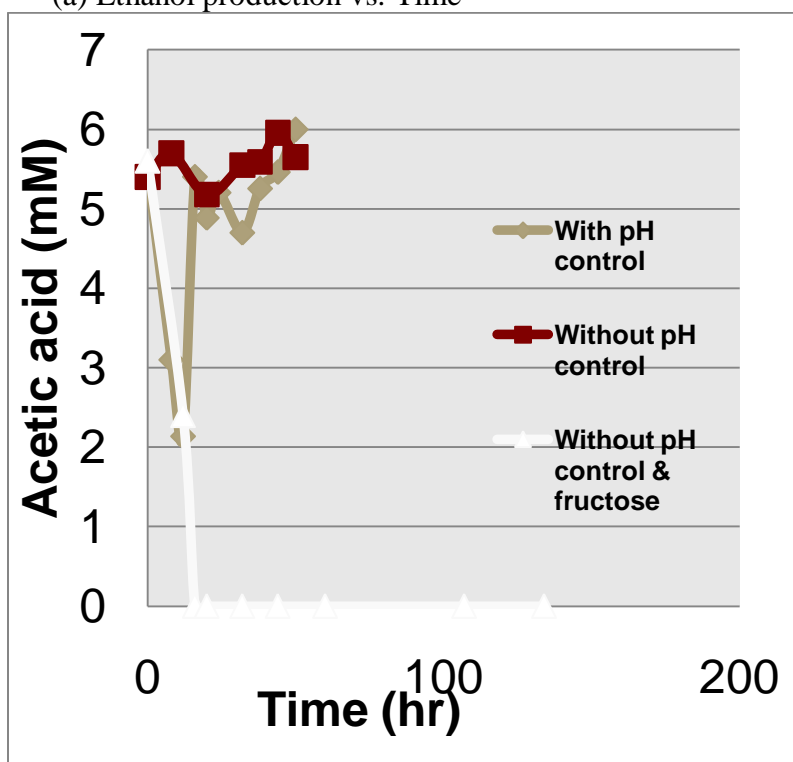
(b) Acetic acid production vs. Time
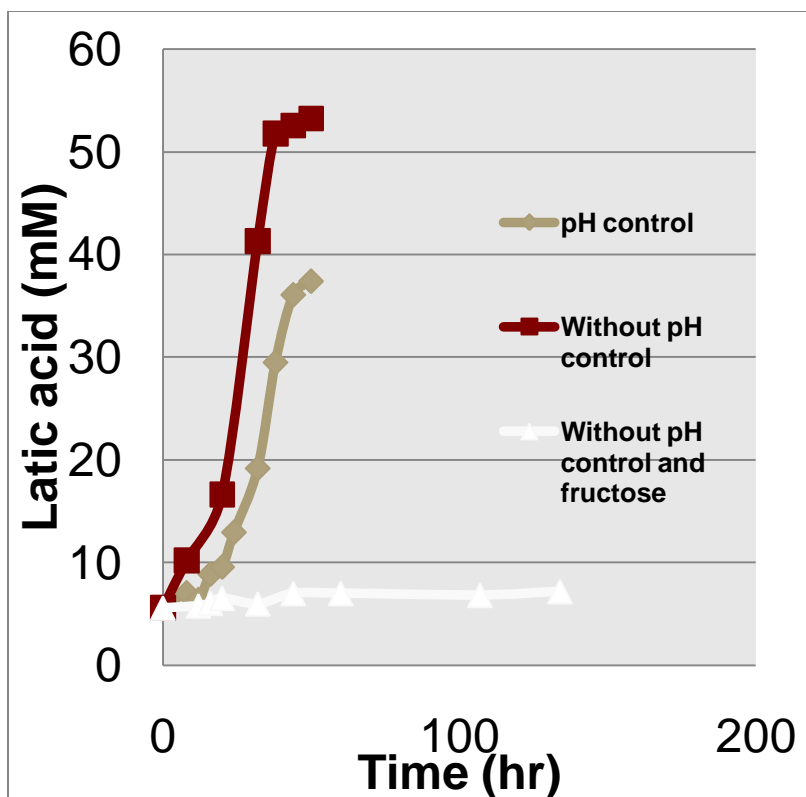
(c) Lactic acid production vs. Time

Fig. 11. Ethanol, acetic acid, and lactic acid production by controlling pH between 6.5 and 7.5 using 100% CO supply with and without fructose on *Clostridium ljungdahlii*
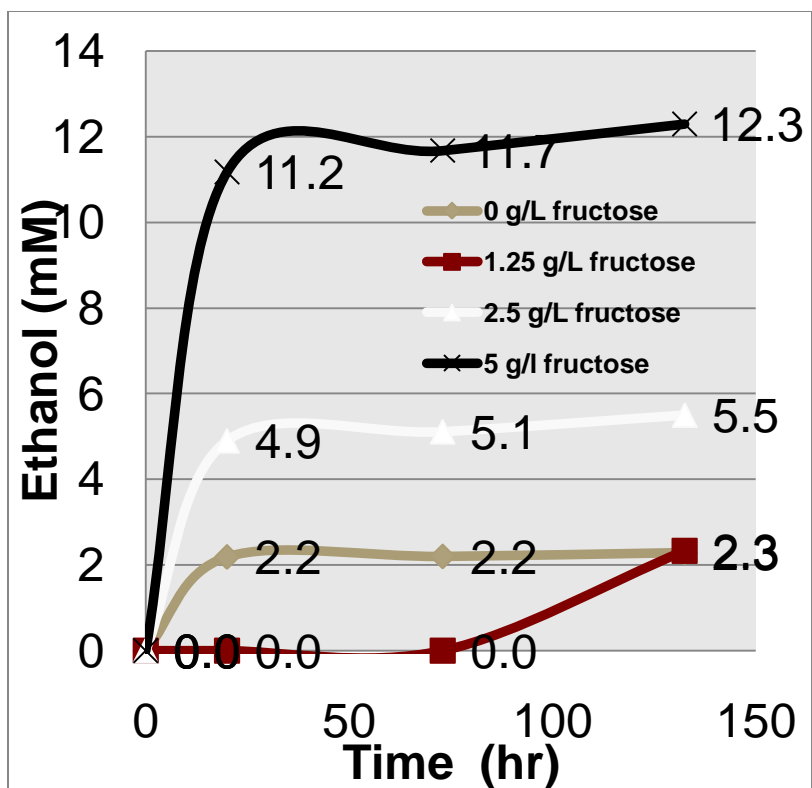
(a) Ethanol production vs. Time
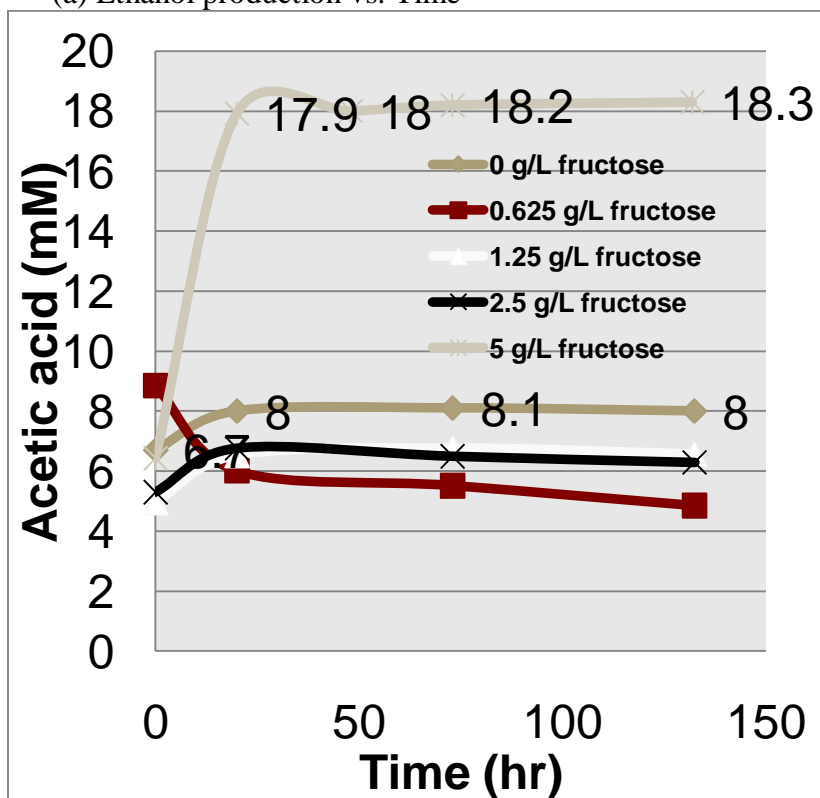
(b) Acetic acid production vs. Time
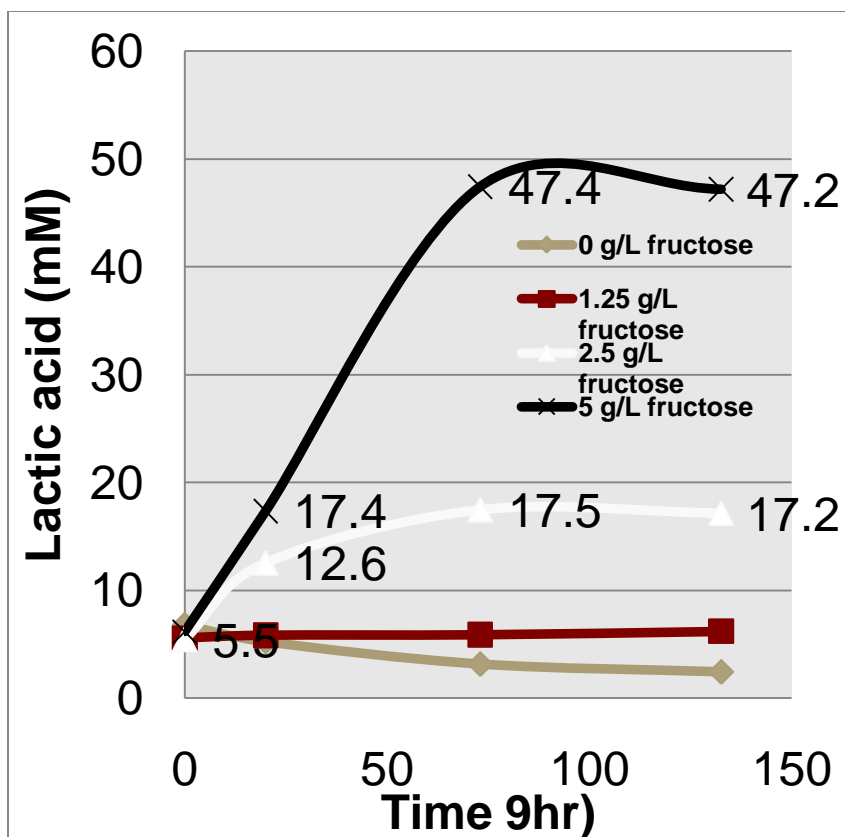
(c) Lactic acid production vs. Time

Fig. 12. Ethanol, acetic acid, and lactic acid production using the syngas supply composition of 15% H_2, 10% CO, 20% CO_2, and 55% N_2 with and without fructose on *Clostridium ljungdahlii*
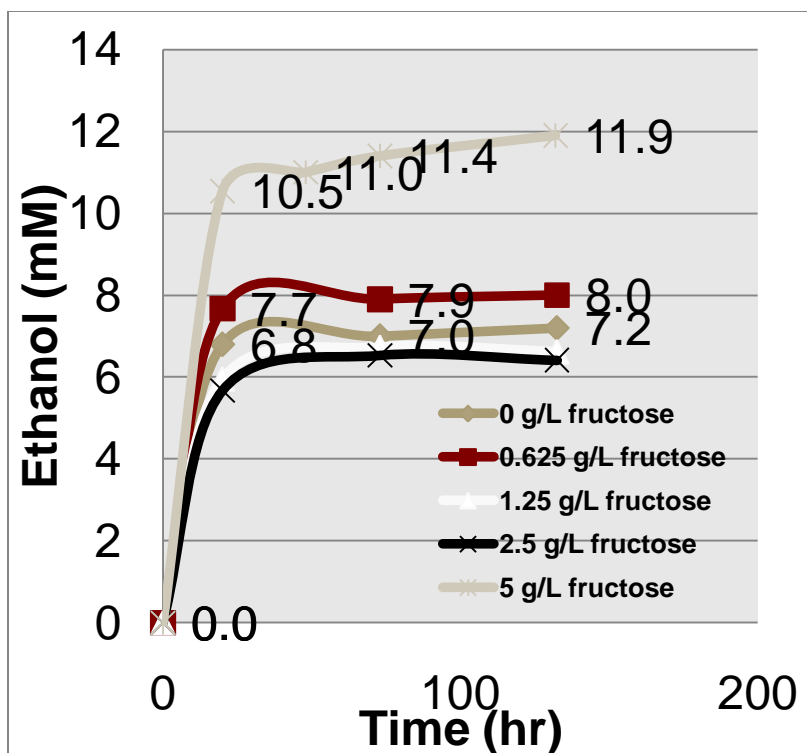
(a) Ethanol production vs. Time
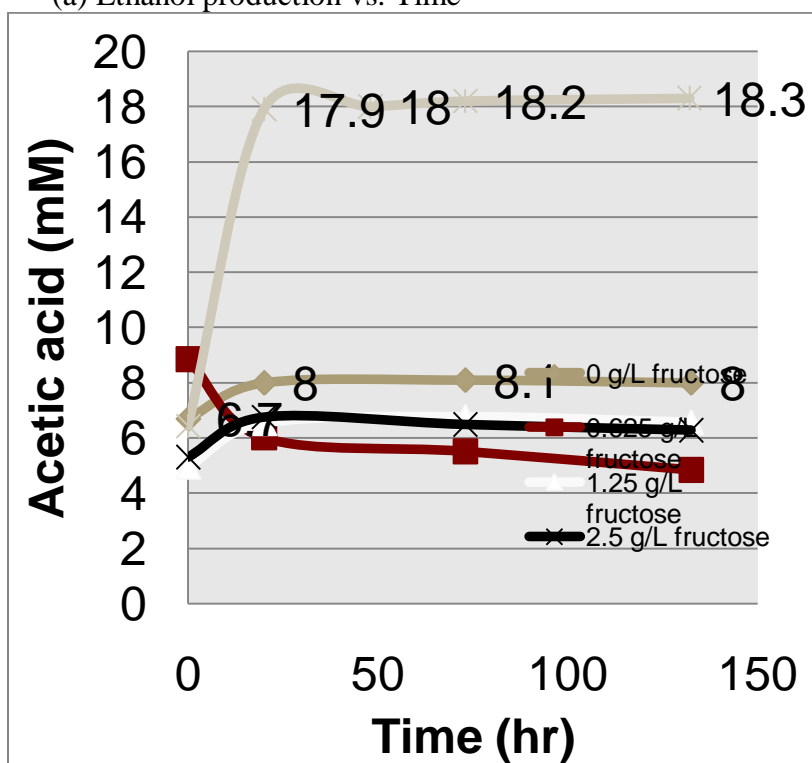
(b) Acetic acid production vs. Time
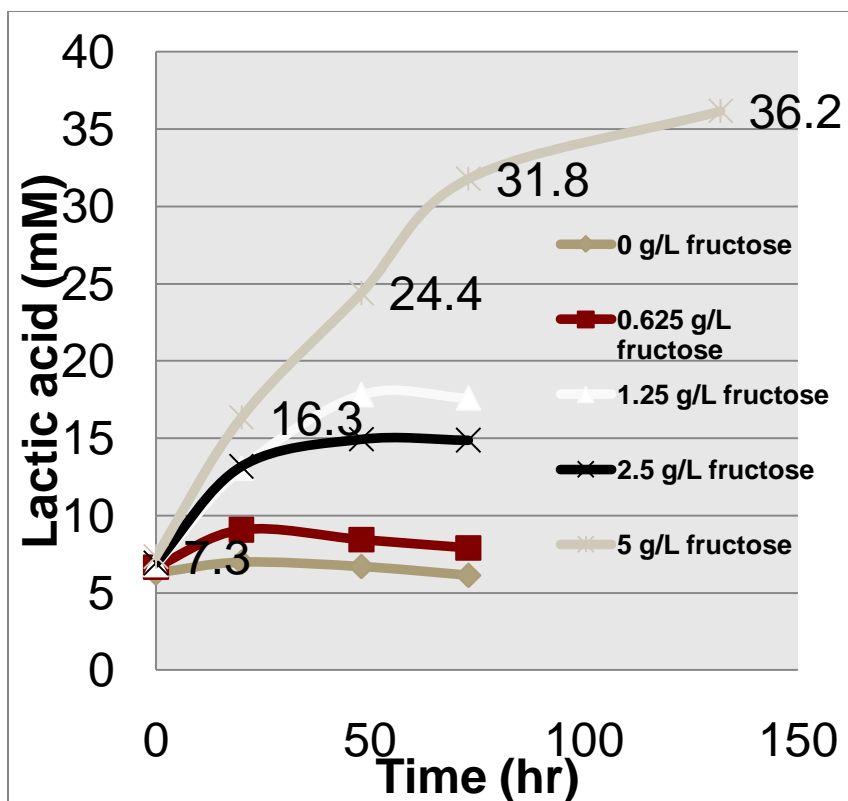
(c) Lactic acid production vs. Time

Fig. 13. Ethanol, acetic acid, and lactic acid production using the syngas supply composition of 50% H_2 and 50% CO with and without fructose on *Clostridium ljungdahlii*

Table 1. ATCC 1754 PETC medium composition in 1-L distilled water

Compounds	Amount
NH_4Cl (g)	1.0
KCl (g)	0.1
$MgSO_4 \cdot 7H_2O$ (g)	0.2
NaCl (g)	0.8
KH_2PO_4 (g)	0.1
$CaCl_2 \cdot 2H_2O$ (mg)	20.0
$NaHCO_3$ (g)	2.0
Fructose (g)	5.0
Nitrilotriacetic acid (g)	2.0
$MnSO_4 \cdot H_2O$ (g)	1.0
$Fe(SO_4)_2(NH_4)_2 \cdot 6H_2O$ (g)	0.8
$CoCl_2 \cdot 6H_2O$ (mg)	20.0
$ZnSO_4 \cdot 7H_2O$ (g)	0.2
$CuCl_2 \cdot 2H_2O$ (mg)	20.0
$NiCl_2 \cdot 6H_2O$ (mg)	20.0
$Na_2MoO_4 \cdot 2H_2O$ (mg)	20.0
Na_2SeO_4 (mg)	2.0
Biotin (mg)	2.0
[a] Reducing agent (ml)	10.0
Folic acid (mg)	2.0
Trace elements (ml)	10
Wolf's vitamin solution (ml)	10
Pyridoxine HCl (mg)	10.0
Thiamine HCl (mg)	5.0
Riboflavin (mg)	5.0
Nicotinic acid (mg)	5.0
Calcium D-(+) pantothenate (mg)	5.0
Cyanocobalamine (µg)	100.0
p-Aminobenzoic acid (mg)	5.0
Thioctic acid (mg)	5.0

[a] Reducing agent composition (per 100 ml): NaOH 0.9 g, L-cysteine·HCl: 4.0 g, and $Na_2S \cdot 9H_2O$: 4.0 g

Table 2. Summary of the buffer solution study on *Clostridium ljungdahlii*

Buffer solutions	Optimal OD	Note
NaHCO$_3$ 2 g/L	0.8	
Citrate 25 mM + NaHCO$_3$ 2 g/L	0.75	
Phosphate 25 mM + NaHCO$_3$ 2 g/L	0.79	
Citrate 25 mM + Phosphate 25 mM	0.7	
Phosphate 25 mM	0.84	Long lag phase
MES 25 mM + NaHCO$_3$ 2 g/L	0.83	
Manual controlling pH from 6.5 to 7.5 + NaHCO$_3$ 2 g/L	0.93	

Table 3. Summary of the carbon source study on *Clostridium ljungdahlii*

Gas Composition	Carbon Source	Optimal OD
	5 g/L fructose w/ MES	0.83
100% CO	5 g/L fructose	0.27
	0 g/L fructose w/ MES	0.26 (long lag time)

Table 4. . Summary of the syngas supply compositions on *Clostridium ljungdahlii*

Gas Composition	Carbon Source	Optimal OD
100% CO	5 g/L fructose	0.8
15% H_2, 10% CO, 20% CO_2, and 55% N_2	0 g/L fructose	0.13
	1.25 g/L fructose	0.15
	2.5 g/L fructose	0.40
	5 g/L fructose	0.66
50% H_2, 50% CO	0 g/L fructose	0.24
	0.625 g/L fructose	0.84
	1.25 g/L fructose	1.05
	2.5 g/L fructose	1.00
	5 g/L fructose	0.73

Table 5. Summary of the yield ratios of the end products

Syngas composition	conditions	Lactic acid (mM)	Acetic acid (mM)	Ethanol (mM)	Lactic acid /Ethanol	Ethanol/ Acetic acid
100 % CO	5 g/L fructose w/ MES	44.6	121.4	0	-	-
	5 g/L fructose	42.4	6.0	8.1	-	-
	0 g/L fructose w/ MES	5.6	124.6	0	-	-
	5 g/L fructose w/ pH control	37.4	6.0	9.9	3.7	1.6
	5 g/L fructose w/o pH control	41.3	5.5	8.5	4.8	1.5
	0 g/L fructose w/o pH control	7.2	5.7	-	-	-
	0 g/L fructose	5.2	10.3	2.2	2.4	0.2
15% H_2, 10% CO, 20% CO_2, and 55% N_2	1.25 g/L fructose	6.2	15.6	2.3	2.6	0.2
	2.5 g/L fructose	17.5	15.9	5.1	3.4	3.1
	5 g/L fructose	47.2	18.9	11.8	3.9	1.5
	0 g/L fructose	6.9	10	6.9	1.0	0.6
	0.625 g/L fructose	7.9	4.4	8	0.98	1.6
50% H_2 and 50% CO	1.25 g/L fructose	17.6	6.6	6.6	2.7	1.0
	2.5 g/L fructose	15.0	6.5	6.5	2.4	1.0
	5 g/L fructose	36.2	18.3	11.6	3.1	0.63

Table 6. The pH effect on ethanol production by *Clostridium ljungdahlii*

Initial pH	Final pH	Acetic acid (mM) at 58 h	Ethanol (mM) at 58 h	OD (600nm) at 58 h
4.0	3.3	3.3	0	0.41
4.6	3.	4.1	0	0.43
4.9	3.4	1.3	0.6	0.44
5.3	3.5	5.6	0	0.41
6.0	4.1	2.0	0	0.40

CHAPTER 5. SYNGAS FERMENTATION TO ETHANOL USING HOLLOW FIBER MEMBRANE AS GAS DELIVERING SYSTEM

Po-Heng Lee, Dong-Won Choi, and Shihwu Sung

Department of Civil, Construction and Environmental Engineering,

Iowa State University, Ames, IA 50011, USA

Abstract

The mass transfer of carbon monoxide (CO) to liquid through hollow fiber membrane was examined for syngas fermentation in which gas transfer is regarded as a limiting step. The design of using a hollow fiber membrane as a syngas delivering system was demonstrated to produce ethanol at 6 g/L using the fructose-free medium with an ethanol to acetate ratio of 2.6, which was the highest ratio in comparison with other previous studies. The use of HFM in syngas fermentation is an innovative approach which can eliminate the mass transfer barrier compared to conventional reactor designs.

1. Introduction

Consumption of unsustainable fossil fuels for energy in human activities results in severe environmental threats, and seeking a reliable and economical alternative energy source has raised a lot of attention recently. Hence, seeking an alternative way to produce energy is a vital issue in today's society. One of the potential solutions is to convert

inexpensive lignocellulosic biomass like straw, wood, and corn stover, which is available in many forms, into fuels. Consequently, it would reduce the stress of dependence on fossil fuels and alleviate environmental concerns (Worden *et al*., 1991). The typical fuel production technology from lignocellulosic biomass is through physicochemical and/or enzymatic hydrolysis followed by fermentation of the formed sugars. This process, however, faces several challenges. These include high enzyme cost and unwanted by-products in physicochemical hydrolysis (Henstra *et al.,* 2007). Moreover, lignin composed of 10-40% lignocellulose cannot be converted to sugars in any known hydrolysis method, which reduces the effectiveness of utilization of lignocellulosic biomass (Bredwell *et al.,* 1999). Another existing technology that could convert biomass into fuels is the hybrid thermochemical/biological approach for the potential commercialization necessary to the address fossil fuel replacement. The process starts with the gasification of biomass to produce synthesis gas (syngas) that is a gas mixture of carbon monoxide (CO), hydrogen (H_2), carbon dioxide (CO_2) and Nitrogen (N_2). Then, syngas serves as a microorganism substrate for several microbial metabolisms and synthesizes various valuable fuels including ethanol and butanol (Henstra *et al.,* 2007).

Many early researches were conducted to produce acetate and butyrate using CO as a substrate. *Eubaterium limosum* isolated from various environments, e.g. human intestine, sewage, rumen, and soil, produces acetate and butyrate exclusively using CO as the sole energy source (Genthner *et al.,* 1982 and 1987). Other acetogens, including *Clostridium aceticum, Peptosteptococcus productus*, etc, were identified to be able to produce acetate from syngas. *Butyribacterium methylotrophicum* has demonstrated its ability to shift

production from acetate to butyrate by inducing pH changes during the fermentation (Grethlein *et al.,* 1991; Lynd *et al.,* 1982; Shen *et al.,* 1999). *Acetobacterium woodii* is also one of the mesophiles capable of producing acetate from CO. However, the research trend of syngas fermentation has shifted from volatile acid production to production of fuel or other high-value derivatives (Genthner *et al.,* 1987).

Microbial production of acetate, formate, butyrate, ethanol, butanol, and hydrogen has been considered to have industrial application in recent years. Among the well-studied microbes, *Clostridium ljungdahlii*, a Gram-positive, motile, rod-shaped anaerobe, was isolated from chicken yard waste. *C. ljungdahlii* grows on syngas in pH 4-7 producing ethanol and acetate (Tanner *et al.,* 1993). It has been used in full-scale production of ethanol from syngas in a commercial process involving gasification, fermentation, and distillation. *Clostridium autoethanogenum* was also reported to be capable of producing ethanol and acetate from CO and CO_2. The conversion efficiency of *C. autoethanogenum* from syngas to alcohol and acetate, however, was much lower than that of *C. ljungdahlii* (Cotter *et al.,* 2009). Another bacterium, *Clostridium carboxidivprans P7*, recently isolated from sediment of an agricultural settling lagoon, was reported to produce acetate, ethanol, butyrate, and butanol from CO and H_2 (Liou *et al.,* 2005). Currently, the most attractive syngas fermentation process is using *C. carboxidivprans P7* to produce butanol, which has a higher energy content, lower vapor pressure and is less corrosive than ethanol.

A photosynthetic purple nonsulfur bacterium, *Rhodospirillum rubrum*, can use CO as the sole carbon and energy source under anaerobic conditions, in the presence or absence of light, to produce H_2 and Poly-β-hydroxyalkanoate (PHA) (Kerby *et al.,* 1995; Do *et al.,* 2007). PHA is a biodegradable plastic with many potential applications, including use as food additive and as the material for bone reconstruction. Thermophilic fermentation has the advantages of less cooling requirement of syngas, high conversion rates, and a separation benefit for alcohols; however, higher temperatures would reduce the syngas solubility (Henstra *et al.,* 2007). Gram-positive thermophiles that can convert CO and H_2O into H_2 and CO_2 also have been isolated recently, including *Carboxydothermus hydrogenoformans* and *Thermolithobacter carboxydivorans.* Other thermophiles, such as *Moorella thermoautotrophica* and *Moorella thermoacetic,* have been reported to use CO producing acetate. However, no thermophiles have been reported to be able to convert CO into fuels (such as ethanol or butanol).

Syngas fermentation could offer several potential advantages over its counterpart-syngas mental-catalyst method, which include higher specificity of the biocatalyst (Klasson *et al.,* 1992). However, the poor solubility of syngas in the aqueous phase (e.g. the solubility of CO is 77% that of oxygen) would limit the full-scale application of syngas fermentation in a bubble sparging fermentor that is commonly used in the fermentation industry (Kapic *et al.,* 2006; Henstra *et al.,* 2007).

Microporous hollow fiber membranes with a hydrophobic surface would enhance the gas-to-liquid mass transfer. The syngas fed to the inside of the hollow fiber membrane

diffuses through the wall of the membrane and dissolves into the aqueous phase on the outside of membrane. The gaseous diffusion by membranes is known to be more efficient than bubble sparging in oxygen and H_2 transfer (Cote *et al.,* 1988; Ahmed *et al.,* 2004). Syngas fermentation using hollow fiber membranes as the gas delivering system, however, has not been reported yet. The objective of this study was to evaluate the performance of the hollow fiber membrane syngas fermentor by *Clostridium ljungdahlii*. Accordingly, the study focuses on determining the operating parameters, i.e. syngas supply flow rate and pH for improvement of ethanol production by syngas fermentation.

2. Materials and Methods

2.1. Reactor setup

Polypropylene hollow fiber membranes manufactured by C2L ENVIRONMENTAL MEMBRANE, LLC (Hangzhou, China) were used in this study. The outer diameter, wall thickness, porosity, and nominal pore size were 426 µm, 50 µm, 40%, and 0.2 µm, respectively. 400 fibers was potted into a Plexiglas insert (inner diameter of 1.90 cm) using Alumilite Regular (Alumilite Corp., Kalamazoo, MI). The length of fibers above the insert was controlled to be 25.0 cm. The other free ends of the fibers were heat-sealed. The insert with fibers was then combined to an external glass shell (inner diameter of 2.54 cm) as shown in Fig 1 (a) and (b). The working volume of the hollow fiber membrane reactor was 0.13 L. A schematic of CO transfer experimental setup is shown in Fig. 1 (c). The membrane reactor was connected to an artificial syngas supply and a reservoir. The artificial syngas was composed of 50% CO, 30% H_2, and 20% CO_2. The 2.4-L reservoir was employed for liquid recirculation and CO mass transfer assay

(Ahmed *et al.,* 2004). In the experiment, the membrane reactor and the reservoir were filled with distilled water. The water was re-circulated using a peristaltic pump (Masterflex I/P 7521-50, Cole-Parmer Inc., Vernon Hills, IL, USA) at a flow rate of 0.31 to 1.07 L/min providing cross flow velocity of 1.02 to 3.52 cm/sec in the membrane reactor. The reservoir was mixed at 90 rpm. Artificial syngas was transferred across the membrane at 50, 150, and 250 ml/min. The mixed-liquor samples were withdrawn through the septa in sampling port using 3-mL syringe. The experiment was performed at 35°C which is the optimal growth condition for *Clostridium ljungdahlii* (Bredwell *et al.,* 1999).

2.2. Organisms and anaerobic medium preparation

In this study, a pure culture of *Clostridium ljungdahlii* purchased from American Type Culture Collection (ATCC), 55383, University Boulevard, Manassa, Virginia, 20110-2209 USA, was used. The inoculum bacterium was grown on ATCC 1754 PETC medium at 35 ^{o}C in sealed stopper hypovials (total volume, 120 ml). This basal mediumcomposition is summarized in Table 1. All media for the studies were prepared anaerobically. Heat stable ingredients were combined and the medium was then boiled and cooled under an argon purge to drive off dissolved oxygen. Two-liter of the deoxygenated medium was transferred to the in a Coy anaerobic chamber with an atmosphere containing 3% H_2 and 97% Ar (Coy Laboratory Products, Inc.). A bottle with 2 L of the deoxygenated medium was capped, and its connecting tubes were sealed with clappers. It was then removed from the chamber, and sterilized at 121$\circ$C for 15 min.

After autoclaving, the 2-L sterilized medium was transferred by a pump into the reservoir

of the hollow fiber membrane fermentor that had been degassed using the artificial syngas at a flow rate of 100 ml for 3 hrs. Heat sensitive ingredients (vitamins and a reducing agent) were reconstituted from a concentrated solution with anaerobic de-ionized water in the anaerobic chamber. These ingredients were filter sterilized and injected into the medium in the 2-L working volume reservoir. The medium were inoculated with 10 ml inoculums.

2.3. Operating parameters

Two operating parameters, i.e. pH and syngas supply flow rate, were investigated to optimize the ethanol production by *C. ljungdahlii* in the growth phase and production phase. pH were controlled manually by adding NaOH and HCl. Syngas flow supply rate was controlled by a control program developed in Labview version 8.2.

2.4. Analytical procedures

Cell density: A 200 μl aliquot from the well-mixed hypovail sample was diluted to 1,000 μl by adding deionized (dI) water in a 1.5 ml disposable polystyrene cuvette (Fisher Scientific). A Cary 50 Conc UV-Visible spectrophotometer (Varian) equipped with the Varian software, Simple Reads, was used to determinate cell density. The measured values were obtained by setting up in the spectrophotometer at an absorbance of 600 nm, a sampling rate of 80 Hz, and a reading period of 3 second. A blank of deionized (dI) water was used as a zero reference. The blank cuvette was re-read at the end of each session in order to check for baseline drift during analysis.

Lactic acid, acetic acid, and ethanol concentration determination: The concentrations of lactic acid, acetic acid, and ethanol were analyzed using a Waters high pressure liquid chromatograph (HPLC). The HPLC system (Millipore Corporation, Milford, MA, USA) included a Waters model 401 refractive index detector, column heater, auto-sampler and computer controller. The Bio-Rad Aminex HPX-87H column (7.8×300 mm; Bio-Rad Chemical Division, Richmond, CA, USA) was used to separate the samples with 0.012 N sulfuric acid as a mobile phase at 0.8 ml/min, an injection volume of 20 μl, and a column temperature of 65 $^{\circ}$C. After harvesting the samples, the samples were centrifuged at 9000 rpm for 10 min and filtered by using Whatman PP 0.45 μm syringe filters. All analyses were carried out in triplicate with the same samples and the mean values reported.

3. Results and discussion

3.1. The effects of syngas flow rate on ethanol production by *C. ljungdahlii* controlling between 6.5 and 7.5 in both of the growth and production phase

Three different experiments were studied to investigate the effects of syngas flow rate on ethanol production by *C. ljungdahlii* controlled between 6.5 and 7.5 in both the growth and production phase. The first stage (grow phase) was operated for 10 days using the medium containing fructose. The second stage (production phase) was operated for 5 days using the medium without fructose. Figs 2, 3, and 4 present the results at the syngas flow rate of 50, 150, and 250 ml/mim syngas. The syngas composition was 50 % CO, 30% H_2, and 20% CO_2. The highest ethanol and acetate production were 60 mM of ethanol and 45 mM of aceate at the syngas supply flow rate of 150 ml/mim. For the result at the syngas supply flow rate of 250 ml/mim, the optimal production was 59 mM of

ethanol and 46 mM of acetate. This result could affirm that a higher syngas flow rate does not increase the production rate result from substrate inhibition.

3.2. The effects of syngas flow rate on ethanol production by *C. ljungdahlii* controlling the production phase at pH 5

Two different syngas flow rates (50 and 150 ml/mim) were studied to investigate the effects of syngas flow rate on ethanol production by *C. ljungdahlii* while controlling pH at 5 in production phase, while pH was maintained between 6.5 and 7.5 in the growth phase. The first stage (growth phase) was operated for 10 days using the medium containing fructose. The second stage (production phase) was operated for 5 days using the medium without fructose. Figs 5 and 6 present the results at the syngas flow rates of 50 and 150 ml/mim. The highest ethanol and acetate production were 60 mM and 30 mM, respectively, at the syngas supply flow rate of 150 mL. For the result at the syngas supply flow rate of 50 mL, the optimal production was 42 mM of ethanol and 19 mM of acetate. The optical density was 0.7 for the syngas supply flow rate of 150 ml/mim and 0.6 for the syngas supply flow rate of 50 ml/mim so that the productivity did not improve in comparison with the results of the section 3.3.

3.3 The effects of syngas flow rate on ethanol production by *C. ljungdahlii* controlling the production phase at pH 5 by retaining the biomass from the semi-batch mode.

In order to retain the biomass in the fermentor, the operating mode was changed to the semi-batch mode (after the growth phase, the mixed-liquor was settled for 30 min and then decanted). Two different syngas flow rate (200 and 250 ml/min) were studied to

investigate the effects of syngas flow rate on ethanol production by *C. ljungdahlii* with controlled pH at 5 in the production phase. Figure 7 and 8 show the results of these two experiments. The highest ethanol and acetate production were 125 mM and 40 mM, respectively, at the syngas supply flow rate of 200 ml/mim. For the result at the syngas supply flow rate of 250 ml/mim, the optimal production was 120 mM of ethanol and 43 mM of acetate.

Table 2 summarizes the production ratios of ethanol to acetate in varied conditions. The average ethanol to acetate ratios for the growth phase, the lag phase, and the production phase were 1.6, 1.1, and 2.6. It demonstrates that the metabolism of *C. ljungdahlii* during the fermentation could be expected. Table 3 summarizes the maximum product from different studies. Most of the studies used the recommended medium from ATCC, which includes fructose in it. This study was conducted without the fructose in the medium. The result, therefore, is also very attractive compared with the previous studies.

4. Conclusion

The design of using hollow fiber membranes as a syngas delivering system was demonstrated to produce ethanol at 6 g/L using the fructose-free medium with an ethanol to acetate ratio of 2.6, which was the highest ratio in comparison with other previous studies. The use of HFM in syngas fermentation is an innovative approach which can eliminate the mass transfer barrier observed in conventional reactor designs.

5. References

Amed, A., Cateni, B.G., Huhnke, R.L., Lewis, R.S. (2006) Effects of biomass-generated producer gas constitutes on cell growth, product distribution and hydrogenase activity of *Clostridium carboxidivorans* P7, *Biomass Bioeng*. 30, 665–672.

Bredwell, M.D., Srivastava, P., and Worden, R.M. (1999) Reactor design issues for synthesis gas fermentations, *Biotechnol. Prog*. 15, 834–844.

Cote PL, Bersillon J-L, Huyard A (1988) Bubble-free aeration using membranes: Mass transfer analysis. J Membrane Sci 47: 91-106.

Do, Y.S., Smeenk, J., Broer, K.M., Kisting, C., Brown, R., Heindel, T.J., Bobik, T.A., and Dispirito, A.A. (2007) Growth of *Rhodospirillum rubrum* on synthesis gas: conversion of CO to H_2 and poly-beta-hydroxyalkanoate, *Biotechnol. Bioeng*. 97, 279–86.

Genthner, B.R.S. and Bryant, M.P. (1987) Additional characteristics of one-carbon-compound utilization by *Eubacterium limosum* and *Acetobacterium woodii*, *Appl. Environ. Microbiol.* 53, 471–476.

Genthner, B.R.S. and Bryant, M.P. (1982) Growth of *Eubacterium limosum* with carbon monoxide as the energy source. *Appl. Environ. Microbiol.* 43, 70–74.

Grethlein, A.J., Worden, R.M., Jain, M.K., and Datta, R. (1991) Evidence for production of n-butanol from carbon monoxide by *Butyribacterium methylotrophicum*, *J. Ferment. Bioeng*. 72, 58–60.

Kapic, A., Jones, S.T., and Heindel, T.J. (2006) Carbon monoxide mass transfer in a syngas mixture, *Ind. Eng. Chem. Res*. 45, 9150–9155.

Liou, J.S.C., Balkwill, D.L, Drake, G.R., and Tanner, R.S. (2005) *Clostridium carboxidivorans* sp. nov., a solvent-producing clostridium isolated from an agricultural settling lagoon, and reclassification of the acetogen *Clostridium scatologenes* strain SL1 as *Clostridium drakei* sp. nov. *Int. J. Syst. Evol. Microbiol.* 55, 2085–2091.

Lynd, L., Kerby, R., Zeikus, J.G. (1982) Carbon monoxide metabolism of the methylotrophic acidogen *Butyribacterium methylotrophicum*, *J. Bacteriol*., 149, 255–263.

Henstra, A.M., Sipma, J., Rinzema, A., and Stams, A.J.M. (2007) microbiology of synthesis gas fermentation for biofuel production, *Current Option in Biotechnol.,* 18, 200–206.

Kerby, R.L., Ludden, P.W., and Roberts, G.P. (1995) Carbon monoxide dependent growth of *Rhodospirillum rubrum*, *J. Bacteriol.* 177, 2241–2244.

Klasson KT, Ackerson MD, Clausen EC, Gaddy JL (1993) Biological conversion of coal and coal-derived synthesis gas. Fuel 72: 1673-1678.

Najafpour, G. and Younesi, H. (2006) Ethanol and acetate synthesis from waste gas using batch culture of *Clostridium ljungdahli*, *Enzyme Microbial Technol*. *38*, 223–228.

Shen, G.J., Shieh, J.S., Grethlein, A.J., Jain, M.K., and Zeikus, J.G. (1999) Biochemical basis for carbon monoxide tolerance and butanol production by *Butyribacterium methylotrophicum*, *Appl. Microbiol. Biotechnol.* 51, 827–832.

Worden, R.M., Grethlein, A.J., Jain, M.K., and Datta, R. (1991) Production of butanol and ethanol from synthesis gas via fermentation, *Fuel* 70, 615–619.

Younesi, H., Najafpour G., Mohamed, A.R. (2006) Liquid fuel production from synthesis gas via fermentation process in a continuous tank bioreactor (CSTR) using Clostridium ljungdahlii, *Iranian J. Botechnol.* 4, 45–53.
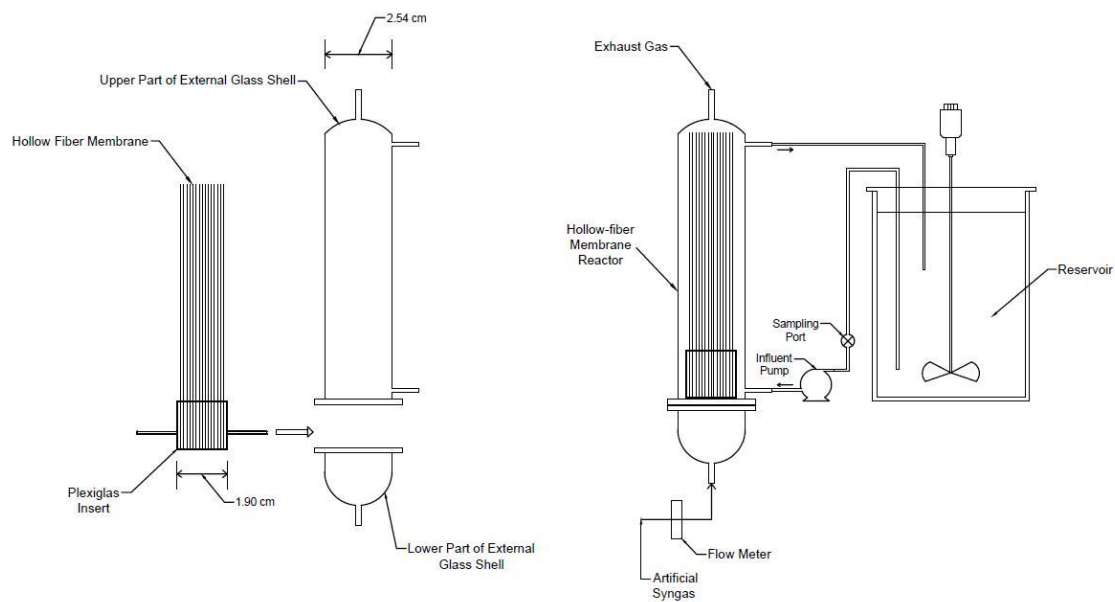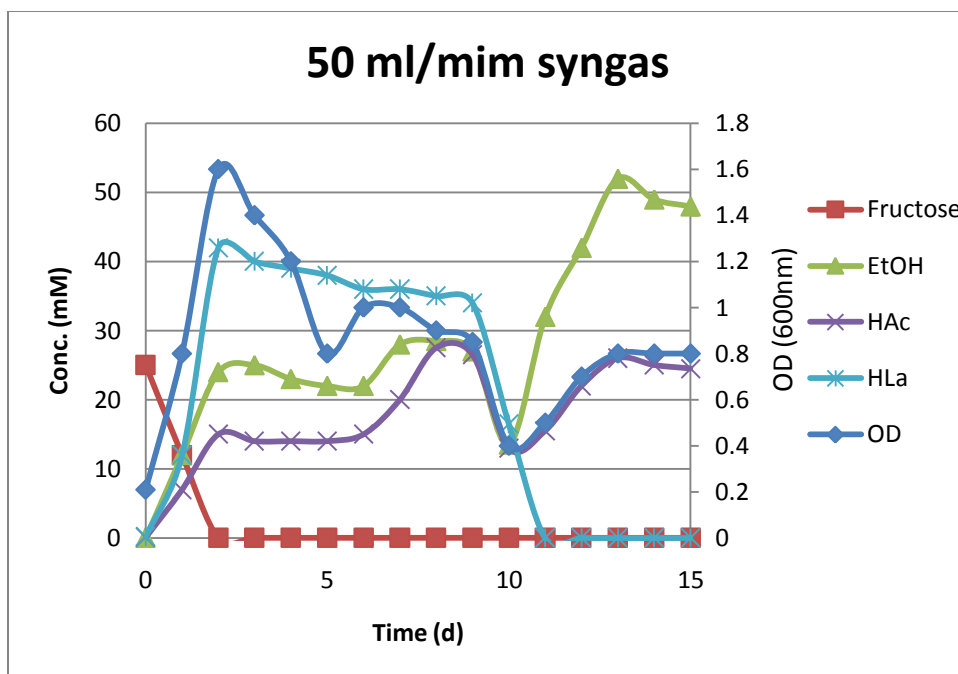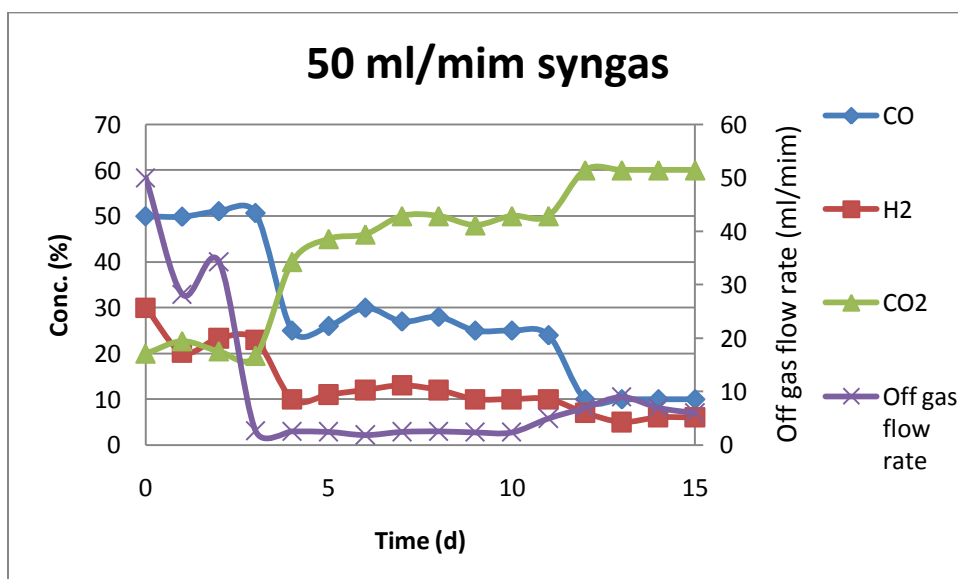
Figure 1. Schematic diagram of experimental setup. (a) Hollow fiber membrane module, (b) Hollow fiber membrane reactor, (c) CO transfer experiment

(a) Production and cell density vs. Time

(b) Off-gas flow rate and composition vs. Time

Figure 2. The end product production by *C. ljungdahlii* at a flow rate of 50 ml/mim of syngas supply controlling between 6.5 and 7.5

(a) Production and cell density vs. Time

(b) Off-gas flow rate and composition vs. Time

Figure 3. The end product production by *C. ljungdahlii* at a flow rate of 150 ml/mim of

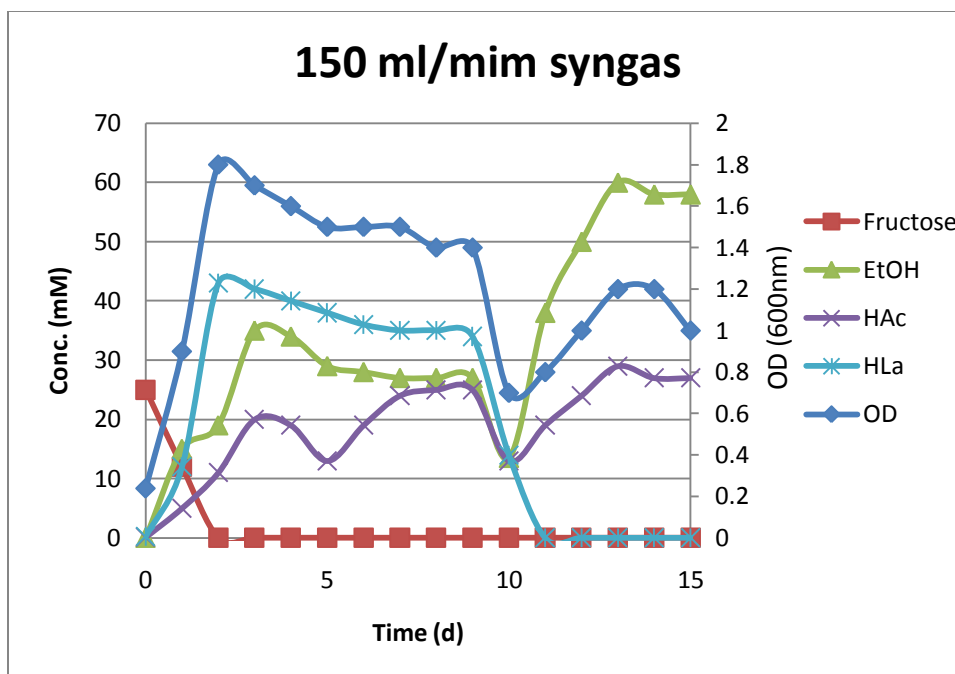syngas supply controlling between 6.5 and 7.5

(a) Production and cell density vs. Time

(b) Off-gas flow rate and composition vs. Time

Figure 4. The end product production by *C. ljungdahlii* at a flow rate of 250 ml/mim of

syngas supply controlling between 6.5 and 7.5

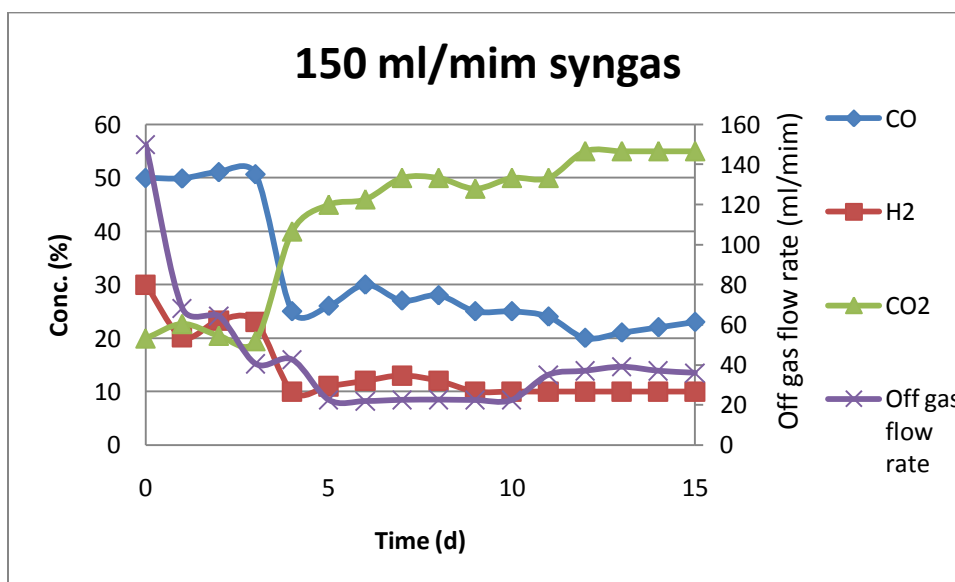(a) Production and cell density vs. Time

(b) Off-gas flow rate and composition vs. Time

Figure 5. The end product production by *C. ljungdahlii* at a flow rate of 50 ml/mim of syngas supply by controlling pH at 5.0 in the production phase
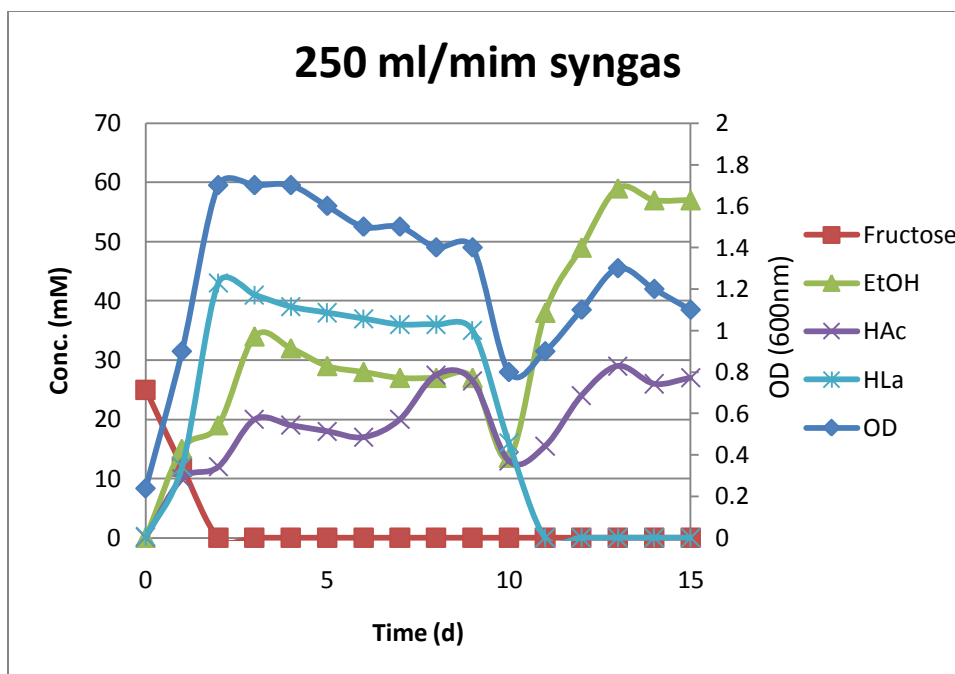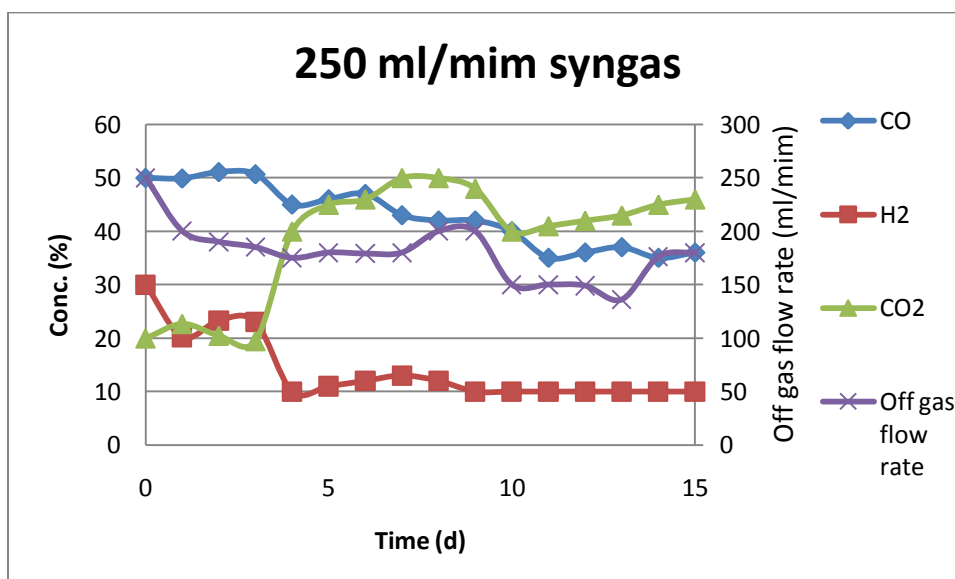
(a) Production and cell density vs. Time

(b) Off-gas flow rate and composition vs. Time

Figure 6. The end product production by *C. ljungdahlii* at a flow rate of 150 ml/mim of syngas supply by controlling pH at 5.0 in the production phase

(a) Production and cell density vs. Time

(b) Off-gas flow rate and composition vs. Time

Figure 7. The end product production by *C. ljungdahlii* at a flow rate of 200 ml/mim of

syngas supply by controlling pH at 5.0 in the production phase with biomass retained
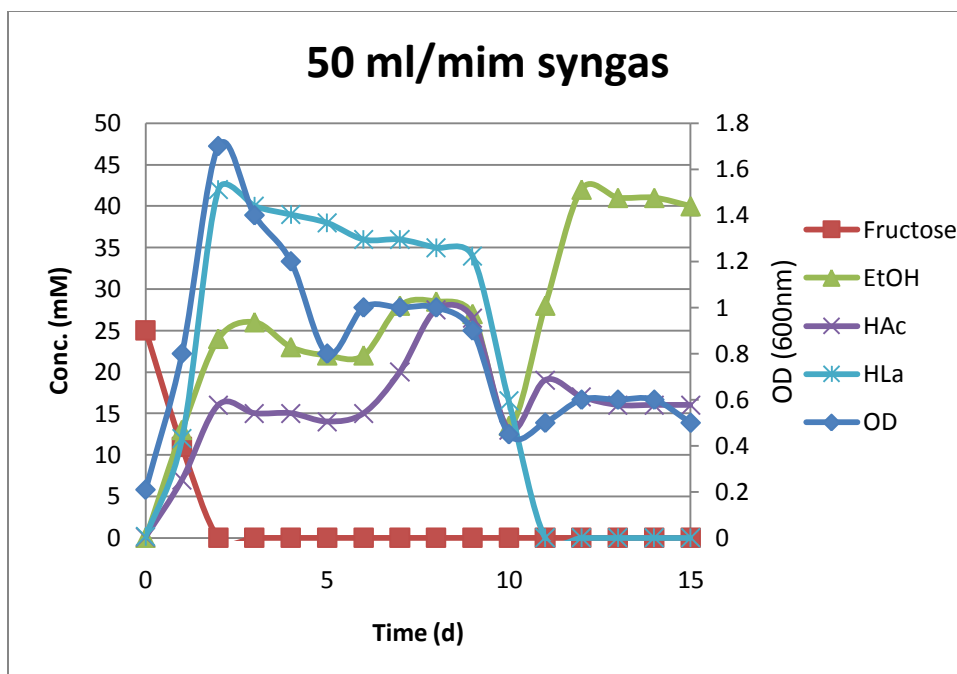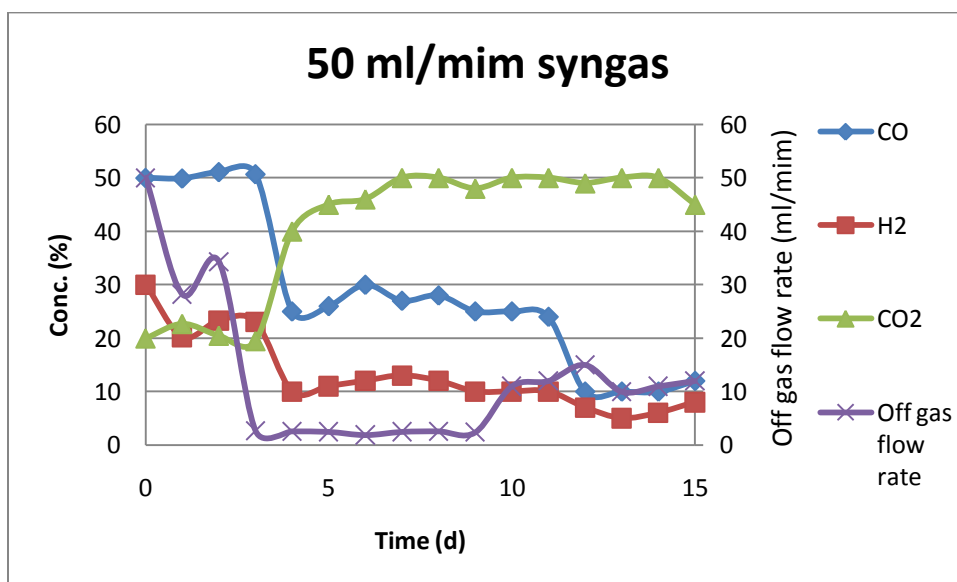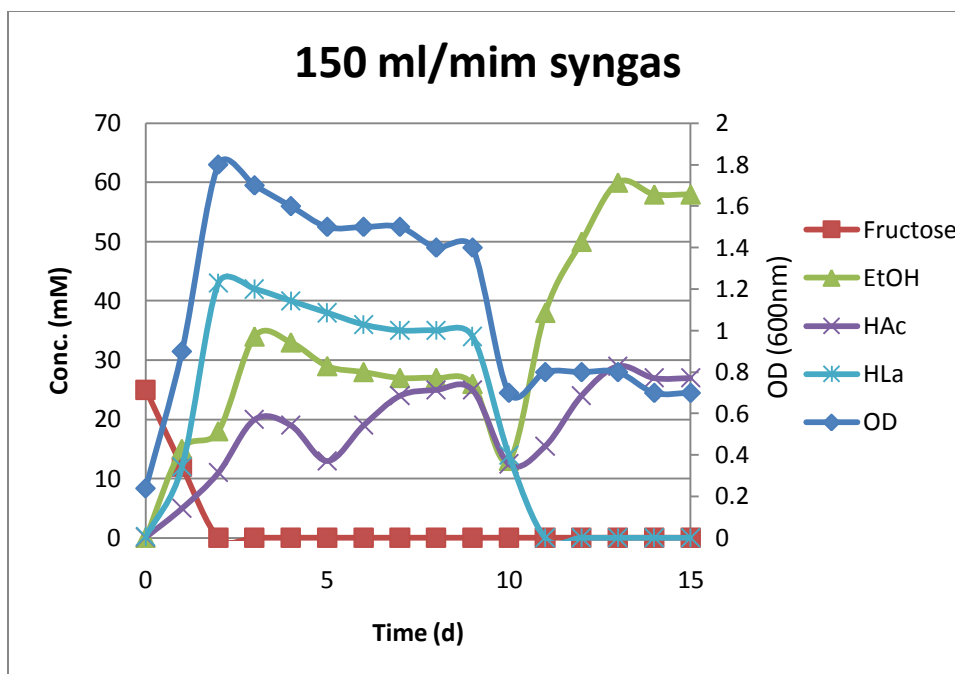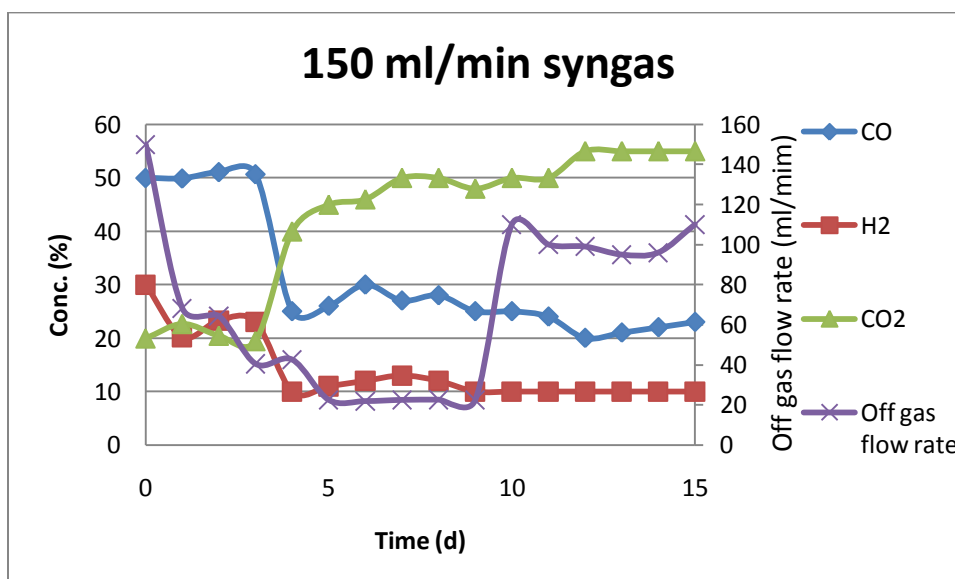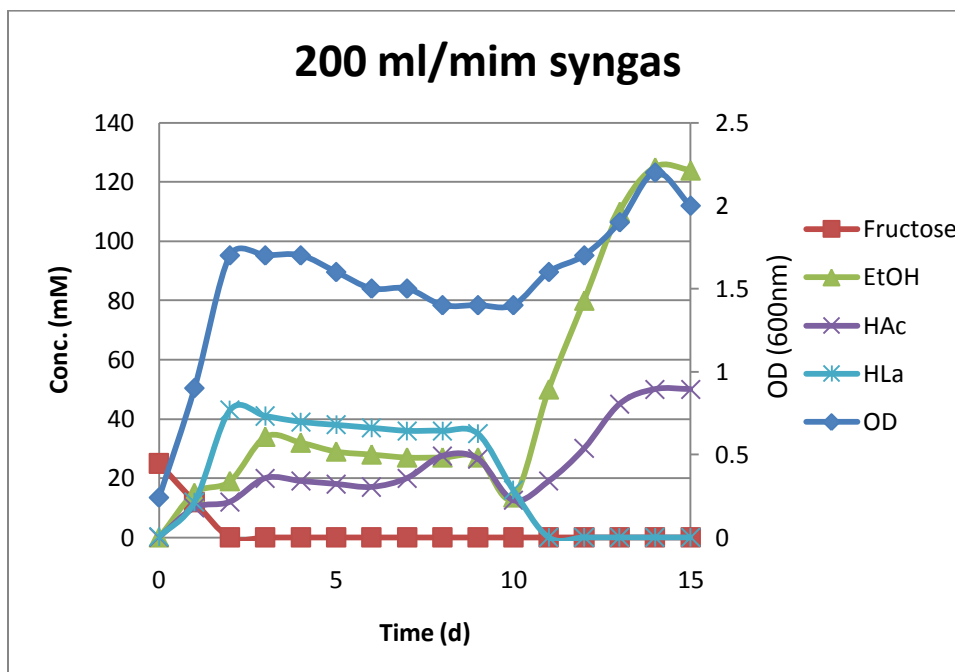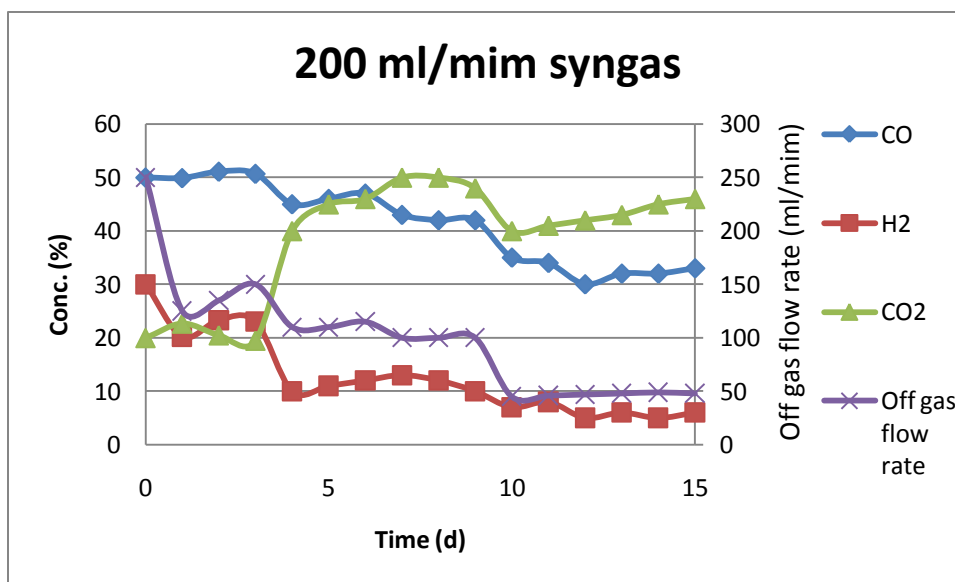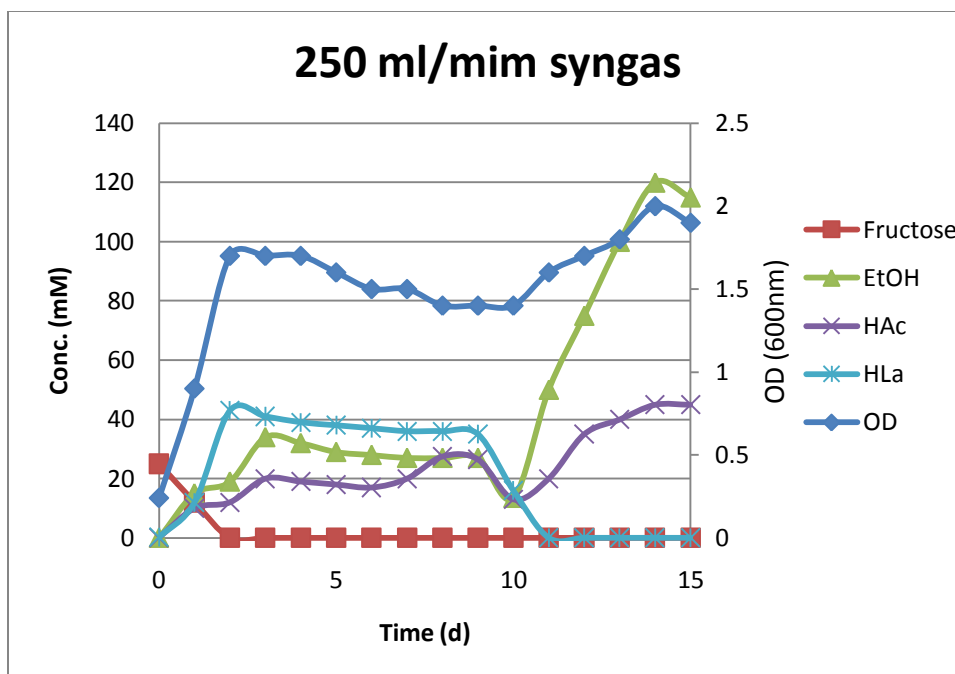
(a) Production and cell density vs. Time
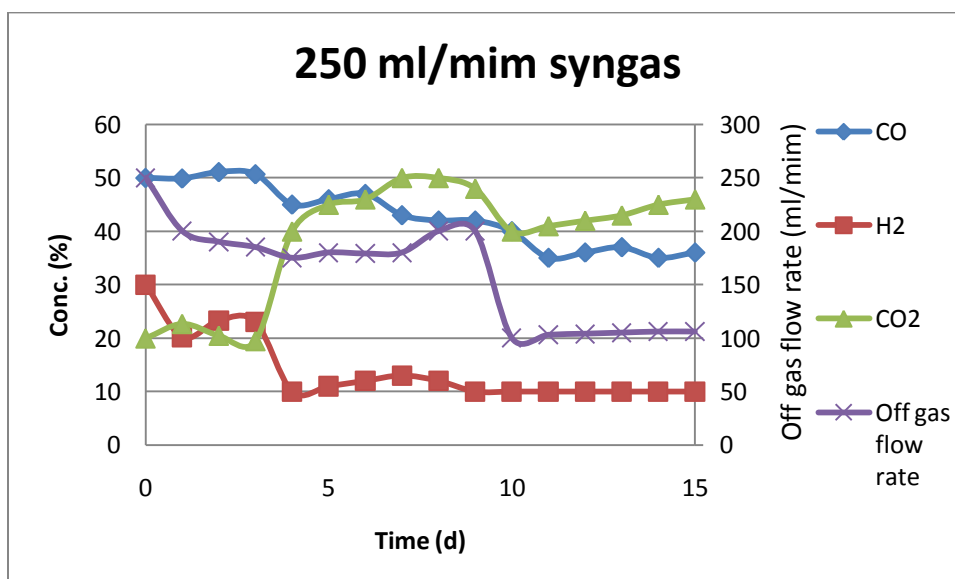
(b) Off-gas flow rate and composition vs. Time

Figure 8. The end product production by *C. ljungdahlii* at a flow rate of 250 ml/mim of

syngas supply by controlling pH at 5.0 in the production phase with biomass retained

Table 1. ATCC 1754 PETC medium composition in 1-L distilled water

Compounds	Amount
NH_4Cl (g)	1.0
KCl (g)	0.1
$MgSO_4 \cdot 7H_2O$ (g)	0.2
NaCl (g)	0.8
KH_2PO_4 (g)	0.1
$CaCl_2 \cdot 2H_2O$ (mg)	20.0
$NaHCO_3$ (g)	2.0
Fructose (g)	5.0
Nitrilotriacetic acid (g)	2.0
$MnSO_4 \cdot H_2O$ (g)	1.0
$Fe(SO_4)_2(NH_4)_2 \cdot 6H_2O$ (g)	0.8
$CoCl_2 \cdot 6H_2O$ (mg)	20.0
$ZnSO_4 \cdot 7H_2O$ (g)	0.2
$CuCl_2 \cdot 2H_2O$ (mg)	20.0
$NiCl_2 \cdot 6H_2O$ (mg)	20.0
$Na_2MoO_4 \cdot 2H_2O$ (mg)	20.0
Na_2SeO_4 (mg)	2.0
Biotin (mg)	2.0
[a] Reducing agent (ml)	10.0
Folic acid (mg)	2.0
Trace elements (ml)	10
Wolf's vitamin solution (ml)	10
Pyridoxine HCl (mg)	10.0
Thiamine HCl (mg)	5.0
Riboflavin (mg)	5.0
Nicotinic acid (mg)	5.0
Calcium D-(+) pantothenate (mg)	5.0
Cyanocobalamine (μg)	100.0
p-Aminobenzoic acid (mg)	5.0
Thioctic acid (mg)	5.0

[a] Reducing agent composition (per 100 ml): NaOH 0.9 g, L-cysteine·HCl: 4.0 g, and $Na_2S \cdot 9H_2O$: 4.0 g

Table 2. Summary of the end product ratios in varied conditions

(a) Growth phase

pH	syngas flow rate (ml/mim)	EtOH (g/L)	HAc (g/L)	EtOH/ HAc	OD	EtOH/ OD
6.5-7.5	50	1.05	0.84	1.8	1.4	0.88
6.5-7.5	150	1.61	1.23	1.8	1.8	0.94
6.5-7.5	200	1.63	1.21	1.7	1.7	0.96
6.5-7.5	250	1.56	1.2	1.7	1.7	0.92

(b) Production phase

pH	syngas flow rate (ml/mim)	EtOH (g/L)	HAc (g/L)	EtOH /HAc	OD	EtOH/ OD
6.5-7.5	50	2.39	1.56	2.0	0.8	3.0
6.5-7.5	150	2.76	1.74	2.1	1.2	2.3
6.5-7.5	250	2.71	1.74	2.1	1.3	2.1
5	50	1.90	1.02	2.4	0.6	3.1
5	150	2.76	1.74	2.1	0.9	3.1
5 (with biomass retained)	100	4.32	1.74	3.1	1.6	2.7
5 (with biomass retained)	200	6.0	3.0	2.0	2.2	3.0
5 (with biomass retained)	250	5.5	2.7	2.5	2.0	2.7

Table 3. Maximum product from different studies

Syngas diffuser types/Reactor	Medium	Ethanol (g/L)	Acetate (g/L)	References
Degassed/Batch	ATCC medium	3.0	2.0-3.0	Klasson *et al.*, (1993)
Bubbled/CSTR	Modified ATCC medium	48.0	3.0	Klasson *et al.*, (1993)
Degassed/Batch	ATCC medium	0.55	1.3	Younesi *et al.*, (2002)
Bubble/CSTR	ATCC medium	12.0	28.0	Najafpour and Younesi (2006)
Degassed/Batch	ATCC medium	0.50	1.1	This study
Degassed/Batch	ATCC medium without fructose	0.029	0.69	This study
Hollow fiber membrane reactor	ATCC medium without fructose	6.0	3.1	This study

CHAPTER 6. GENERAL CONCLUSIONS

1. Conclusions

The following conclusions are drawn from the performance of this research effort:

The mass transfer of carbon monoxide (CO) to liquid through hollow fiber membrane was examined for syngas fermentation in which gas transfer is regarded as limiting step. Hollow fiber membrane would be beneficial, as the membrane enabled higher CO mass transfer than previous studies. The maximum observed volumetric CO mass transfer coefficient of 0.107 s^{-1} was observed at 400 fibers, cross flow velocity of 2.20 cm·sec^{-1}, and specific gas flow rate of 1.02 min^{-1}. The mass transfer would be improved along with increasing cross flow velocity, specific gas flow rate, and fiber numbers

The mass transfer rates of carbon monoxide (CO) to liquid through a microporous polypropylene hollow fiber membrane and nonporous silicone hollow fiber membrane (HFM) were examined in this study for improving CO-liquid mass transfer in the syngas fermentation process. The study is conducted using a statistic, experimental design: Box-Behnken design to determinate the significant operational parameters (water recirculation velocity, specific gas flow rate, and mixing power input per volume) and to fit a model for full-scale applications. The highest CO mass transfer rate of 1.49 s^{-1} which is over its counterpart (nonporous silicone HFM) and previous studies was obtained using the

microporous polypropylene HFM.   A model is calculated for commercialization of syngas fermentation.

Clostridium ljungdahlii demonstrated its highest growth rate on PETC 1754 with 5 g·l^{-1} fructose and 1 g·l^{-1} yeast extract with pH between 6.5 and 7.5. Since the medium without fructose in the medium is desired for ethanol production, pH at 5 in the production phase is recommended for the optimal ethanol production from *C. ljungdahlii*.

The design of using hollow fiber membrane as syngas delivering system was demonstrated to producing ethanol to 6 g·L^{-1} using the fructose-free medium with an ethanol to acetate ratio of 2.6 which was the highest ratio in compared with other previous studies.   The use of HFM in syngas fermentation is an innovative approach which can eliminate the mass transfer barrier compared to conventional reactor designs.

2. Recommendations for Future Research

An investigation into the different hollow fiber membrane reactors configurations, including stirrers, different geometries, particles, and different porous size hollow fiber membrane, should be performed to determine the best possible configuration for maximizing the gas-liquid mass transfer rate. Additional work should be completed to understand the complex relationship between gas-liquid mass transfer rates for differing gas species such as hydrogen so that mass transfer rates may be accurately estimated using one of the theoretical models. Also, different types of hollow fiber membranes, especially design for low soluble gaseous, should be developed and tested for syngas fermentation.

A medium for *Clostridium ljungdahlii* to optimize ethanol production in the production phase should be developed, since the PETC 1754 medium from ATCC is for the growth of *Clostridium ljungdahlii*. A medium with different carbon to nitrogen ratio should be investigated for *Clostridium ljungdahlii* using an experimental design method for maximizing ethanol production. Future studies could include examining other medium components such as biotin, phosphate, and 3-(N-morpholino) propanesulfonic acid (MOPS).

References

Amed, A., Cateni, B.G., Huhnke, R.L., Lewis, R.S. (2006) Effects of biomass-generated producer gas constitutes on cell growth, product distribution and hydrogenase activity of *Clostridium carboxidivorans* P7, *Biomass Bioeng*. 30, 665–672.

Barik, S., Prieto, S., Harrison, S.B., Clausen, E.C., and Gaddy, J.L. (1988) Biological production of alcohols from coal through indirect liquefaction, *Appl. Biochem. Biotechnol.* 28, 363–378.

Barik, S., Prieto, S., Harrison, S.B., Clausen, E.C., and Gaddy, J.L. (1990) *Bioprocessing and Biotreatment of Coal*, I[st] Ed. Wise, D. L., Chapter 8 'Biological production of ethanol from coal synthesis gas," (Marcel Dekker In., New York) 1231–1154.

Berberich, J.A., Knutson, B.L., Strobel, H.J., Tarhan, S., Nokes, S.E., and Dawson, K.A. (2000) Product selectivity shifts in *Clostridium thermocellum* in the presence of compressed solvent, *Ind. Eng. Chem. Res.* 39, 4500–4505

Bredwell, M.D., Srivastava, P., and Worden, R.M. (1999) Reactor design issues for synthesis gas fermentations, *Biotechnol. Prog*. 15, 834–844.

Charpentier, J.C. (1981). Mass transfer in gas-liquid absorbers and reactors, *Adv. Chem. Eng.* 11, 1–103.

Cotter, J.L., Chinn, M.S., and Grunden, A.M. (2009) Influence of process parameters on growth of *Clostridium Ljungdahlii* and *Clostridium autoetahanogenum* on synthesis gas, *Enzyme Microbial Technol.* 44, 281–288.

Cotter, J.L., Chinn, M.S., and Grunden, A.M. (2008) Ethanol and acetate production by *Clostridium ljungdahlii* and *Clostridium autoethanogenum* using resting cells, *Bioprocess Biosyst. Eng.* 32, 369–380.

Datar R.P., Shenkman, R.M., Cateni, B.G., Huhnke, R.L, and Lewis, R.S. (2004) Fermentation of biomass-generated producer gas to ethanol, *Biotechnol. Bioeng*. 86, 587–594

Diekert, G.B., and Thayer, R.K. (1982) Carbon monoxide oxidation by *Clostridium thermoaceticum* and *Clostridium formicoaceticum*, *J. Bacteriol.* 136, 597–606.

Do, Y.S., Smeenk, J., Broer, K.M., Kisting, C., Brown, R., Heindel, T.J., Bobik, T.A., and Dispirito, A.A. (2007) Growth of *Rhodospirillum rubrum* on synthesis gas: conversion of CO to H_2 and poly-beta-hydroxyalkanoate, *Biotechnol. Bioeng*. 97, 279–86.

Drake, H.L. (1994) *Acetogenesis,* 1st ed. (Chapman and Hall, New York).

du Preez, L.A., Opendaal, J.P., Maree, J.P., Ponsonby, M. (1992) Biological removal of sulfate from industrial effluents using producer gas as energy source, *Environ. Technol*. 13, 875–882.

du Preez, L.A., and Maree, J.P. (1994) Pilot-scale biological sulfate and nitrate removal utilizing producer gas and energy source, *Wat.. Sci. Technol*. 30, 275–285.

Fischer, C.R., Klein-Marcuschamer, D., and Stephanopoulos, G. (2008) Selection and optimization of microbial hosts for biofuels production, *Metabolic Eng*. 10, 295–304.

Fordyce, A.M., Crow, V.L., and Thomas, T.D. (1984) Regulation of product formation during glucose or lactose limitation in nongrowing cells of streptococcus, *Appl. Environ. Microbiol.* 48, 332–337.

Gaddy, J.L. and Clausen, E.C. (1992) US Patent 612:221

Genthner, B.R.S. and Bryant, M.P. (1987) Additional characteristics of one-carbon-compound utilization by *Eubacterium limosum* and *Acetobacterium woodii*, *Appl. Environ. Microbiol.* 53, 471–476.

Genthner, B.R.S. and Bryant, M.P. (1982) Growth of *Eubacterium limosum* with carbon monoxide as the energy source. *Appl. Environ. Microbiol.* 43, 70–74.

Grethlein, A.J., Worden, R.M., Jain, M.K., and Datta, R. (1991) Evidence for production of n-butanol from carbon monoxide by *Butyribacterium methylotrophicum*, *J. Ferment. Bioeng*. 72, 58–60.

Hedderich, R. (2004) Energy-converting [NiFe] hydrogenases from archaea and extremophiles: ancestors of complex I. *J. Bioenerg. Biomembr.* 36, 65–75.

Henstra, A.M., Sipma, J., Rinzema, A., and Stams, A.J.M. (2007) microbiology of synthesis gas fermentation for biofuel production, *Current Option in Biotechnol.,* 18, 200–206.

Kapic, A., Jones, S.T., and Heindel, T.J. (2006) Carbon monoxide mass transfer in a syngas mixture, *Ind. Eng. Chem. Res*. 45, 9150–9155.

Kerby, R.L., Ludden, P.W., and Roberts, G.P. (1995) Carbon monoxide dependent growth of *Rhodospirillum rubrum*, *J. Bacteriol.* 177, 2241–2244.

Kim, S.H., Lee, P.H., Chang, H.I., and Sung, S. Carbon monoxide mass transfer characteristics of hollow-fiber membranes for syngas fermentation, manuscript in progress.

Klasson, K.T., Ackerson, M.D., Clausen, E.C. and Gaddy, J.L. (1992) Bioconversion of synthesis gas into liquid or gaseous fuels. *Enzyme Microbial Technol. 14*, 602–608.

Lee, P.H., Ni, S.Q., Choi, D.W., and Sung, S. pH effect on the growth of *Clostridium ljungdahlii* for ethanol production from syngas fermentation, manuscript in progress.

Lindahl P.A. (2002). The Ni-containing carbon monoxide dehydrogenase family: light at the end of the tunnel?. B*iochem.* 41, 2097–2105.

Liou, J.S.C., Balkwill, D.L, Drake, G.R., and Tanner, R.S. (2005) *Clostridium carboxidivorans* sp. nov., a solvent-producing clostridium isolated from an agricultural settling lagoon, and reclassification of the acetogen *Clostridium scatologenes* strain SL1 as *Clostridium drakei* sp. nov. *Int. J. Syst. Evol. Microbiol.* 55, 2085–2091.

Lynd, L., Kerby, R., Zeikus, J.G. (1982) Carbon monoxide metabolism of the methylotrophic acidogen *Butyribacterium methylotrophicum*, *J. Bacteriol*., 149, 255–263.

Maness, P. C., Huang, J., Smolinski, S., Tek, V., Vanzin, G. (2005) Energy generation from the CO oxidation-hydrogen production pathway in *Rubrivivax gelatinosus*, *Appl. Environ. Microbiol.* 71, 2870–2874.

Najafpour, G. and Younesi, H. (2006) Ethanol and acetate synthesis from waste gas using batch culture of *Clostridium ljungdahli*, *Enzyme Microbial Technol*. *38*, 223–228.

Phillips, J.R., Clausen, E.C., Gaddy, J.L. (1994) Synthesis gas as substrate for biological production of fuels and chemicals., *Appl. Biochem. Biotechnol*. 45, 145–157.

Ragsdale, S.W. (2004) Life with carbon monoxide, *Crit. Rev. Biochem. Mol. Biol*, 39, 165–195

Ragsdale, S.W. and Pierce, E. (2008) Acetogenesis and Wood-Ljungdahl pathway of CO_2 fixation, *Biochimica et Biophysica Acta* 1784, 1873–1898.

Riggs, S.S. and Heindel, T.J. (2006) Measuring carbon monoxide gas-liquid mass transfer in a stirred tank reactor for syngas fermentation, *Biotechnol. Prog*. 22, 903–906.

Rajagopalan, S., Datar, R.P., and Lewis, R.S. (2002) Formation of ethanol from carbon monoxide via a new microbial catalyst, *Biomass Bioenergy* 23, 487–493.

Selvaraj, P.T., Little, M.H., Bredwell, M.D., and Kaufman, E.N. (1996) Bioreactors for flue gas biodesulfurization using coal synthesis gas as feedstock. *Proc. American Insti. of Chem. Eng. Fall Annual Meeting.*, 10-15, 1996, (in Chicago, IL).

Shen, G.J., Shieh, J.S., Grethlein, A.J., Jain, M.K., and Zeikus, J.G. (1999) Biochemical basis for carbon monoxide tolerance and butanol production by *Butyribacterium methylotrophicum*, *Appl. Microbiol. Biotechnol.* 51, 827–832.

Singer S.W., Hirst, M.B., Ludden, P.W. (2006) CO-dependent H_2 evolution by *Rhodospirillum rubrum*: role of CODH:CooF complex, *Biochim. Biophys. Acta. – Bioenerg.* 1757, 1582–1591

Tanner, R.S., Miller, L.M., and Yang, D. (1993) *Clostridium ljungdahlii* sp. nov., an acetogenic species in clostridial ribosomal-RNA homology group-I. *Int. J. Syst. Bacteriol*. 43, 232–236.

Ungerman, A.J. and Heindel, T.J. (2007) Carbon monoxide mass transfer for syngas transfer for syngas fermentation in a stirred tank reactor with dual impeller configurations, *Biotechnol. Prog.* 23, 613–620.

van Houten, R.T., Hulshoff Pol, L.W., Lettinga, G. (1994) Biological sulfate reduction using gas-lift bioreactors fed with hydrogen and carbon dioxide as energy and carbon source, *Biotechnol Bioeng.* 44, 586–594.

Worden, R.M., Grethlein, A.J., Jain, M.K., and Datta, R. (1991) Production of butanol and ethanol from synthesis gas via fermentation, *Fuel* 70, 615–619.

Younesi, H., Najafpour G., Mohamed, A.R. (2005) Ethanol and acetate production from synthesis gas via fermentation processes using anaerobic bacterium, *Clostridium ljungdahlii*, *Biochem. Eng. J.* 27, 110–119.

Younesi, H., Najafpour G., Mohamed, A.R. (2006) Liquid fuel production from synthesis gas via fermentation process in a continuous tank bioreactor (CSTR) using *Clostridium ljungdahlii*, *Iranian J. Botechnol.* 4, 45–53.

ACKNOWLEDGEMENTS

I would like to thank those who helped me throughout this research project and the writing of this disseration. First and foremost, thank you to Dr. Shihwu Sung for providing guidance and support review of my work that was helpful in improving my understanding and research. Thank you to Dr. Dong-Won Choi, Dr. Sang-Hyoun Kim, Shouqing Ni, Sam Cottor, David Chipman and my fellow graduate students for advice and help. I would also like to thank my committee members, Dr. Ong, Dr. Alleman, Dr. Loynachan, and Dr. Moorman, for their help and support with this project throughout my time at Iowa State.   Most of all, I would like to thank my family, especially my parents (Chao-Ming Lee and Shu-Mei Leehuang) and my wife (Chiao-Hua Li), for their love, support, and patience throughout this process.